



University of  
**Salford**  
MANCHESTER

# **Molecular Pathways Controlling DNA Damage Response**

**Hasen Alhebshi**

School of Environment & Life Sciences  
The University of Salford, UK

Submitted in partial fulfilment of the requirements of the Degree of  
Doctor of Philosophy, 2018

<b>Table of contents.....</b>	<b>2</b>
<b>List of figures.....</b>	<b>7</b>
<b>List of tables .....</b>	<b>11</b>
<b>Declaration of originality.....</b>	<b>12</b>
<b>Acknowledgements.....</b>	<b>13</b>
<b>List of abbreviations.....</b>	<b>14</b>
<b>Abstract.....</b>	<b>17</b>
<b><u>Chapter 1. Introduction</u> .....</b>	<b>19</b>
<b>1.1 Cancer.....</b>	<b>19</b>
1.1.1 Lung Cancer .....	20
1.1.2 Malignant pleural mesothelioma.....	21
<b>1.2 P53 tumour suppressor .....</b>	<b>23</b>
1.2.1 P53 roles .....	23
1.2.2 P53 structure.....	25
1.2.3 Levels of control of p53 activity.....	26
1.2.3.1 P53 : Posttranslational modifications.....	26
1.2.3.1.1 Protein phosphorylation.....	27
1.2.3.1.2 Acetylation .....	28
1.2.3.1.3 Ubiquitination.....	29
1.2.4 P53-MDM2 relationship.....	30
1.2.5 P53 cofactors.....	30
1.2.6 P53- TTC5 Crosstalk.....	31
1.2.7 P53 pathways.....	33
1.2.7.1 Cell cycle arrest .....	35
1.2.7.2 Apoptosis.....	36
1. 2. 8. P53 and the regulation of microRNAs.....	38
1. 2. 8. 1. MiRNA-34 family and p53 pathway.....	39
1. 3. Aims of the study.....	43
<b><u>Chapter 2. Materials and methods</u>.....</b>	<b>44</b>
<b>2.1 Growing and maintaining cells.....</b>	<b>44</b>
2.1.1 Cell lines maintenance.....	44

2.1.2 Passage of A549, Mero-25 and M-14 cell lines .....	44
2.1.3 Freezing of cell lines .....	44
2.1.4 Thawing of cell lines.....	45
<b>2.2 Immunoblotting .....</b>	<b>45</b>
2.2.1 Extract preparation.....	45
2.2.2 Determination of protein concentration.....	46
2.2.3 SDS Gel electrophoresis.....	46
2.2.3.1 SDS Gel preparation.....	47
2.2.3.2 Sample loading and running .....	47
2.2.3.3 Western transferring .....	47
2.2.3.4 Western blot development .....	48
2.2.4.4 Stripping of the membrane .....	49
<b>2.3 Immunohistochemistry approach.....</b>	<b>50</b>
2.3.1 Tissue Processing.....	50
2.3.1.1 Fixation.....	50
2.3.2.2 Tissue sections and mounting.....	50
2.3.2 Antigen retrieval .....	51
2.3.3 Blocking endogenous enzymes .....	51
2.3.4 Primary antibodies.....	51
2.3.5 Secondary antibodies .....	52
2.3.6 Immunochromogenic staining.....	52
2.3.7 Counter staining.....	52
2.3.8 Microscopic examination .....	52
<b>2.4 CO-IP.....</b>	<b>53</b>
<b>2.5 Immunofluorescent approach.....</b>	<b>54</b>
<b>2.6 MiRNA Isolation, Reverse Transcription and Quantitative Real-time-PCR.....</b>	<b>54</b>
<b>2.7 Statistical Analysis.....</b>	<b>54</b>
<b><u>Chapter3. Results</u>.....</b>	<b>56</b>
<b>3.1 Immunoblotting results.....</b>	<b>56</b>
<b>3.1.1. Analysis of the total p53 protein levels in A549 human lung cancer cell line.....</b>	<b>56</b>

<b>3.1.1.2</b> Analysis of the phosphorylated p53 at Serine 46 protein levels in A549 human Lung cancer cell line.....	57
<b>3.1.1.3</b> Analysis of the acetylated p53 at lysine 382 protein levels in A549 human Lung cancer cell line.....	59
<b>3.1.1.4</b> Analysis of the TTC5 protein levels in A549 human lung cancer cell line .....	60
<b>3.1.2.1</b> Analysis of the total p53 protein levels in Mero-25 human Mesothelioma cancer cell line.....	62
<b>3.1.2.2</b> Analysis of the phosphorylated p53 at Serine 46 protein levels in Mero-25 human Mesothelioma cancer cell line .....	63
<b>3.1.2.3</b> Analysis of the acetylated p53 at lysine 382 protein levels in Mero-25 human Mesothelioma cancer cell line.....	64
<b>3.1.2.4</b> Analysis of the TTC5 protein levels in Mero-25 human Mesothelioma cancer cell line.....	66
<b>3.1.3.1</b> Analysis of the total p53 protein levels in Mero-14 human Mesothelioma cancer cell line.....	67
<b>3.1.3.2</b> Analysis of the phosphorylated p53 at Serine 46 protein levels in Mero-14 human Mesothelioma cancer cell line.....	68
<b>3.1.3.3</b> Analysis of the acetylated p53 at lysine 382 protein levels in Mero-14 human Mesothelioma cancer cell line.....	70
<b>3.1.3.4</b> Analysis of the TTC5 protein levels in Mero-14 human Mesothelioma cancer cell line.....	71
<b>3.2 Immunohistochemistry results</b> .....	73
<b>3.2.1</b> The optimization process.....	73
<b>3. 2. 2</b> The tissue microarrays results.....	75

3. 2. 2. 1. Total p53 protein expression in the human lung cancer tissue microarrays.....	81
3. 2. 2. 2. Detection of the actylated-p53 at lysine 382 protein expression in the human lung cancer tissue microarrays.....	85
3. 2. 2. 3. Detection of the phosphorylated-p53 at Ser-46 protein expression in the human Lung cancer tissue microarrays.....	86
3. 2. 2. 4. Detection of TTC5 protein expression in the human Lung cancer tissue microarrays.....	90
<b>3. 3. CO-Immunoprecipitation results.....</b>	<b>92</b>
<b>3.4. Immunofluorescence results.....</b>	<b>94</b>
3.4.1 Determination of the acetylated p53 (K382) expression location in the A549 cell lines.....	95
3.4.2 Determination of the acetylated p53 (K382) expression location in the U2OS cell lines.....	97
3. 5 Detection of the expression of microRNA-34 in lung and mesothelioma cell lines using QRT-PCR.....	100
3. 5. 1 Determination of the expression of miR-34a and miR-34b family members in the lung cancer (A549) cell lines in the presence or absence of DNA damage.....	100
3. 5. 2 Determination of the expression of miR-34a and miR-34b family members in the Mesothelioma (Mero-25) cell lines in the presence or absence of DNA damage.....	101
3. 5. 3 Determination of the expression of miR-34a and miR-34b family members in the Mesothelioma (Mero-14) cell lines in the presence or absence of DNA damage.....	102
<b><u>Chapter 4. Discussion</u>.....</b>	<b>104</b>
4. 1. Analysis of p53 total, its modified isoforms and TTC5 protein levels in cancer cell lines.....	105

<b>4. 2. Detection of p53 total, its modified isoforms and TTC5 protein levels in cancer tissues.....</b>	<b>107</b>
<b>4. 3. Subcellular location of p53, its isoforms and TTC5 in cell lines.....</b>	<b>109</b>
<b>4. 4. MiR-34 expression detection.....</b>	<b>110</b>
<b>4. 5. Conclusions.....</b>	<b>112</b>
<b>4. 6. Future Directions.....</b>	<b>113</b>
<b>4. 7. Appendix.....</b>	<b>114</b>
<b>References.....</b>	<b>117</b>

**List of figures:**

**Figure 1. 1.** Cancer mortality in UK for 2012. ....21

**Figure 1. 2.** Mesothelioma (C45): European Age-Standardised Incidence Rates per 100,000 Populations, by Sex, Great Britain 1979-2013. ....23

**Figure. 1. 3.** Schematic representation of the p53 structure. ....26

**Figure 1. 4.** P53 pathway: Phosphorylation of p53 and mdm2 disrupt the interaction between the two proteins. ....28

**Figure. 1. 5.** Role of JMY and Strap in the p53 response. ....32

**Figure. 1. 6:** P53 pathway: Upstream pathway. ....34

**Figure 1. 7.** A p53-mediated apoptosis model. ....37

**Figure 1. 8.** Model of miRNAs biogenesis and function. ....40

**Figure 2. 1.** The sandwich assembly for western transfer process. ....48

**Figure 3. 1.** Expression of the total p53 protein in A549 Lung cancer cell lines in the absence and presence of induced DNA damage. ....57

**Figure 3. 2.** Quantification of the total p53 protein levels of the blots shown in figure 3. 1 was carried out using ImageJ software. ....57

**Figure 3. 3.** Analysis of the phosphorylated p53 at Serine 46 protein levels in A549 cell lines with and without DNA damage. ....58

**Figure 3. 4.** Quantification of the phosphorylated p53 at Serine 46 protein level of the blots shown in figure 4 have carried out using ImageJ software. ....58

**Figure 3. 5.** Analysis the acetylated p53 at lysine 382 protein levels in Lung cancer cell lines (A549) with and without inducing DNA damage. ....59

**Figure 3. 6.** Densitometric analysis of acetyl-p53 at lysine 382 in A549 cell lines in presence or absence of induced DNA damage via Etoposide by using ImageJ software. ....60

**Figure 3. 7.** Detection of the TTC5 protein in the A549 cell lines in presence or absence of induced DNA damage using SDS PAGE assay. ....60

<b>Figure 3. 8.</b> Quantification of the TTC5 protein level of the blots in A549 cell lines shown in figure 3. 7. was carried out using ImageJ software. ....	61
<b>Figure 3. 9:</b> Conclusion figure for densitometric analysis of Tp53, P-p53 at S46, acetyl-p53 at lysine 382 and TTC5 proteins in the A549 cell lines with or without of induced DNA damage. ....	61
<b>Figure 3. 10.</b> Detection of the Total p53 protein level in the Mero-25 cell lines with and without DNA damage. ....	62
<b>Figure 3. 11.</b> Quantification of the wild-type p53 protein level of the blots shown in figure 3. 10, which carried out using ImageJ software. ....	63
<b>Figure 3. 12.</b> Analysis of the phosphorylated p53 at Serine 46 protein levels in Mero-25 cell lines with and without DNA damage by treated and incubated with 20 $\mu$ M Etoposide for 24 hours. ....	64
<b>Figure 3. 13.</b> Quantification of the phosphorylated p53 at Ser46 protein level has carried out using ImageJ software in the Mero-25 cell lines shown in figure 3. 12. ....	64
<b>Figure 3. 14.</b> Analysis the acetylated p53 at lysine 382 protein levels in Mesothelioma cell lines (Mero-25) with and without DNA damage. ....	65
<b>Figure 3. 15.</b> Densitometric analysis of acetyl-p53 at lysine 382 in Mero-25 cell lines in presence or absence of DNA damage via Etoposide has carried out by using ImageJ software.....	65
<b>Figure 3. 16.</b> Detection of the TTC5 protein in the Mero-25 cell lines in presence or absence of DNA damage via using SDS PAGE and WB. ....	66
<b>Figure 3. 17.</b> Quantification of the TTC5 protein levels shown in figure 3. 16 have carried out using ImageJ software. ....	66
<b>Figure 3. 18.</b> Quantification of Tp53, Ser-46 and K382 protein levels in association with TTC5 in the Mero-25 cells concluded and showed in C. ....	67
<b>Figure 3. 19.</b> Detection of the Total p53 protein level in the Mero-14 cell lines with and without DNA damage by using SDS PAGE and Western Blotting. ....	68

<b>Figure 3. 20.</b> Quantification of the wild-type p53 protein levels in the Mero-14 shown in figure 3. 19. which generated by using ImageJ software. ....	68
<b>Figure 3. 21.</b> Detection of the phosphorylated p53 at Serine 46 protein levels in Mero-14 cell lines with and without DNA damage by treated and incubated the cells with 20 $\mu$ M Etoposide for 24 hours. ....	69
<b>Figure 3. 22.</b> Quantification of phospho-p53 at Ser46 protein levels has generated using ImageJ software in the Mero-14 cell lines shown in figure 3. 21. ....	69
<b>Figure 3. 23.</b> Analysis the acetylated p53 at lysine 382 protein levels in Mesothelioma cell lines (Mero-14) with and without an induced DNA damage. ....	70
<b>Figure 3. 24.</b> Densitometry analysis of the p53 acetylation form (K382) in the Mero-14 cell lines in presence or absence of an induced DNA damage has carried out by using ImageJ software. ....	70
<b>Figure 3. 25.</b> Detection of the TTC5 protein expression level in Mero-14 cells with or without of the induced DNA damage using SDS PAGE and immunoblotting assay. ....	71
<b>Figure 3. 26.</b> Quantification of the TTC5 expression levels in Mero-14 shown in figure 3. 25 by using ImageJ software. ....	71
<b>Figure 3. 27.</b> Quantification of Total p53, Ser-46 and K382 proteins levels in addition to TTC5 protein in the Mero-14 cell lines. ....	72
<b>Figure 3. 28.</b> Shown the TMA human lung cancer slides 1 and 2 included 92 +120 cases. ....	75
<b>Figure 3. 29.</b> Immunoreactivity of the Tp53 protein in paraffin-embedded Human lung cancer tissue microarrays using the Tp53 (DO-7) antibody. ....	82
<b>Figure 3. 30.</b> Immunostaining of the acetylated-p53 at lysine 382 protein expression in paraffin-embedded, human lung cancer tissue microarrays using the polyclonal anti-acetyl-p53 (K382) antibody. ....	86
<b>Figure 3. 31.</b> Immunostaining of the phospho-p53 at Ser-46 protein expression in paraffin-embedded human Lung cancer tissue microarrays using anti-phospho-p53 (Ser-46) antibody. ....	87

<b>Figure 3. 32.</b> The TTC5 protein expression in paraffin-embedded human Lung cancer tissue microarrays using the polyclonal anti-TTC5 antibody. ....	90
<b>Figure 3. 33.</b> CO-Immunoprecipitation results for Mero-14 cells shows the bands with the Tp53 Ab (DO-1). ....	92
<b>Figure 3. 34.</b> CO-Immunoprecipitation results for Mero-14 showed the blotting bands with the Actin. ....	92
<b>Figure 3. 35.</b> The location of p53 acetylated at lysine 382 protein in untreated A549 cell lines. ....	94
<b>Figure 3. 36.</b> The location of p53 acetylated at lysine 382 protein in untreated A549 cell lines. ....	95
<b>Figure 3. 37.</b> Shown the location of K382 protein expression in U2OS cell lines. ....	97
<b>Figure 3. 38.</b> Shown the location of K382 protein expression in U2OS cell lines for zoomed images. ....	98
<b>Figure 3. 39.</b> Histograms show relative expressions of miR-34a, b in the A549 cancer cells with or without an induced DNA damage by used 20 $\mu$ M of Etoposide for 24 hours. ....	100
<b>Figure 3. 40.</b> Bar charts show the relative miR-34a, b expression in the Mero-25 Mesothelioma cells in presence and absence of DNA damage. ....	101
<b>Figure 3. 41.</b> Histograms show the relative expression of the two members of miR-34 family (a, b) in the Mero-25 Mesothelioma cells with or without induced DNA damage. ....	102

## List of tables

<b>Table 1.</b> The miRNA family members' details. ....	55
<b>Table 2.</b> TaqMan™ microRNA Control Assay products details. ....	55
<b>Table 3.</b> Optimization conditions with the antibodies and buffers. ....	74
<b>Table 4.</b> Specification Sheet for 92 cases adapted from: <a href="http://www.biomax.us/tissue-arrays/Lung/OD-CT-RsLug04-001">http://www.biomax.us/tissue-arrays/Lung/OD-CT-RsLug04-001</a> . ....	76
<b>Table 5.</b> Supplementary table for specification Sheet for 120 cases adapted from: <a href="https://www.biomax.us/tissue-arrays/Lung/BC041115c_">https://www.biomax.us/tissue-arrays/Lung/BC041115c_</a> .....	114
<b>Table 6.</b> The relationship between the total p53 and its acetylated form protein expression and various clinicopathological features of the 202 Lung cancer patients using SPSS statistics software and Chi-square test. ....	84
<b>Table 7.</b> The correlation between each of the phosphorylated form of p53 (Ser-46) and The TTC5 protein expression with various clinicopathological features of the 202 Lung cancer patients using SPSS statistics software and Chi-square test. ....	89

**Declaration of originality**

This thesis is submitted in fulfilment of the requirements for the degree of Doctor of Philosophy.

I clarify that no part of these thesis has been submitted in support of any other degree, qualification or university.

I certify that the work reported in this thesis is the product of my own work and all the assistance received in preparing this thesis and sources have been fully acknowledged.

## **Acknowledgements**

First and before myself and all I thank **Allah** almighty for his never-ending blessings and mercy always.

There are no proper words to express my extreme grateful and appreciations to my supervisor Professor **Maria Krstic-Demonacos** for her kind support and guidance and enthusiasm. It has been a great pleasure and opportunity to work with her.

My sincere thanks and gratitude must go also to **Dr. Constantinos Demonacos** for his invaluable advices and constructive suggestions.

There is no way to express how much it meant to me to be a member of this team and work among the most supportive, inspired friends, honestly this work and these four years would be more hard and difficult without having brilliant friendship. Special thanks must go to everyone worked with me through these four years.

I cannot forget **my lovely wife, kids and parents** who went through hard times with me, cheered me up and encouraged me and for their endless patience and trust.

## List of abbreviations

μM	Micromolar
3' UTR	3 untranslated regions
A549	Adenocarcinomic human alveolar basal epithelial cells
AF-1	Activating factor-1
AF-2	Activating factor-2
ATM	Ataxia telangiectasia mutated
ATP	Adenosine triphosphate
ATR	Ataxia telangiectasia RAD 3 related
BAX	BCL2 associated protein
BCL2	B cell / lymphoma 2
B-CLL	B-chronic lymphocytic leukaemia
BRCA1	Breast cancer 1
CBP	(CAMP-Response Element Binding)-binding protein
CBP	CREBB binding protein
CCND1	Cyclin D1
CCNE2	Cyclin E2
CD44	CD44 molecule (Indian blood group)
CDK	Cyclin-dependant kinase
CDK4	Cyclin dependent kinase 4
CDK6	Cyclin dependent kinase 6
CDKI	Cyclin dependent kinase inhibitors
CDKNA1	p21
cDNA	Complementary DNA
CHEK- 1	Checkpoint kinase1
CHEK-2	Checkpoint kinase 2
Chip	Chromatin immunoprecipitation
c-MET	MET proto-oncogene, receptor tyrosine kinase
c-MYC	Transcriptional regulator Myc-like
COPD	Chronic Obstructive Pulmonary Disease
DBD	DNA binding domain

DMEM	Dulbecco`s modified Eagle`s medium
DMSO	Dimethyl Sulfoxide
DNA	Deoxyribonucleic acid
DNA-PK	DNA protein kinase
E2F3	E2F transcription factor 3
G1	Gap 1
G2	Gap 2
GADD45	Growth arrest and DNA damage
HATs	Histone acetyltransferases
HDAC	Histone deacetylase
HSF1	Heat shock protein factor 1
JMY	Junction mediating and regulatory protein, p53 co- factor
JNK	c-Jun N-terminal kinase
kDa	Kilodalton
LBD	Ligand binding domain
M phase	Mitosis
MDM2	Murine double minute 2
MDMX	Murine Double Minute X
MEFs	Mouse embryonic fibroblasts
MiRNAs	MicroRNAs
ml	Millilitre
mM	Millimolar
MPM	Malignant Pleural Mesothelioma
mRNA	Messenger ribonucleic acid
MYCN	Proto-oncogene, bHLH transcription factor
NICE	National institute for health and care excellance
NSCLC	Non-small-cell lung carcinoma
OncomiRs	Oncogenic miRNAs
p/CAF	P300/CBP-Associated Factor
P/S	Penicillin and streptomycin
P300	E1A binding protein 300

P300	Protein 300
P53	Tumour suppressor protein p53
PCR	Polymerase chain reaction
qRT PCR	Quantitative real time PCR
RNA	Ribonucleic acid
RPM	Rotation per minute
S phase	Synthesis phase
SCLC	Small cell lung cancer
SDS PAGE	Sodium dodecyl sulfate -poly acrylamide gel electrophoresis
Ser	Serine
SHG-44	Suzhou Human Glioma-44
SIRT1	Sirtuin 1
Strap	Stress responsive activator of p300
SUMO	Small ubiquitin-like modifier
Thr	Threonine
TMA	Tissue microarrays
<i>TP53</i>	P53 gene
TPR	Tetratricopeptide repeat
TTC5	Tetratricopeptide repeat domain 5
U251	p53 -mutant glioma cell line
UV	Ultraviolet

## Abstract

P53 is inactivated in around 50 % of human neoplasms and more than 26,000 somatic mutations of the p53 have reported in human cancers. P53 network is activated after cells are exposed to the DNA damage and depending on diverse conditions and type of DNA damage, p53 upregulation could lead to repression of the cell cycle progression and induction of apoptosis. Consequently, the p53 protein is considered vital to cancer progression and treatment and has been the focus of intense research. TTC5 (Tetratricopeptide repeat domain 5) or STRAP was identified as p53 cofactor and a key component of the p300/CBP (CREBB binding protein) complex. TTC5 enhances the interaction of JMY (Junction mediating and regulatory protein, p53 co- factor) and P300, leading to increase in HAT (Histone acetyltransferase) activity of P300, increase in p53 acetylation, stability and transcriptional activity.

In this study, we investigated crosstalk between the total p53, p53 phosphorylated at serine 46 (S46), p53 acetylated at lysine 382 (K382) and the TTC5 protein expression in Etoposide treated lung and mesothelioma cancer cell lines (A549, Mero-14, and Mero-25). Our results suggest there is no impact of Etoposide treatment on the TTC5 protein levels in all treated cell lines. Upregulation of p53, K382 and S46 protein expression levels as a response to the DNA damage in A549 and Mero-14 but not in Mero-25 cell lines was observed. Co-immunoprecipitation results showed evidence of the interaction between p53 protein and its co-factor (TTC5). MiRNA-34 family members that are transcriptional p53 targets were also investigated in studied cancer cell lines. Decrease in the miR-34a expression was observed in treated A549, Mero-25, and Mero-14 cancer cells compared to untreated cells, whereas the expression of miR-34b was elevated in treated A549 and Mero-25 but not in Mero-14 mesothelioma cells. We also analysed expression of above mentioned proteins in 220 tissue microarrays (TMA) in human lung cancer tissues using immunohistochemistry (IHC) approach and correlated these data with clinicopathological features of patients. Significant correlation was detected between the p53 expression levels and the grade of lung cancer, which might support the theory that mutant p53 acts as an oncoprotein. In addition, significant correlation was observed between the TTC5 protein expression and age, grade, tumour size and the intensity of Ser-46 protein expression. Interestingly, some cases showed cytoplasmic staining of acetylated p53 at lysine 382 rather than nuclear staining.

Immunofluorescence (IF) was used to demonstrate a nuclear staining of the K382 protein in A549 and U2OS cell lines, suggesting that cultured cancer cells might behave differently and/or that in patients tissues there is heterogeneity of K382 subcellular location. Overall, our results indicate that p53 isoforms analysis together with TTC5 expression might have future use as biomarkers, prognostic factors or drug targets in cancer. However, further research is needed to confirm these findings.

## Chapter 1. Introduction

### 1.1 Cancer

The most straightforward definition of cancer refers to the condition as abnormal cell growth occurring due to alterations in gene expression and modified cellular functions, which lead to the deregulated balance between the cell growth and the death. This process can lead to the generation of a population of cells that form a tumour, spread to neighbouring tissues and throughout the body to other organs; therefore, inducing significant morbidity and death of the patient if the condition is left untreated (Salwiczek *et al.*, 2009).

Cancer hallmarks include sustaining of signalling mediated proliferation, angiogenesis, rejecting cell death programme, evading growth suppressors, permitting replicative immortality, and triggering invasion while spreading to other parts of the body organs (Hanahan & Weinberg, 2011). Tumour cells display a standard set of characteristics, which include the ability of unlimited cells division, resisting apoptotic and anti-proliferative signals, and autonomy in growth signals. Additionally, cancer cells need support from surrounding tissues, to build fresh blood vessels that aid in obtaining oxygen and nutrients, avoid detection by the immune system, and eventually spread to other organs and body tissues (Pepperberg, 2004). Cancer has these properties because of the genetic changes that include the gain-of-function mutation, amplification, and critical oncogenes overexpression together with or without mutations leading to epigenetic inhibition of crucial tumour suppressors, genetics deletion, and altered function (Zorina, 2005). Tumour cells gain these phenotypes by altering and reactivating numerous existing programs in the cell itself usually used through development, which coordinates processes for instance cells division and proliferation, migration, cell death, and differentiation throughout embryogenesis and tissue homeostasis. Tumour cells arise from epigenetic variations and random mutations that alter cellular functions, followed by the clonal selection of tumour cells, which can continue growing, survival and dividing under some conditions that would generally be deleterious (Luo *et al.*, 2009). Though many of oncogenes and tumour suppressors, like Rb, p53, and p16, are commonly mutated in tumour cells, it is also evident that numerous low-frequency variations can add to oncogenesis (Luo *et al.*, 2009).

Cancer has been considered as one of the main causes of deaths globally. World Health Organization reported, "Cancer is amongst the highest cause of mortality and morbidity globally, with about fourteen million fresh cases and eight million deaths attributed to cancer in 2012" (WHO, 2015). In the next two decades, the number of new cancer cases is expected to reach twenty-two million per year. Furthermore, predictions indicate that in the next 2 decades, cancer deaths are going to rise from about eight million to thirteen million per year (WHO, 2014). In the United Kingdom, cancer is a leading cause of death and it only comes second to cardiovascular diseases. More than three hundred and twenty-four thousand patients were diagnosed with cancer in 2010 (Cancer Research UK, 2013). Additionally, according to Cancer Research UK report, there were about one hundred and sixty-one deaths in 2012 from cancer in the United Kingdom, which means one hundred and sixty-eight people per one hundred thousand people (Longo *et al.*, 2012).

### **1.1.1 Lung Cancer**

Generally, Lung cancer is defined as lung carcinoma or pulmonary carcinoma, which is a malignant tumour characterised by uncontrolled cell multiplication and tissue growth in the lungs. Globally, lung cancer leads regarding deaths and cancer incidences. Only fifteen percent of lung cancer patients are diagnosed at an early phase, and the five-year survival rate is about fifty percent for cases detected when cancer did not metastasise to distal organs. Most tumours that grow in the lungs are referred to as primary lung cancers, and they are malignant tumours derived from epithelial tissues (Collins *et al.*, 2007). The World Cancer Report 2014 indicated that lung cancer was the most common cancers diagnosed in 2012 making 13.0% of the total (1.8 million cases), followed by breast cancer 11.9% (1.7 million) and 9.7% (1.4 million) for large bowel cancer.

Moreover, lung cancer was also described as the most common cause of cancer death comprising 19.4% of the total (1.6 million), 9.1% (0.8 million) for liver cancer and then stomach cancer 8.8% (0.7 million) of the total (WHO, 2014). Smoking is linked to ninety percent of lung cancer cases, and it is regarded as the primary cause of lung cancer (Collins *et al.*, 2007). Only 10–15% of lung cancer is found in non-smokers, causes are often

attributed to a combination of air pollution including radon gas, asbestos, second-hand smoke, and genetic elements (Emery & Clayton, 2009). Histologically, lung cancer can be categorised into two types based on its appearance, which are small cell lung cancer (SCLC) and non-small cell lung cancer (NSCLC). SCLC makes up about 20% to 25% of lung cancers (Collins *et al.*, 2007).

In the United Kingdom, National Institute for Health Care Excellence showed that new patients of lung cancer are more than thirty-nine thousand each year while about thirty-five thousand deaths are attributed to this condition; therefore, having a more substantial effect than colorectal and breast cancer combined. Furthermore, due to an increase in the number of women smokers, lung cancer has become the leading cause of cancer death in women. On the other hand, there is a decrease of deaths for men by more than a quarter (27% reduction between 1971 and 2006) because of the reduced number of smoking men (NICE, 2011). Fig.1. 1. shows the cancer mortality in the UK for 2012.

In the United States, it has been established that lung cancer is the main cause of cancer-related deaths. It caused over one hundred and fifty-eight thousand deaths in 2006, which were more than the deaths caused by breast, colorectal, and prostate cancers combined (Salwiczek *et al.*, 2009).



**Figure 1. 1.** Cancer mortality in UK for 2012

Adopted from: <http://www.cancerresearchuk.org/health-professional/cancer-statistics/mortality>

Each year more than a million new patients of lung cancer are diagnosed in the world (Tokino & Nakamura, 2000), and around eighty percent of the lung cancer involve non-small cell lung cancer, which includes large cell carcinomas, adenocarcinomas, and squamous cell carcinoma. Several cases are diagnosed with advanced stages of the disease and as a

consequence, five years' survival across all stages of disease is only about 14% (Suzuki & Matsubara, 2011). Kandoth et al. (2013) indicate that surgery is still considered the best treatment strategy, however potentially curative resection is appropriate for only around twenty-five percent of non-small cell lung cancer (Kandoth *et al.*, 2013).

### **1.1.2 Malignant pleural mesothelioma**

Mesothelioma, also called malignant pleural mesothelioma (MPM) refers to a rare tumour originating from the pleural mesothelium cells and is an aggressive disease with poor diagnosis (Peto *et al.*, 1999). Usually, malignant pleural mesothelioma is linked to the history of long-lasting asbestos exposure. MPM is a disease that has created numerous legal issues and consequently has resulted in the elimination of asbestos usage in the industrial areas, mainly in construction and shipping in individual countries (Ismail-Khan *et al.*, 2006). The first observation of malignant mesothelioma was in 1870 (Wagner *et al.*, 1960), and asbestos connection to the mesothelioma was discovered at the beginning of 1960 in South Africa when the report was published about the link between MPM and both incidental and occupational asbestos exposure (Carbone *et al.*, 2003; Robinson & Lake, 2005). In 2005, Europe prohibited the use of asbestos due to its involvement in the pathogenesis of MPM, but other developed countries including Russia (the largest producer), China, and Canada still produce large amounts of asbestos (Ismail-Khan *et al.*, 2006).

Malignant mesothelioma and lung cancer have been considered separate entities in the second half of the 20th century. Universally, the incidence of the disease is raising, which is predicted to peak in 2020 (Robinson & Lake, 2005). Approximately 2,500 patients per year in the United States are diagnosed with MPM. Besides, 5,000 patients die because of the disease in Western Europe every year (Ismail-Khan *et al.*, 2006). According to UK cancer research studies in 2013, rates of MPM incidence have increased by 497% in England since the late 1970s; also, this showed a significant increase of the rate for males than for females (Cancer Research UK, 2013), (Fig. 1. 2).

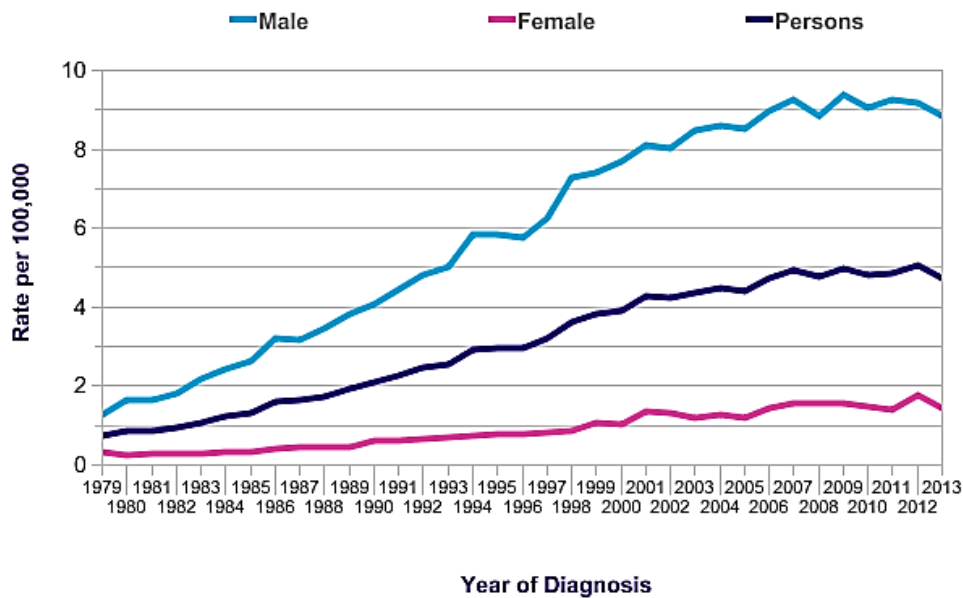


**Figure 1. 2.** Mesothelioma (C45): European Age-Standardised Incidence Rates per 100,000 Populations, by Sex, Great Britain 1979-2013

Adapted from Cancer Research UK, <http://www.cancerresearchuk.org/health-professional/cancer-statistics/statistics-by-cancer-type/mesothelioma/incidence#heading-Two> , [Accessed: 15/May/2016]

The Malignant pleural mesothelioma disease may occur thirty to forty years after exposure to asbestos, which makes diagnosis more difficult. Also, the differential diagnosis based on pleural biopsy followed by immunohistochemistry between MPM and metastasis of adenocarcinoma or benign pleural disease may be difficult in some cases (Scherpereel & Group, 2007);(Scherpereel, 2006). Experts from the European Society of Thoracic Surgeons and the European Respiratory Society recommend identification of particular immunohistochemistry markers on pleural biopsies to achieve a reliable and earlier diagnosis of Malignant pleural mesothelioma since standard staining procedures are insufficient in about ten percent of the cases (Scherpereel *et al.*, 2010). Numerous recommendations from the International Mesothelioma Panel to use the immunohistochemical method rely upon whether a mesothelioma tumour is of epithelioid or sarcomatoid subtype. The use of two markers with positive diagnostic value for mesothelioma is recommended in distinguishing between adenocarcinoma and epithelioid mesothelioma. For diagnosis of epithelioid mesothelioma, it is recommended to use nuclear

markers like anti-Wilms tumour antigen-1 and anti-calretinin, and membrane marker like anti-epithelial membrane antigen (EMA). On the other hand, it is recommended to utilise two markers with negative predictive value (like anti-S100, anti-B-cell lymphoma two markers, anti-CD34, and anti-desmin,) and two broad-spectrum anti-cytokeratin antibodies to establish the diagnosis (Scherpereel *et al.*, 2010).

## **1.2 P53 tumour suppressor**

### **1.2.1 P53 roles**

In 1979, the p53 gene was identified as the first neoplasm-suppressor gene. At first, the p53 was perceived as an oncogene; however, later it was realised that it was a tumour suppressor based on genetic and functional data. In around fifty percent of human neoplasms, p53 is inactivated resulting from the gene mutations (Jen & Wu, 2008).

Over 26,000 somatic mutations of the p53 are recorded in human cancers (Kandoth *et al.*, 2013). When mutations cause loss of function, this can fail suppressive activities with deregulation of linked pathways that control cellular senescence, apoptosis, and cell cycle. As a result, the p53 protein is considered vital to cancer progression and as such has been the focus of extensive research for the p53 role in both tumour development and new treatments (Lane *et al.*, 2010). Cancer is characterized by a pathological appearance of uncontrolled cell proliferation; therefore, the understanding of the fundamental rules of cell cycle control is expected to lead to effective cancer treatments (Asghar *et al.*, 2015).

The p53 network is usually off and only reactivated when cells are stressed or exposed to the DNA damage. Upregulation of p53 expression could inhibit the proliferation of stressed cells, and repress the cell cycle progression. Depending on diverse conditions, p53 can also induce apoptosis to control the damage. Consequently, p53 protein acts as a significant brake on tumour advancement, so that could serve as the reason why the protein is often mutated or deactivated in cancer (Jen & Wu, 2008).

The p53's capability to prevent cell multiplication via blocking cell cycle development, and facilitating repair of damaged DNA or activating apoptotic cell death allows this protein to inhibit cancer cell growth; thus, preventing cancer development. Activation of p53 is controlled through a broad range of stress signals including hypoxia, activation of oncogenes, loss of standard cell contacts, and genotoxic damage (Vousden & Prives, 2009).

Although the p53 functions of suppressing tumours have been identified, its contribution to several features of the disease and healthy life (metabolism) has only been appreciated recently. P53's vast array of responses are reflected via a different mechanism through which p53 functions, though to trigger transcription capability remains essential to p53's pathway. When determining which response of p53 is activated, it is vital to control p53's transcriptional activity. This has been used to develop the next generation of drugs which can be selectively used to activate or inhibit p53 (Vousden & Prives, 2009). Principally, sequence specific transcription factors' proteins like op53 act through binding to DNA-regulatory sequences of the target genes that could be enhancers and silencers leading to activation or repression of transcription respectively. Through this process, transcription factors raise or decrease gene transcription (Barnes *et al.*, 2009).

### **1. 2. 2. P53 structure**

Human's p53 protein consists of 393 amino acids and involves various functional domains: proline-rich and N-terminus transactivation domains, followed by the central core DNA-binding domain, and lastly the C-terminus-regulatory domain (Fig. 1.3). Most of the mutations in more than fifty percent human tumours are found in the central core DNA-binding domain (Emery & Clayton, 2009). The p53 gene is situated on the short arm of the chromosome 17. p. 13, and it is encoded by 20 kb gene with ten introns and 11 exons. It is a nuclear protein that contains five essential functional domains, which is mediating interactions. Both the proline-rich domain (64–91 residues) and the C-terminal domain (364–393 residues) are vital for activating the apoptosis network, whereas the N-terminal domain (1-43 residues) with the two adjacent transactivation domains, (TAD1 and TAD2) includes the majority of phosphorylation sites (Zhu *et al.*, 2000). The TAD2 joins the proline-

rich domain and plays vital roles in transcriptional activation, repression, and apoptosis (Lin *et al.* 1994).

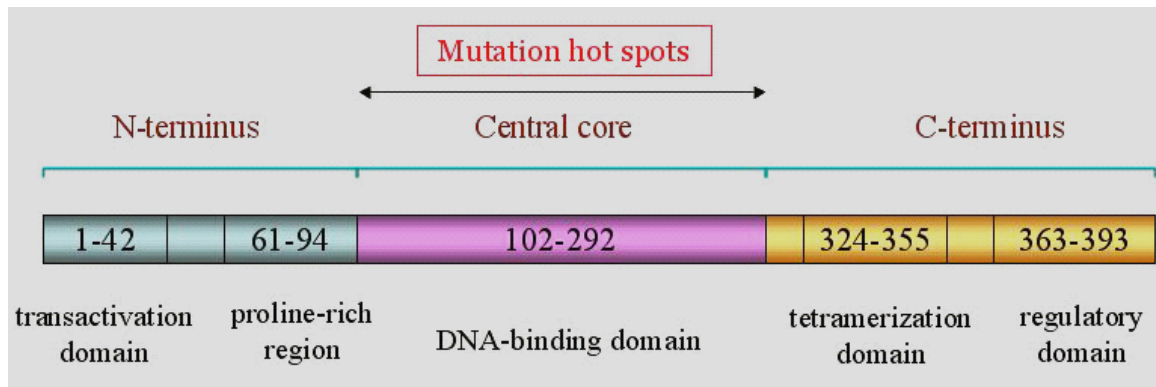


**Figure. 1. 3:** Schematic representation of the p53 structure (Bai & Zhu, 2006).

Adapted from: <http://www.surescreen.com/lifesciences/pdf/p53-forms%26function.pdf>

### 1. 2. 3 Levels of control of p53 activity

#### 1. 2. 3. 1 P53: Posttranslational modifications

Regulation of P53's activity and specificity can be done by determining the proteins that can bind to various domains of p53. When it comes to downstream signalling, the involvement of numerous series of genes is required to activate the process via p53 trans-activating attributes. This can be achieved via particular DNA binding of p53 protein to p53's response element (p53 RE), which are DNA sequences located in regulatory regions of target genes (El-Deiry, 1992;) (Tokino & Nakamura, 2000)

Comprehensive research has determined several post-translational modifications with the function of each one connected to a particular role of p53. For instance, phosphorylation and acetylation of P53 have been suggested to modulate expression of p53 transcriptional targets. Other modifications involving, neddylation, sumoylation, and ubiquitination, have been linked to p53's nuclear export, protein stability, and suppression of p53-mediated transcription (Lee & Gu, 2010). Specifically, methylation has been demonstrated to be linked with both the enhancement and repression of p53 role, according to the particular location of methylation (Scoumanne & Chen, 2008). Various modifications from these have been shown to affect p53's lysine residues, showing complicated regulation of p53. P53's

ubiquitynation has been noted to control the localization and stability of p53, and perhaps is the master regulator of cellular senescence, cell proliferation, or cell death (Lee & Gu, 2010).

#### 1.2.3.1.1 Protein phosphorylation

P53 protein has a crucial function in DNA damage, cellular stress response signalling, and other genomic aberrancies. Through posttranslational modifications, the p53 can be activated, thus, leading to DNA repair or apoptosis or cell cycle arrest (Chehab *et al.*, 1999). Phosphate groups can be added to a specific serine and threonine residues at the N-terminal transactivation region. Phosphorylation of p53 protein elevates the protein levels and increases the affinity of protein-protein interaction (Jenkins *et al.*, 2012). P53 phosphorylation at the transactivation domain results in p53 stabilization and activation (Ohki *et al.*, 2007). In contrast, ubiquitination leads to destabilization and protein degradation (Berger, 2010). Many p53 residues can be phosphorylated *in vivo* and different protein kinases can phosphorylate the p53 protein *in vitro* (Levine, 1997; Meek, 1994) (Fig. 3).

Phospho-p53 at Ser15 or Ser20 during the DNA damage results in inhibition of p53- MDM2 interaction and elevating p53 levels. MDM2 represses the p53 expression levels through ubiquitination process leading to its degradation via S26 proteasome proteins (Milczarek *et al.*, 1996) (Figure 1.4). P53 phosphorylate by protein kinases ATR (ataxia telangiectasia-related), DNA-PK (DNA-dependent protein kinase), and ATM (ataxia telangiectasia mutated) at Ser-37 and Ser-15 leads to increase the activation and accumulation of p53 in response to stress signalling and DNA damage (Milczarek *et al.*, 1996; Tibbetts *et al.*, 1999). Furthermore, Chk2 and Chk1 phosphorylate p53 protein at Ser20, supporting its stability and transcriptional activity of the protein (Hirao *et al.*, 2000). In addition, phosphorylation of p53 at Ser46 can increase the ability of p53 to induce apoptosis (Knippschild *et al.*, 1997). Numerous protein kinases can induce the phosphorylation of p53 at serine 46 including homeodomain interacting protein kinase 2 (HIPK2) (Hofmann *et al.*, 2002), ataxia-telangiectasia mutated (ATM) (Kodama *et al.*, 2010), and p38 mitogen-activated protein kinase (p38 MAPK) (Perfettini *et al.*, 2005). This important modification was proposed to

participate in the apoptotic target genes selectivity, like the p53 apoptosis inducing protein 1 (p53AIP1) as DNA damage response (Oda *et al.*, 2000). Previous study showed that S46 was significantly increased in Etoposide treated U2OS cells, and binding to variety of direct transcriptional target genes involved in apoptosis induction (Smeenk *et al.*, 2011).

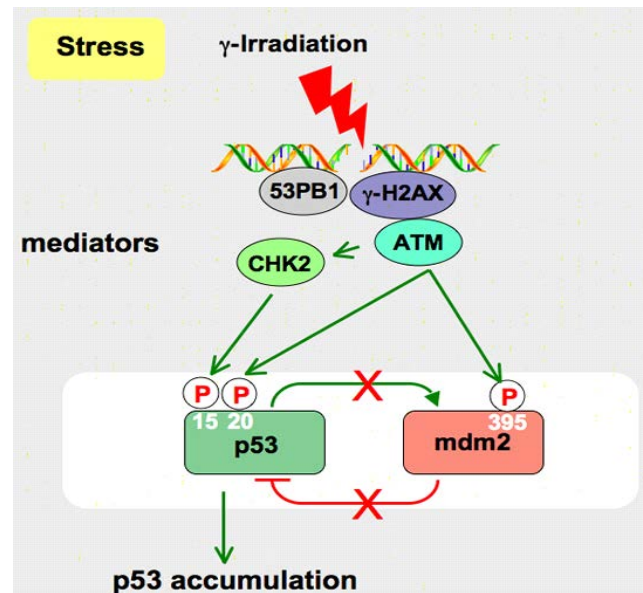


**Figure 1. 4:** P53 pathway: Phosphorylation of p53 and mdm2 disrupt the interaction between the two proteins. Adapted from: [http://p53.free.fr/p53\\_info/p53\\_Pathways.html](http://p53.free.fr/p53_info/p53_Pathways.html)

### 1. 2. 3. 1. 2. Acetylation

Acetylation is one of the posttranslational modifications that is extensively studied, and the process can be defined as “adding an acetyl group to the ε- amino group of the lysine residues presents within nonhistone and histone proteins” (Glozak *et al.*, 2005). The process involves mediation by the histone acetyltransferase enzymes (HATs), which also target non-histone proteins and are called K-acetyltransferases (KATs) (Allis *et al.*, 2007). The acetyl group could be removed through the process histone deacetylation mediated by histone deacetylase enzymes (HDACs). Histone tails acetylation reduces their net positive charge (Rajendran *et al.*, 2011), thus decreasing the ability of chromatin-binding to DNA, that can make it more accessible to the transcription initiation complexes and the RNA polymerase (Clayton *et al.*, 2006; Jenuwein & Allis, 2001). Regulation of gene transcription is a multifactorial process including numerous posttranslational modifications of histone and

non-histone proteins (Rajendran *et al.*, 2011). Generally, histone tails acetylation is linked to gene expression activation whereas deacetylation is associated with gene expression inhibition (Shahbazian & Grunstein, 2007). The histone acetyltransferases p300 and CBP play a vital role in p53 acetylation at many C-terminal lysines involving K382, K381, K373, K372, and K370 (Gu & Roeder, 1997). The vital study illustrated that the S46 phosphorylation of p53 mediated by HIPK2 is required for efficient p300-p53 co-recruitment onto apoptotic genes' promoters after cellular exposure to DNA damage, resulting in acetylation of the p53 at lysine 382 and ultimately leading to apoptosis, (Puca *et al.*, 2009).

### **1. 2. 3. 1. 3. Ubiquitination**

P53 function is controlled at several levels including the regulation of p53 stability. Tsvetkov *et al.* (2010) indicate that p53 degradation has been studied intensively and turned into a model for examining 26S ubiquitin-dependent proteasome degradation (Tsvetkov *et al.*, 2010). Generally, to determine the p53 protein level in cells, the ratio of degradation and synthesis of that protein needs to be determined. This degradation proceeds through an ubiquitin-mediated proteolysis process. Ubiquitin refers to a small protein, which binds covalently to proteins like the p53 protein leading to its degradation. The ubiquitin chain marks p53 for the protein degradation (Vogelstein *et al.*, 2000). Ubiquitination process involves three enzymes: (E1) ubiquitin-activating enzymes, (E2s) ubiquitin-conjugating enzymes, and (E3s) ubiquitin ligase enzymes. The enzymes often lead to monoubiquitination by catalysing the establishment of an isopeptide bond among a common substrate lysine and the C terminus of ubiquitin (Komander & Rape, 2012). MDM2 protein is among the enzymes needed in targeting p53 with ubiquitin, and the process is referred to as a feedback loop. P53 protein can regulate the transcription of MDM2 protein by binding to the regulatory region of the MDM2 gene, which leads to stimulation of the gene's transcription, hence increasing the MDM2 levels. The increase in MDM2 protein levels leads to increase of its p53 binding and stimulates addition of ubiquitin groups to p53, and then degradation. Degradation process leads to a decrease in the level of p53 followed by a decrease in transcription of the MDM2 gene, ending feedback loop, and permitting the p53 levels to increase again (Vogelstein *et al.*, 2000). Various particular E3 ubiquitin ligases have been described to polyubiquitinate and bind p53, leading to degradation by the 26S proteasome

(Tsvetkov *et al.*, 2010). Through determination of crystal structure of MDM2 in complex with a p53 it was suggested that p53's residues 15–29 are critical in binding to MDM2 (Nagata *et al.*, 2014).

#### **1.2.4 P53- MDM2 Relationship**

Fakharzadeh *et al.* (1991) show that Mdm2 was identified in mice cells as being gene-amplified on double-minute chromosomes (Fakharzadeh *et al.*, 1991). Human Mdm2 protein comprises four hundred and ninety-one amino acids and four regions defined on Mdm2 include: a zinc finger region at the central part of the protein, an acidic region, a binding site region for p53 at the N terminus, and a RING finger region situated at the C terminus (Marine *et al.*, 2007; Wade *et al.*, 2010). The latter, which comprises of Mdm2's RING finger region functions as a binding site with MdmX, and functions as the ubiquitin ligase activity (Manfredi, 2010).

Through two essential mechanisms, MDM2 protein interacts with p53, the tumour suppressor protein; thus, negatively regulating the p53. Firstly, Mdm2 binds directly to p53's N-terminal end, hence inhibiting the transcriptional activation function of p53 (Momand *et al.*, 1992); (Oliner *et al.*, 1993). Secondly, Mdm2 possesses ubiquitin ligase activity of E3, which targets p53 for modification and then degradation by the 26S proteasome (Manfredi, 2010).

P53 can be mono and polyubiquitinated. MDM2 high levels could induce p53 polyubiquitination and lead to degradation, with co-factors such as CBP/p300 mediating this process. Whereas, lower levels of MDM2 induce mono ubiquitination leading to p53 nuclear exportation and cytoplasmic translocation (Brooks & Gu, 2006). Transcriptionally, MDM2 protein expression is regulated by p53 through an autoregulatory feedback loop. This regulation is achieved via direct MDM2 transcriptional activation by p53, thus maintaining adequate levels of its negative regulator (Wu *et al.*, 1993).

### 1.2.5 P53 cofactors

Growth arrest or apoptosis occurs when stress signals cause DNA damage, hence activating DNA damage response. Zhou and Elledge, (2000) mention that DNA damage activates PI3 kinase like Chk1 and Chk2, ATR, and ATM, which promote a signalling cascade that eventually leads to activation of different responsive proteins like p53. One of the most significant tumour suppressor proteins is p53, which has crucial roles in response to DNA change and the cell cycle checkpoints. Xu and La Thangue (2008) also indicate that some forms of environmental stress, for instance, oxidative stress, chemical stressors, and heat shock, can contribute to the cellular response by accelerating the process of synthesising chaperone proteins, which are defined as heat shock proteins. (Xu & La Thangue, 2008). Nevertheless, transcription factors need a multiplicity of additional co-factors and co-activators to coordinate and ensure successful transcription. CBP/ P300 are an essential example of a coactivator that interacts with a wide range of transcription factors. Furthermore, it possesses several types of enzyme activity, such as acetyltransferase (Chan & La Thangue, 2001). By interacting with transcription factors, P300/CBP can acetylate target proteins found in the local chromatin granule environment. Junction-mediating and regulatory protein (JMY) is a co-factor that interacts with CBP/P300 by inducing activities specific transcription factors, such as p53. Stress-responsive activator of p300 (Strap) is another example of a transcription co-factor, which interacts with Junction-mediating and regulatory protein (JMY) while also included in complex with JMY and p300. (Demonacos *et al.*, 2001).

### 1.2.6 P53 - TTC5 crosstalk

In 2001, TTC5 the tetratricopeptide motif five was firstly identified and also was named Strap, which means stress responsive activator of p300. Demonacos *et al.* (2001) showed that Strap is an essential element of CBP/p300 complex, which is created on p53 as a reaction to stress signalling (Demonacos *et al.*, 2001). For all purposes in this report, this protein will be referred to as TTC5. TTC5 consists of four hundred and forty amino acids in humans, and the protein was observed to be made up of six TPR motifs (Adams *et al.*,

2008). The TTC5 structure consists of a domain with an unexpected binding made up of oligosaccharide/oligonucleotide besides the having an atypical or irregular six tetratricopeptide repeat (TPR) motifs (Adams *et al.*, 2012). It is reported that a tetratricopeptide repeat (TPR) motif protein has vital functions regarding heat-shock responses and DNA damage. In the first place, TTC5 was observed in a complex that included a histone acetyltransferase (HAT), an EP300-interacting protein, which was recognised as JMY (junction mediating and regulatory protein), and the EP300 (p300, an E1A-binding protein p300). Demonacos *et al.* (2001) state that TTC5 increases interaction between JMY and EP300; therefore, resulting in heightened HAT activity of EP300, which increases p53's acetylation, stability, and transcriptional processes throughout the DNA damage responses (Demonacos *et al.*, 2001). It was also observed that TTC5 protein had two phosphorylation sites for checkpoint kinase 2 (CHK2) and ataxia telangiectasia mutated (ATM) (Adams *et al.*, 2008). ATM phosphorylates TTC5 at S203 while Chk2 phosphorylates TTC5 at S221; therefore, leading to an increase in its stability and nuclear accumulation, hence the p53 activity (Demonacos *et al.*, 2004). Upon DNA damage- TTC5 is phosphorylated and activated, hence stimulating p53 acetylation by employing JMY/p300, which later on lead to increase in p53-dependent apoptosis (Fig.1.5), (Coutts & La Thangue, 2005). Moreover, TTC5 increases the response of p53 by down-regulation of Mdm2's activity (Demonacos *et al.*, 2004). TTC5 stability is increased through DNA-damage resulting from phosphorylation by the DNA damage responsive protein kinases, Chk2 and ATM, and accumulates in the nucleus (Adams *et al.*, 2008). Several studies are supporting the importance of TTC5 in mediating an adequate stress response (Adams *et al.*, 2008; Demonacos *et al.*, 2001; Xu & La Thangue, 2008).

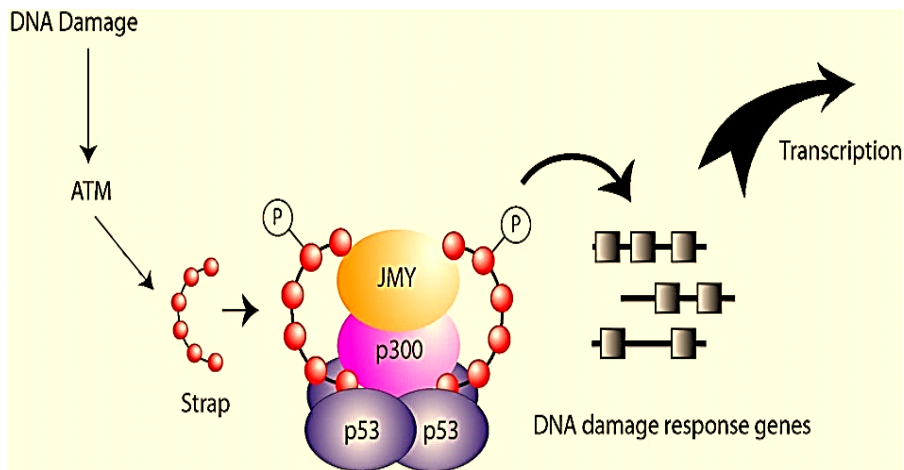


**Figure. 1. 5.** Role of JMYP and Strap in the p53 response. Model summarising the role of Strap in linking ATM kinase with the DNA damage response (Coutts & La Thangue, 2005).

### 1.2.7 P53 pathways

P53 is a significant tumour suppressor whose importance is indicated by showing increasing functions for p53 including the ability to regulate metabolism, senescence, apoptosis, DNA repair, cell cycle progression, and the recently reported tasks in differentiation and fertility. Vousden and Prives (2009) indicate that p53 also determines the expression of different genes, which mediate the p53 response while serving as a transcription factor (Vousden & Prives, 2009). Vogelstein et al. (2000) suggested that P53 networks can be activated using at least three independent metabolic pathways (Vogelstein *et al.*, 2000).

Firstly, a pathway can be induced through DNA damage, for instance, inducing through ionizing radiation. P53 network activation depends on two protein kinases that provide other proteins with phosphate groups. These two proteins are ataxia telangiectasia mutated (ATM), which is activated via double-strand DNA breaks; and checkpoint kinase 2 (Chk2), which is stimulated through ATM (Jen & Wu, 2008).

Secondly, the other pathway is activated via growth signals that are aberrant, for instance, growth signals originating from the expression of the oncogenes Ras or Myc. p53 network activation in this pathway relies upon a protein known as p14ARF.

Thirdly, the last pathway is brought about by protein-kinase inhibitors, chemotherapeutic drugs, and ultraviolet light. This pathway differs from the others as it does not depend on Chk2 genes, ATM, or intact p14ARF, but instead includes other kinases referred to as casein kinase II, and Ataxia Telangiectasia Related (ATR) (Fig. 1. 6).

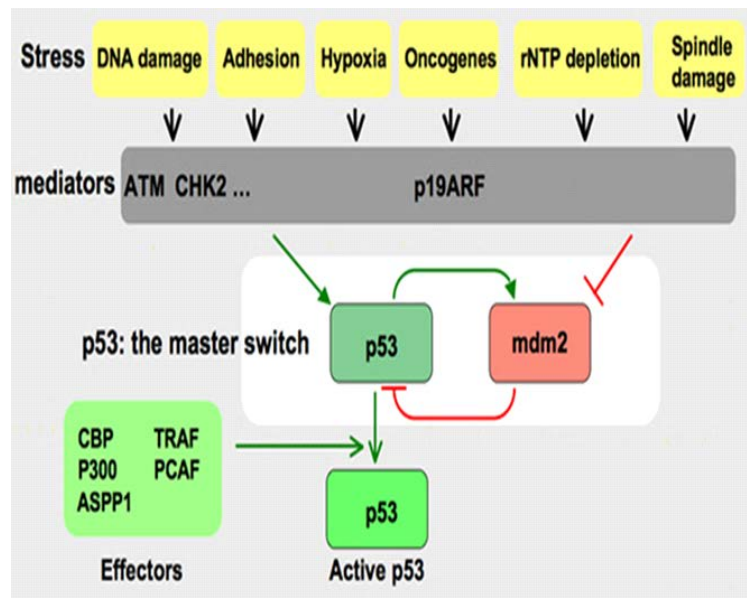


**Figure. 1. 6:** P53 pathway: Upstream pathway. i) The stress signals that activate the pathway. ii) The upstream mediators that detect and interpret the upstream signals. iii) The core regulation of p53 through its interaction with several proteins that modulate its stability. Adapted from: [http://p53.free.fr/p53\\_info/p53\\_Pathways.html](http://p53.free.fr/p53_info/p53_Pathways.html)

These pathways prevent p53 protein's degradation and increase its stability. The increase in the p53 levels allows the protein to perform its vital function through binding to specifically targeted genes and activate their expression (Jen & Wu, 2008). P53's quantitative and qualitative roles generally depend upon the level of p53, integrity, in addition to its posttranslational modifications which are induced by activating various stress-induced signalling pathways. Lacroix et al. (2006) report that the results indicate different association patterns between p53 and numerous different co-regulatory protein, which could be cell or tissue-type-specific (Lacroix *et al.*, 2006).

According to Levine et al. (2006), the pathways of p53 have been categorised into five sections:

- a) Stress signals, which trigger p53 pathway

- b) Upstream mediators with functions of detecting and interpreting upstream signals.
- c) p53's central regulation and the interaction with various proteins that regulate its stability.
- d) The downstream actions, mostly activation of transcription or protein-protein interactions.
- e) The outcomes, apoptosis or DNA repair, or cell cycle arrest (Levine *et al.*, 2006).

Vousden and Lu (2002) state that depending on the stress type, the final result of the activation of p53 is also apoptosis or DNA repair and growth arrest; nevertheless, the mechanism controlling the alternative between the events is yet to be clarified. "However, in spite of this great attempt, people still have a lot to learn, and p53 is an area of study that is expanding fast and highly dynamic" (Vousden & Prives, 2009).

#### 1.2.7.1 Cell Cycle arrest

The cell cycle includes G<sub>0</sub>, G<sub>1</sub>, G<sub>2</sub>, M, and S phases. S represents the phase where DNA synthesis takes place, and cell replicates the genetic material; M represents mitosis phase where the nucleus undergoes division succeeded by cytokinesis or cell division; in gap phase, G<sub>0</sub> cells stop dividing and in G<sub>1</sub> increase in cell size RNA production and protein synthesis takes place. In G<sub>2</sub>, there is an increase in the protein production and checkpoint for the genetic material errors before the mitosis. In response to numerous stresses like DNA damage, the division of cells may go through growth arrest at the different checkpoints to prevent the mutation of the DNA and stop the replication process. To ensure reliability and accuracy of cell division throughout each phase, checkpoints are vital stages before proceeding to replication. Several checkpoints are regulated by various cyclins, CDKs (Cyclin-dependent kinases) and their inhibitors, CDKIs (Cyclin-dependent kinase inhibitors) (Li *et al.*, 2013). Negative modulators of the cell cycle, CDKIs constitute two families; KIP/CIP (p21<sup>Cip1</sup>, p27<sup>Kip1</sup>, and p57<sup>Kip1</sup>), and the INK4 family (p16<sup>Ink4a</sup>, p15<sup>Ink4b</sup>, p18<sup>Ink4c</sup>, and p19<sup>Ink4d</sup>) While responding to DNA damage, p53 trans-activates the downstream effectors to induce cell

cycle arrest (Li *et al.*, 2013). ATM/ATR pathway was reported to be being essential for the activation of p53 and that is followed by promoting the expression of downstream target genes for G1 arrest as observed in murine embryo fibroblasts exposed to DNA damage. The p21 transactivation via p53 may inhibit CDK2/cyclin E, leaving a non-phosphorylated inactive form of RB, which in turn suppresses E2F, a G1/S phase promoting protein. Consequently, cells undergo arrest of the proliferation for repair of the DNA damage leading to failure of cell cycle completion (Dulić *et al.*, 1994).

### 1.2.7.2 Apoptosis

Kerr and his group in 1972 were the first to use the term 'apoptosis.' Kerr *et al.* (1972) state that characterisation of cells dying by apoptosis starts with cell shrinking and fragmentation of the nucleus, followed by membrane blebbing to end with cellular components separating into apoptotic bodies (Kerr *et al.*, 1972). The principle of the apoptosis is explained via two essential pathways. First, through the intrinsic pathway, the death signal originates from within the cell and includes various non-receptor-mediated stimuli generating intracellular signals that target cell components directly through mitochondrial-induced phenomena. Degterev *et al.* (2003) explain extrinsic pathway as a process that involves activating cell surface receptors using a death signal located outside the cell, and eventually, converging to activate effector caspases (Degterev *et al.*, 2003).

Extrinsic apoptotic pathway starts with stimulation to bind the tumour necrosis factor (TNF) and TNF-related apoptosis-inducing ligand (TRAIL) with their corresponding cell surface death receptors, which include Fas, TNF receptor 1 (TNFR1), TRAIL receptor 1 (TRAILR1), and TRAIL receptor 2 (TRAILR2) (Fulda & Debatin, 2006);(Lavrik *et al.*, 2005). To produce the death-inducing signalling complex (DISC), substance binds to the death receptors and activates clustering and receptor trimerisation of the intracellular cytoplasmic death domains that utilises many adaptor molecules (Fulda & Debatin, 2006);(Walczak & Krammer, 2000). To signal TRAILR1, TRAILR2 and Fas the death-inducing signalling complex (DISC) constitutes FAS-associated death domain (FADD) in addition to pro-caspase-8 while the DISC created downstream of TNFR1 signalling comprises additional molecules like TNFR-

associated factor 2 (TRAF2) and TNFR-associated death domain (TRADD) (Fulda & Debatin, 2006);(Lavrik *et al.*, 2005). DISC formation followed by pro-caspase-8 cleavage and activation transmits the signal of death, also induces mitochondria outer membrane permeabilisation (MOMP) or through activation of a protease cascade of effector caspases-3, -6 and/or -7, eventually causing cell death (Fulda *et al.*, 2002); (Scaffidi *et al.*, 1998).

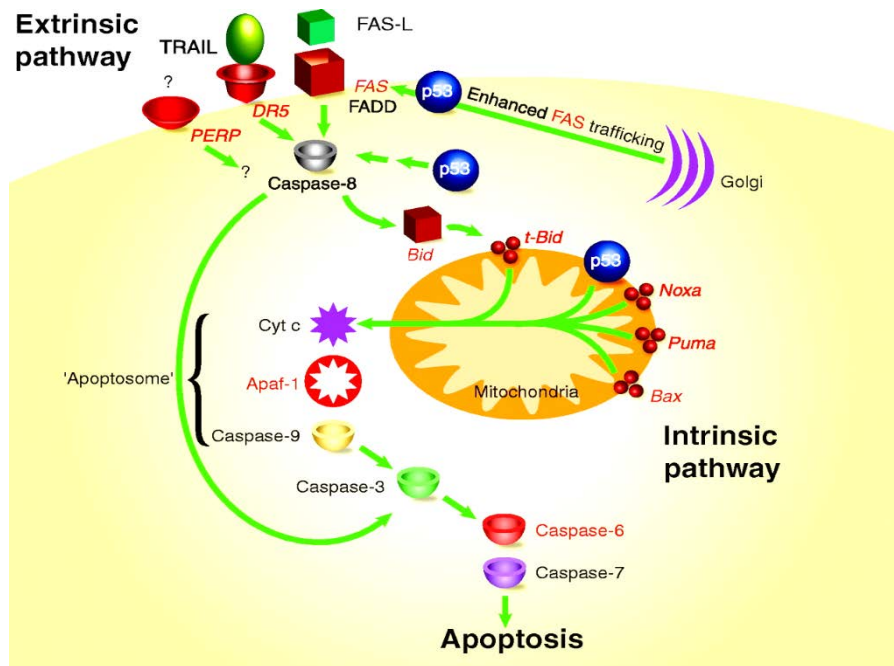


**Figure 1. 7.** A p53-mediated apoptosis model. The model illustrates the p53 involvement in the extrinsic and intrinsic apoptotic pathways (Haupt *et al.*, 2003).

Additionally, activating intrinsic apoptotic pathway is induced via different intracellular stimuli, involving growth factor-starvation, DNA damage, and oxidative stress (Mayer & Oberbauer, 2003), which leads to stimulating MOMP, producing the mitochondrial proteins that release apoptotic machinery (Hengartner, 2000); (Saelens *et al.*, 2004). From the mitochondria, cytochrome c (cyt c) that stimulates Apaf-1 oligomerisation and helps in activating caspase-9, an initiator, by forming Apaf-1, cyt c, or caspase-9 apoptosis (Long & Ryan, 2012). Caspase-9 activation leads to cleaving and activation of executioner caspases-3, -6 and/or -7, which is followed by cleavage of numerous cellular targets, like polymerase (PARP), poly (ADP-ribose), inhibitor of caspase-activated lamin and DNase, which starts the process of breaking down components of the and inducing its death (Degterev *et al.*, 2003).

Interactions among anti- and pro-apoptotic components of the B-cell lymphoma-2 (Bcl-2) family are complicated, but they control MOMP. The Bcl-2 proteins are characterized depending on their domain organisation in respect to the Bcl-2 homology:

- Pro-apoptotic effectors comprising BH1–BH3 domains (Bax, Bok, and Bak,) whose role is to execute the MOMP process directly.
- Anti-apoptotic effectors consisting of BH1–BH4 domains (A1, Bcl-XL, Bcl-w, Bcl-2, and mcl-1), which regulate and bind Bak and Bax.

BH3 only domain proteins include Noxa, BNIP3, Bid, Bim, Puma, Bad, Bik, BMF, and HRK, which are tasked with stimulating MOMP by inhibition of anti-apoptotic Bcl-2 components; thus, activating Bax and Bak, or via repressing Bak and Bax directly (Chipuk & Green, 2008); (Tait & Green, 2010).

### **1. 2. 8. P53 and the regulation of microRNAs**

Numbers of researchers have demonstrated p53 as a crucial player at the centre of a very complex molecular regulating network. As a response to cancer-related stress, p53 can promote cell cycle arrest, cell senescence, and programmed cell death through transactivation of variety of downstream genes (Oren, 2003);(Xu-Monette *et al.*, 2012). In addition to its roles for regulating the expression of different protein-coding genes as transcription factor, p53 also can transcriptionally activate non-coding genes like microRNAs (miRNAs). MiRNAs are considered as a non-coding RNAs consisting of single-stranded RNA and around ~22 nucleotides in length, which mediate post-translational silencing of number of target mRNAs via inhibition of the translation or cleaving of RNA transcripts (Filipowicz *et al.*, 2008). They have essential functions in fundamental biological processes by controlling of multiple proteins, leading to negatively regulating the gene expression (Oliveto *et al.*, 2017). MiRNAs can bind to the 3' untranslated regions (3' UTR) of the targeted mRNA (Li, Ren, *et al.*, 2014), which leads to degradation and inhibition of the translation and protein production (Bartel, 2009). Some research showed that deregulation of miRNAs expression can play important roles in the tumourigenesis and cancer progression and suggested that these discoveries could improve the patient therapeutic results with some type of cancer (Li,

Ren, *et al.*, 2014). As long hairpin molecules (pri-miRNAs), transcribed miRNAs are afterward processed over many steps, then DICER cuts them to produce duplexes of their final ~22-nucleotide length (Di Martino *et al.*, 2014). MiRNAs may inhibit the expression of the targeted genes at the transcriptional level by interact with the ribonucleoproteins and create the RNA-induced silencing complex -independent manner (Di Martino *et al.*, 2014) or by binding directly to the DNA (Kim *et al.*, 2008).

Some studies have reported that miRNAs can be classified as oncogenes or tumour suppressor genes depending on their contribution in the cancer development and progression. MiRNAs, which were highly expressed in tumour cells and participated in carcinogenesis via tumour suppressor genes inhibition have been identified as oncogenic miRNAs (Esquela-Kerscher & Slack, 2006), whereas miRNAs with low expression levels, which normally prevent the cancer development through inhibition of the oncogenes expression, were considered as a tumour suppressor miRNAs (Dimopoulos *et al.*, 2013). Growing studies illustrate that using a specific miRNAs' inhibitors for silencing OncomiRs or synthetic miRNA mimics for replacing tumour suppressor miRNAs were elucidating a beneficial experimental strategy for solid and haematological cancers treatments (Amodio *et al.*, 2012); (Di Martino *et al.*, 2013); (Raimondi *et al.*, 2014); (Leotta *et al.*, 2014).

#### **1. 2. 8. 1. MiRNA-34 family and p53 pathway**

Depending on the nature of the targeted genes, miRNAs play essential roles in carcinogenesis through affecting the functions of tumour suppressor genes or oncogenes (Esquela-Kerscher & Slack, 2006).

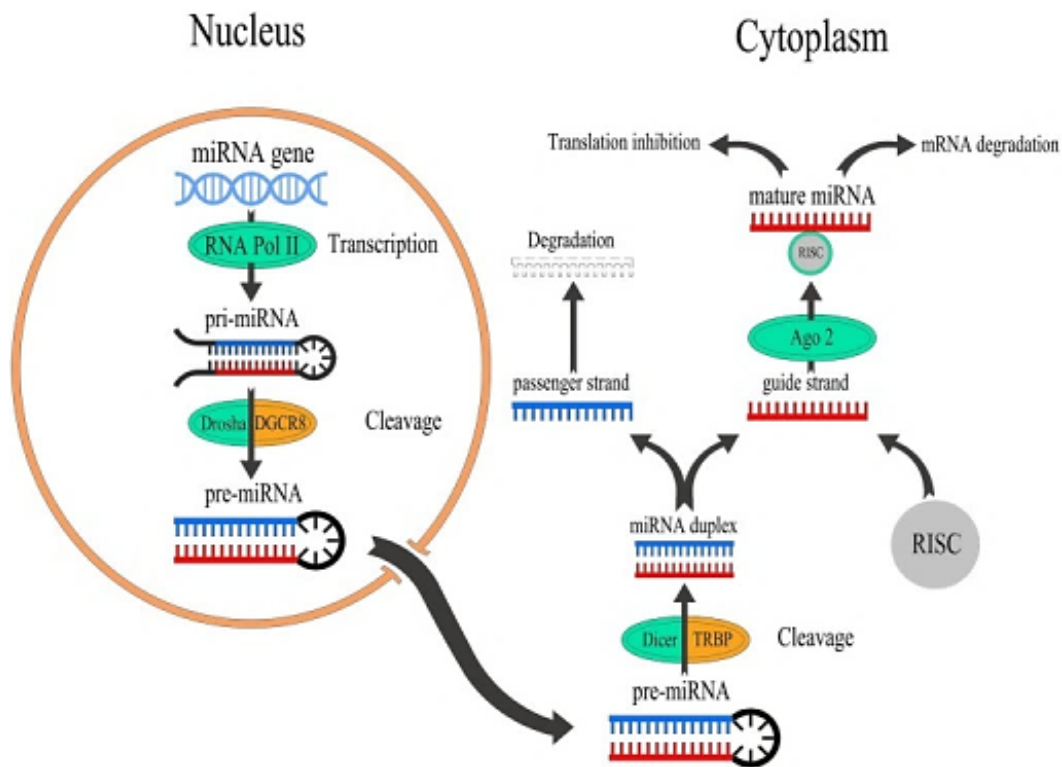


**Figure 1. 8.** Model of miRNAs biogenesis and function (Alsharafi *et al.*, 2015).

One of the important miRNAs families included in the p53 pathways is the mir-34 family, which is a direct targeted via p53 to increase their expression in response to the stress and oncogenic signals (Gallardo *et al.*, 2009). This family consists of three miRNAs members encoded by 2 different genes. MiR-34a member is encoded by its own transcript, whereas the other two members' miR-34b and c are encoded by shared common primary transcript (Antonini *et al.*, 2010). Researchers showed that ectopic expression of these family members (miR-34a, miR-34b and miR-34c) inhibits the migration and invasion, also promotes cell cycle arrest, apoptosis and cell senescence (Hermeking, 2010). MiR-34 family is involved in p53 downstream effects on cell cycle arrest and apoptosis induction, through affecting c-MYC, c-MET, and CDK6 (Misso *et al.*, 2014).

It has been illustrated that miR-34 family's promoters were frequently silenced through CpG islands methylation in variety types of cancers during the tumourigenesis suggesting their roles as tumour suppressor genes (Lodygin *et al.*, 2008); (Vogt *et al.*, 2011). Studies on the mice showed that the highest expression of miR-34a is observed in the brain, whereas, more expression of 34b and 34c was observed in the mice lung tissues (Hermeking, 2010). Downregulation of miR-34a expression has been observed in association with the status of

p53 deletion or mutation in variety types of cancers such as prostate cancers, gastric cancers, and B-CLL (B-chronic lymphocytic leukaemia) (Fujita *et al.*, 2008); (Ji *et al.*, 2008) ;(Dijkstra *et al.*, 2009). Comparison Studies on wild-type and p53-deficient mouse embryonic fibroblasts (MEFs) miRNA expression profiles suggested that miRNA-34a can be reflecting the status of p53 and is transactivated directly via p53 as a miRNA component of the p53 network (He *et al.*, 2007); (Raver-Shapira *et al.*, 2007). Luan, S et al reported that miR-34a levels are significantly decreased in p53-mutant glioma (U251) cells comparing with p53-wild type A172, SHG-44 glioma cell lines and normal brains, which is consistent with the view that miRNA-34a could reflect the status of p53 (Luan *et al.*, 2010). MiR-34a via directly targeting and repressing CD44, inhibits prostate cancer stem cells and metastasis, suggesting the role of miR-34a and CD44 in tumour progression (Liu *et al.*, 2011). Furthermore, miR-34a has been assessed in lung cancers as a replacement therapy candidate and transfected miR-34a-mimics has determined to substantially inhibit the cancer growth (Yamakuchi & Lowenstein, 2009). Several studies demonstrated that miR-34a can induce cell cycle arrest at G0/G1 and apoptosis through directing different cell cycle genes or oncogenes involving hepatocyte growth factor receptor (MET), CDK6, CDK4, E2F3, cyclin D1 (CCND1), Bcl-2, cyclin E2 (CCNE2), MYCN, and SIRT1 (He *et al.*, 2007; Sun *et al.*, 2008; Wei *et al.*, 2008). Significant cell growth inhibition was detected in transfected glioma cell line U251 with miR-34a mimics and cell cycle arrest at G0/G1 phase have been detected 48 hours after the cells were transfected. This triggers caspase-3 activation and leads to apoptotic cell death and researchers concluded that miR-34a is a powerful inhibitor of the migrative and invasive abilities of U251 cells (Luan *et al.*, 2010). It has been shown that downregulated miR-34a expression contributed to the initiation and development of cancer, and thus, it has been categorised or characterized as tumour suppressor in some types of neoplasm (Fujita *et al.*, 2008; Ji *et al.*, 2008; Li *et al.*, 2009; Yan *et al.*, 2009), while other researchers have demonstrated that in different types of cancers miR-34a was overexpressed and maintains cellular proliferation in rat Fe-NTA-induced renal carcinogenesis (Saunders & Verdin, 2007). Additionally, MiR-34a expression has been reported in association with regulation of cancer stem cells function in different type of cancer such as medulloblastoma (Stankevicius *et al.*, 2013), prostate cancer (Liu *et al.*, 2011), pancreatic (Nalls *et al.*, 2011), and glioblastoma cancer (Guessous *et al.*, 2010). Evidently, in human cancer cells with absent p53 function, certain tumour-suppressing signalling pathways can be restored by overexpression of miR-

34a through targeting and regulation of cell cycle or cell death-related genes (Luan *et al.*, 2010).

There is a suggestion that p53 acetylation status could be significant in the cancer biology and a published research illustrated that the miR-34a impact as tumour suppressor also involves an upregulation in p53 acetylation through SIRT1 downregulation (Yamakuchi *et al.*, 2008). Functionally, the acetylated-p53 (Ac-p53) and deacetylated-p53 balance could be vital for p53 tumour suppression function (Baylin & Ohm, 2006; Chen *et al.*, 2005). Moreover, recent research considered closely association between the SIRT1 protein levels and tumour progression in the malignant tissues (Jang *et al.*, 2008; Jang *et al.*, 2012; Lovaas *et al.*, 2013). The type III histone deacetylase SIRT1 (silent mating type information regulation 2 homolog 1) was first identified to have a longevity related role under cellular stress situations (Luo *et al.*, 2001; Vaziri *et al.*, 2001). It has beneficial effects in some non-tumoural disorders such as a protective role in the metabolic diseases (Lee *et al.*, 2008). SIRT1 mechanisms by promoting survival in stressed cells could have oncogenic potential and even with increased studies provided strong evidences and suggested its roles as tumour progression factor through inhibition of the tumour suppressor genes and inducing activation of numerous of oncogenes; therefore, its roles are still controversial (Lee *et al.*, 2011). The tumour suppressor protein p53 demonstrated to be of central importance in the functional roles of SIRT1, which can deacetylate and regulate p53 (Chen *et al.*, 2005; Vaziri *et al.*, 2001). As earlier reports showed that miRNA-34 family was found to be directly targeted and regulated by p53 and functioning downstream of p53 as tumour suppressor. In particular, miR-34a was illustrated to represent the status of p53 and contribute in cancers initiation and development, so we established this study to explore the role of miR-34a, b in the lung and mesothelioma cancer cell lines.

### **1. 3. Aims of the study**

The main aim of this project is to increase understanding of the p53 roles in cancer development and therapy.

In particular:

- Analysing if the p53 or its modified forms such as acetylated p53 (K382) or phosphorylated p53 at Ser15 or Ser46 correlate with the presence of TTC5 in Lung cancer and Mesothelioma cell lines and human tissues to determine if there is a link in expression of these proteins with the disease progression.
- Analysing the TTC5 cofactor interaction with Total p53 and its isoforms in Lung cancer and Mesothelioma TMA slides by using Immunohistochemistry (IHC) techniques and also if there is any significant correlation of expression of TTC5 with the clinical data of the patients.
- Analysing the expression of miR-34 family members (miR-34a, miR-34b) in the lung cancer (A549) and mesothelioma (Mero-14 and Mero-25) cell lines by using qRT-PCR technique.

## **Chapter 2. Materials and Methods**

### **2.1 Growing and maintaining cells**

#### **2.1.1 Cell lines maintenance**

Adherent human lung cancer cell lines A549 and malignant mesothelioma Mero-25, M-14 cancer cell lines (all WT p53) were maintained at 5% CO<sub>2</sub> and 37°C in the incubator (Wolf Laboratories, Galaxy S). Cell culture protocol were performed in culture cabinets (Esco Class II Biological Safety Cabinet) under sterile conditions by using 70% ethanol and Virkon spray, also using UV light for 20 minutes before starting experiment. T<sub>75</sub> cm<sup>2</sup> culture flasks were used to grow A549, Mero-25 and M-14 cell lines in Lonza Biowhittaker RPMI 1640 medium (Roswell Park Memorial Institute 1640) Lonza, Belgium) complemented with 10 % (v/v) Foetal Bovine Serum (FBS), 0.05U/ml of streptomycin and 0.05U/ml penicillin antimicrobial agents.

#### **2.1. 2 Passage of A549, Mero-25 and M-14 cell lines**

Every 2-3 days all the adherent cell lines were passaged to avoid over confluence. When cells reached 80% confluence, sub-culture of cancer cells was performed. Trypsin-Ethylenediaminetetraacetic acid (trypsin) (Sigma, UK) and Phosphate buffered saline (PBS) warmed in the water bath at 37°C for 5 minutes were used to detach the cells from the flask's surface. RPMI 1640 media was removed and cells were washed in 8 ml of sterile PBS for removal of the media and any dead cells. 1 x PBS was subsequently aspirated followed by addition of 1ml of trypsin and 3 min incubation at 37°C for detachment of adherent cells. Then Cells were removed from incubator and analysed under the microscope to be sure that all cells are detached and 7-10 ml of fresh media was added. About 2.5 ml of suspension was transferred to new flasks that contained 10 ml of fresh media and incubated at 37 °C.

#### **2.1.3 Freezing of cell lines**

Media was taken out from the fully confluent flasks followed by washing the cells in 8 ml of sterile PBS then 1 ml trypsin was added and incubated for 3 minutes in 37°C. The dislodged the cells were visualized under the microscope. 10ml of fresh media was added to each flask and transferred to two white-capped universal tubes, 5ml in each tube. By centrifugation the cells were pelleted at 2000 rpm for 1 min (Meadowrose Scientific Ltd HERMLE Z 400), 1ml PBS was added to the tube, and then centrifuged again for one minute at 2000 rpm. Finally, cells were re-suspended in 1 ml FBS/ 20% DMSO (Dimethyl Sulfoxide) solution to prevent intracellular ice crystal formation. Resultant cell suspension was quickly transferred into cryovials and stored at - 80°C for 24 hours through slow freezing process to avoid shock to cells and finally stored in liquid nitrogen -196°C.

#### **2.1.4 Thawing of the cell lines**

At 37°C cells were quickly defrosted (about 1 min) and transferred to 5ml of pre-warmed medium in the water path 37°C for recovery in T<sub>25</sub> cm<sup>2</sup> flasks. Quick thawing to avoid cells damaging during the rehydration process and prevent ice crystals within the cells. To remove DMSO, cells were centrifuged and pelleted, prior to re-suspension in RPMI 1640 medium. Later cells were moved to T<sub>75</sub> cm<sup>2</sup> flasks when 70-75 % confluence was reached.

## **2. 2 Immunoblotting**

### **2. 2. 1 Extract preparation**

Cultured cells that were 80% confluent in T<sub>75</sub> cm<sup>2</sup> flasks were treated with 20µM Etoposide (Sigma, UK) for 24 hours pre-extraction. After removing the media from the flasks, cells were washed two times with cold PBS, flasks transferred onto ice. 250µl of high salt lysis buffer (HSLB) was added to each flask (45mM Hepes, 1mM EDTA, 400mM NaCl, 5mM NaPPi, 10 % glycerol, 0.5 % IgePal; 2mM sodium orthovanadate, and 20mM β glycerol phosphate and 1 µg /ml protease inhibitor cocktail comprising pepstain A, aprotinin, 1mM DTT, leupeptin, and 1mM PMSF was freshly added. Cells were scraped and extracts collected in a new eppendorf tube (1.5 ml) and put on the rotator (Mini Labroller<sup>TM</sup>, LabnetInc) for 20 mins at

4 °C, then centrifuged (GenFuge 24D, Progen Scientific) for 20 mins at 4°C and 13,000rpm. After discarded the pellets, supernatant transferred to another Eppendorf tubes and kept on ice.

### **2.2.2 Determination of protein concentration**

Using Bio-Rad protein assay reagent protein concentration of the cells' extract was determined (Biorad), based on Bradford method. Biorad reagent was diluted 1/5 by distilled water, Biorad diluted reagent was applied to calibrate the spectrophotometer (Jenway, G305). 2 µl of the cellular extraction was mixed with the Biorad working solution and incubated at room temperature (RT) for 5 minutes before absorbance measured at 595 nm. Protein concentration was measured in duplicates and equal amount of protein calculated using the equation:

Lowest absorbance = 40 (µl)

$(\text{Lowest absorbance} * 40) / 2\text{nd lowest absorbance} = \text{extract volume } (\mu\text{l})$

This ensures samples loaded are compared on an equivalent basis. The resultant extracts were put into another fresh eppendorf tubes and 3X Sodium dodecyl sulphate sample buffer (6% SDS, 187 mM Tris, 2-Mercaptoethanol, 30% Glycerol, 0.01% bromophenol blue) were added and mixed properly before stored at -20 °C.

### **2.2.3 SDS Gel Electrophoresis**

The main use of electrophoresis techniques is to separate macromolecules depending on the molecular weight of the molecular. The polyacrylamide gel has used as a supportive medium, whereas the SDS used for denature the proteins. Throughout electrophoresis the denatured and unfolded proteins carry a negative charge and consequently migrate and move to the direction of the positive electrode upon voltage application.

### **2.2.3.1 SDS Gel preparation**

10% Resolving Gel was made by using the Biorad Mini Protean 3 apparatus. 10.74 ml dH<sub>2</sub>O, 30% Acrylamide w/0.8% bis 9.33 ml, 0.2M EDTA 0.28 ml, 10% SDS 0.28 ml, 1.5M Tris (pH 8.95) 7 ml, 10% Ammonium persulfate (APS) 157 µl and at the end 17 µl N,N,N,N-Tetramethylethylenediamine (TEMED) was mixed for running gel preparation. 500µl isopropanol was added to remove any air bubbles that could affect the quality of the gel. After solidification of the resolving gel, SDS 10% stacking gel was prepared by adding dH<sub>2</sub>O 6.73 ml, Acrylamide 1.67 ml, 1M Tris (pH 6.95) 1.25 ml, 0.2M EDTA 100 µl, 10% SDS 100 µl, 10% APS 157 µl, and the last step TEMED 17 µl was added. Immediately combs were inserted before stacking gel solidification.

### **2.2.3.2 Sample loading and running**

SDS-Gel was put into a Bio-Rad electrophoresis mini buffer tank, which then filled with 1X SDS PAGE running buffer containing 1.9M glycine, 0.25M Tris, and 30mM SDS. The comb was removed once samples were ready to load. By using heating block (TechneDri-Block, DB-2P) samples were heated at 95°C for 7-10 min before loaded. 5µl of Page Ruler protein ladder (Fermentas, UK) was loaded in the first well using a fine microsyringe, followed by the heated samples into respective wells. At 80 volts for 20 min, samples were subsequently run until samples reached the resolving gel, after that the voltage was increased to 110 volts for about 95 min.

### **2.2.3.3 Western transferring**

Transferring process was done by using western transfer apparatus (Bio-Rad, UK) filled with western transferring buffer comprising 25mM Tris-HCl, 150mM Glycine, pH 8.3, and added 20% methanol. For protein transfer, PVDF (Polyvinylidene fluoride) membranes (Millipore, UK) were applied. Before starting the transferring process, sponges, and filter paper were soaked in western transfer buffer, while PVDF membranes were soaked in methanol for 30 secs and then rinsed in western transfer buffer followed by assembly of the cassette (Fig.6.)

The cassettes were layered with sponge, filter paper, SDS gel, PVDF membranes, filter paper and sponge respectively. An ice pack and magnet piece were placed in the tank and transfer run for 1 hour at 0.4 Amp, then fresh ice pack was used and transfer run another 1 hour.

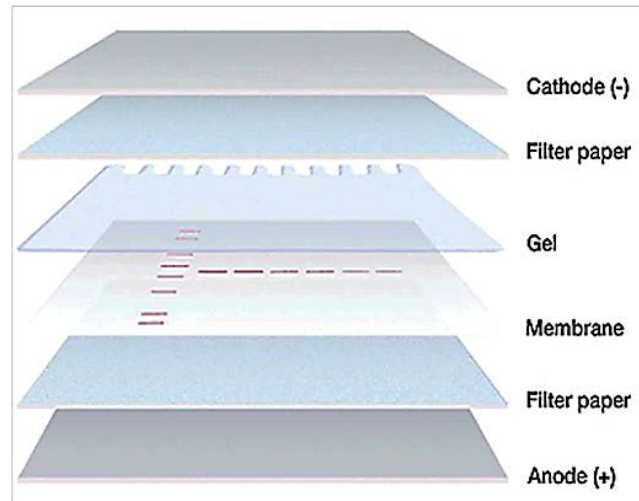


**Figure 2. 1.** The sandwich assembly for western transfer process. Adapted from Bio- Rad, UK website <http://www.bio-rad.com/en-uk/applications-technologies/protein-blotting-methods>

After the transferring process was completed, 5% dried milk in PBS was used for blocking the membrane for 1 hour at RT, followed by incubation with specific primary antibody (depending on the target protein) in 2.5% milk PBS/ included 0.1 % Tween solution put on a rotator machine overnight at 4°C. Diluted primary antibody were added as the supplier's recommendations and membranes were washed with 10ml PBS/0.1% Tween many times for to remove unbounded antibodies. Next a secondary anti – rabbit or anti – mouse IgG horseradish antibody (Amersham, GE Healthcare) prepared in 2.5 % of dried milk in PBS Tween were used for the incubation for 1 hour at Room Temperature on a shaker (Stuart Platform Rocker, STR6). Finally; membranes were washed again for at list three times at 7-10 min each time with 1X PBS Tween at Room Temperature on the Shaker prior to immuno-detection.

#### **2.2.4.4 Western blot development**

For detecting the target protein 1.5 ml of SuperSignal West Pico Chemiluminescent Substrate (ThermoScientific, USA) was applied for 2-3 min at Room Temperature to the membranes and then the membrane was exposed using X ray films (Fujifilm, UK) then

developed by using an X-ray film processor (AFP). To detect low levels of protein 1 ml of SuperSignal™ West Femto Maximum Sensitivity Substrate (ThermoScientific, UK) was used for 30 seconds at RT to the membranes and the bands were detected as above.

#### **2.2.3.4 Stripping of the membrane**

This process was performed to remove the antibodies and the detection materials on the membrane surface. Stripping buffer was prepared (100mM 2-Mercaptoethanol, 2% SDS, and 62.5 mM Tris-HCl pH 6.7) and membranes were incubated in for 30 min at 50 °C and washed three times in 10ml of PBS Tween at 7-10 min. The membrane was then blocked in 5% dried milk in PBS at RT for 1 hour, and incubated again with a primary antibody for detecting new target protein.

## **2. 3 Immunohistochemistry approach**

Immunohistochemistry is the localization of a target in tissue sections by using labelled antibodies as specific reagents through antigen-antibody interactions which could be visualized by using a marker like fluorescent dye, radioactive element, enzyme or colloidal gold. With the development of immunohistochemistry approach, enzyme labels have been presented such as alkaline phosphatase and peroxidase. One of important labels is Colloidal gold label which is used to identify immunohistochemical reactions at both light and electron microscopy level. Radioactive elements and the immunoreaction labels can be visualized by autoradiography.

### **2. 3. 1 Tissue Processing**

#### **2. 3. 1. 1. Fixations**

Tissue preparation is very important process in the immunohistochemistry technique. To ensure the preservation of tissue architecture and cell morphology, prompt and adequate fixation is essential. Furthermore, unsuitable or lengthy fixation may significantly reduce the antibody binding capability.

#### **2. 3. 2. 2 Tissue sections and mounting**

Paraffin wax is widely used as embedding medium in the histological laboratories for diagnostic histopathology. Tissue sections were performed by using a microtome LEICA RM2125RT (Leica Microsystems, UK) to cut 4-5-micrometer in thickness tissue sections, which were mounted on a microscope slide. These slides were used for optimizing the antibodies and to obtain the appropriate dilutions. Histo-clear1 and histo-clear2 solution were used to remove the paraffin wax from the slide sections for 5 min intervals and followed by transferring the slides through different concentration of ethanol to add the water to the tissue (Rehydration), starting with 100% for 5 min, 90% for 3 min, 75% 2 min, and finally 50% for 1 min.

### **2. 3. 2 Antigen Retrieval**

The demonstration of many antigens can be significantly improved by the pre-treatment with the antigen retrieval reagents that break the protein cross-links formed by formalin fixation and thereby uncover hidden antigenic sites. The techniques involved the application of heat for varying lengths of time to formalin-fixed, paraffin-embedded tissue sections in an aqueous solution. In this step the slides were placed in the coplin jar then transferred to a 1L beaker full of Tris- EDTA Buffer pH 9.0 (1.21g Tris-Base, 0.37g EDTA, 1000ml dH<sub>2</sub>O, and 0.5ml Tween-20) or Tri-sodium citrate buffer PH 6.0 (2.1g Tri-sodium citrate, 1000ml dH<sub>2</sub>O), depended on the antibody used in the experiment. The beaker/ Buffer/ coplin jar Assembly was placed in the microwave for 15-20 min at 310-440W then left it to cool for another 20 min. Later it was placed under running water for 5 min.

### **2. 3. 3 Blocking endogenous enzymes**

Blocking endogenous enzymes is necessary in this method because of the use of a peroxidase-based detection system. Cells that have endogenous peroxidase (RBCs for example) will appear as positive without performing this step. The slides incubated with peroxidase blocking solution which include 0.3% H<sub>2</sub>O<sub>2</sub> (Dako REAL™ EnVision™ Detection System, HRP/DAB, Rb/Mo, UK) for 15 mins and then rinsed with distilled water and placed in Tris-Buffer Saline buffer (TBS PH 7.4) for 5- 10 mins without bubbles.

### **2. 3. 4 Primary antibodies**

Incubation with primary antibodies for 1.30-2 hours at RT was performed by using different dilutions of the primary antibody for optimization process (see table 1.). The dilution was started with 1:50, 1:100, 1:200, 1:300, and 1:500 to obtain the best quality of tissue staining. Antibody Diluent with Background Reducing Components (Dako, UK) was used to dilute the antibodies.

### **2. 3. 5 Secondary antibodies**

Before adding biotinylated secondary antibody (Dako REAL™ EnVision™ Detection System, HRP/DAB, Rb/Mo, UK) slides were washed 3 times for 3min with 1X TBS Tween (PH 7.4) to remove unbound primary antibody. Two drops (about 100µl) Biotinylated secondary antibody was added to the slides for 30 min at RT followed by washing the slides 3 times for 3 min with 1X TBS Tween (PH 7.4).

### **2. 3. 6 Immunochromogenic staining**

The slides were placed in horizontal position and DAB substrate (Dako REAL™ EnVision™ Detection System, HRP/DAB, Rb/Mo, UK) was added to cover the tissues on the slide for 5-10 mins at room temperature. The reaction was stopped via dH<sub>2</sub>O and rinsed the DAB substrate.

### **2. 3. 7 Counter staining**

Counter staining was performed by using haematoxylin stain for 20-54 seconds followed by running water for 5 min then dehydrated through ethanol, starting with low concentration 50% for 1 min, 75% for 2 min, 90% for 3 min, and 5min 100%, later histo-clear2 for 5 min and histoclear1 for 5 min. Finally, slides were covered with cover slip by using DPX.

### **2. 3. 8 Microscopic examinations**

The slides were examined under the microscope (Leica Microscope DM500) to detect the protein expression in the tissues, using magnification 10x and 40x.

## 2. 4 CO-Immunoprecipitation (CO-IP)

The cells were cultured in the T<sub>75</sub> flasks to get enough amount of protein for extraction at 37°C and 5% CO<sub>2</sub> incubator and treated as mentioned above. Cells were washed two times with cold 1x PBS and scraped in 250 µl of TNN buffer (Tris-Cl (1 M, pH 7.5), 25 ml NaCl (5 M), 5 ml EDTA (0.5 M), 25 ml NP-40 (10%), 5 ml Pefabloc (40 mg/ml), 500 µl leupeptin (10 mg/ml), 1 ml pepstatin (2 mg/ml), 250 µl aprotinin (10 mg/ml), and then the lysates were transferred to Eppendorf tubes and rotated for 20 minutes in the cold room 4°C. The lysates then were centrifuged for 15 minutes at 12000 rpm; 4°C followed by protein concentration measured using JENWAY spectrophotometer to calculate the required volumes of the samples. About 50 µl of the sample was removed as input sample and one-half volume of 3x SDS was added. Each sample was divided to two, one to incubate with the IgG Ab as a negative control and the other sample to incubate with the target antibody (TTC5). TNN buffer was added to each tube up to 1 ml each followed by added 30 µl of protein A Agarose, Fast Flow (Sigma). After overnight incubation, the samples were centrifuged for 2 mins at 13.000 rpm to remove the supernatant then the beads were washed with TNN buffer and cold PBS for three times to remove unbound antibodies and proteins. To release the antibody bound to the target protein, 30 ml of 3x SDS was added and then heated for 5 mins at 95 °C, followed by centrifugation to remove the beads and the supernatant was kept for analysis by the western blot.

## 2.5 Immunofluorescence

The A549 cells have grown on the slides in the RPMI 1640 Medium as described previously and treated later with 20  $\mu$ M Etoposide for 24 hours. After washing the cells 3 times with cold PBS the cells were fixed by using 4% formaldehyde for 15 mins and followed by 5 mins in 1% Triton in PBS then washed again with PBS 3 times. For blocking step 1% BSA (Bovine serum Albumin) was used for one hour. Because TTC5 Abcam antibody was rabbit polyclonal (510 antibody), mouse monoclonal antibody against acetylated p53 at lysine 382 was used. 1:200 dilution of the TTC5 antibody was mixed with 1:1000 dilution of K382 Abcam antibody in the 1% BSA for one hour. The slides were then washed again to remove unbound antibodies via 1% BSA followed by incubation for an hour, dilution 1:1000 with fluorescent secondary antibodies green for the anti-TTC5 antibody and red for the anti-K382 antibody. Finally, DAPI staining was added and the cover slip has placed before checked under the Leica microscope.

## 2.6 MiRNA Isolation, Reverse Transcription and Quantitative Real-time-PCR

To assess expression of 34a and 34b family members (Gene Family ID: MIPF0000039, mir-34) in presence and absence of DNA damage by using the Etoposide treatment as mentioned previously, total miRNA was isolated from grown A549, Mero-14 and Mero-25 cell lines using mirVana™ miRNA Isolation Kit (Invitrogen, Carlsbad, Cal, USA) according to the manufacturer's instructions, followed by RNA quantification by NanoDrop ND-1000 Spectrophotometer (NanoDrop Technologies, Wilmington, DE). CDNA was reverse-transcribed using the TaqMan® MicroRNA Reverse Transcription Kit (Applied Biosystems™) and each 15 $\mu$ l reaction tube included 5 $\mu$ l RNA sample and 3 $\mu$ l primer plus 7 $\mu$ l Master mix. Quantitative PCR was performed in triplicate for each reaction. Each 20 reactions' tube consisted of 10  $\mu$ l TaqMan® Universal Master Mix II, with UNG (Uracil-N- Glycosylase), 2x in addition to 1  $\mu$ l TaqMan® Assay, 20x and 9  $\mu$ l cDNA/DNA template +RNase-free water as per manufacturer recommendation. The followed tables (Table 1, 2.) show the miRNA family members and the microRNA Control Assay products details respectively.

**Table 1.** The miRNA family members' details.

Family members	Forward Sequence	Stem-loop	Chromosome Location	miRBase ID	miRBase Accession #
<b>miRNA-34a</b>	UGGCAGUGUCUUAG CUGGUUGU	GGCCAGCUGUGAGUGUUUCUUUGGCAGUGUCUUA GCUGGUUGUUGUGAGCAAUAGUAAGGAAGCAAUC AGCAAGUAUACUGCCCUAGAAGUGCUGCACGUUGU GGGGCC	Chr. 1 - 9151668 - 9151777 [-] on Build GRCh38	hsa-miR-34a-5p	MIMAT0000255
<b>miRNA-34b</b>	UAGGCAGUGUCAUU AGCUGAUUG	GUGCUCGGUUUGUAGGCAGUGUCAUUAGCUGAUU GUACUGUGGGUUACAACUACUAAACUCCACUGCC AUCAAAACAAGGCAC	Chr. 11 - 111512938 - 111513021 [+] on Build GRCh38	hsa-miR-34b-5p	MIMAT0000685

As control, two TaqMan™ microRNA Control Assay products have been applied and showed in the next table.

**Table 2.** TaqMan™ microRNA Control Assay products details.

Assay Name	Sequences	NCBI Accession Number
<b>U6 snRNA</b>	GTGCTCGCTTCGGCAGCACATATACTAAAATTGGAACGATACAGAGAAGATTAGCATGGCCCT GCGCAAGGATGACACGCAAAATTCGTGAAGCGTTCCATATTT	NR_004394
<b>RNU44</b>	CCTGGATGATGATAGCAAATGCTGACTGAACATGAAGGTCTTAATTAGCTCTAACTGACT	NR_002750

## 2.7 Statistical Analysis

Data statistically analysed in figures represents the average of at least three independent experiments +/- SEM (standard error of the mean). Unless otherwise stated, asterisks (\*) above bars indicate statistical significance at  $p \leq 0.05$  when compared to the control, as assessed by a paired two-tail *t*-test. For Immunohistochemistry, SPSS software and chi-square was used and also the results were statistically considered as a significant at  $p \leq 0.05$  compared to the control.

## Chapter 3. Results

To investigate possible interaction between the total p53 protein levels and its isoforms originating from post-translational modifications, with the TTC5 co-factor, western blot analysis have been carried out to evaluate the protein levels of these proteins isolated from cells incubated in the presence and absence of DNA damage. We chose to study p53 tumour suppressor as it is mutated frequently in lung cancer and in over 50% of all other human cancers. In addition, p53 phosphorylated at S46 is one of the main phosphorylation site directing p53 to promoters of pro-apoptotic genes (Smeenk *et al.*, 2011). Finally K382 is residue targeted for acetylation by p300 transcriptional cofactor and Histone acetyltransferase (Puca *et al.*, 2009), whereas TTC5 is an important cofactor of p53 that interacts with p300 and affects acetylation status of its targets (Demonacos *et al.*, 2001).

### 3.1 Immunoblotting results

#### 3.1.1. Analysis of the total p53 protein levels in A549 human lung cancer cell line

To investigate protein levels of the total p53 in Etoposide treated lung cancer cell line, western blot analysis was performed (figure 3.1, top panel, compare lane 1 and lane 2). A549 cell lines were treated for 24 hours with 20  $\mu$ M Etoposide, protein was extracted from control and cells exposed to Etoposide induced DNA damage to determine the effect on the total p53 protein level. Three independent cell protein extractions were undertaken and analysed to determine reproducibility of results.  $\beta$ -actin was used as control to ensure equal loading of a protein extract, along with total p53 protein (figure 3. 1. Bottom panel lane 1 and 2).

Image J software was employed for densitometric measurements of total p53 protein levels. Intensity of the band was analysed and normalised to  $\beta$ -actin intensity (Figure 3. 2). Densitometric analysis of p53 protein indicated upregulation of protein levels in A549 Etoposide treated cells in response to DNA damage When compared to untreated cells (Fig. 3. 2, compare lane 1 to lane 2).

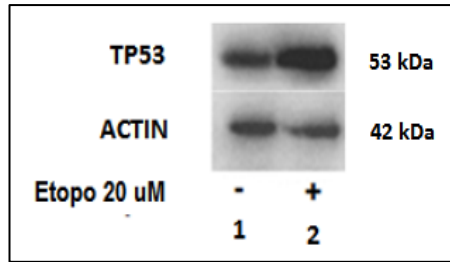


**Figure 3. 1.** Expression of the total p53 protein in A549 lung cancer cell lines in the absence and presence of induced DNA damage. A549 cells were incubated with or without Etoposide (20 μM) for 24 hours. Tp53 has detected using western blotting assay and specific antibody against p53 (DO-1). Blot is representative of three independent experiments. β-Actin was used as control for equal loading of proteins on the gel.

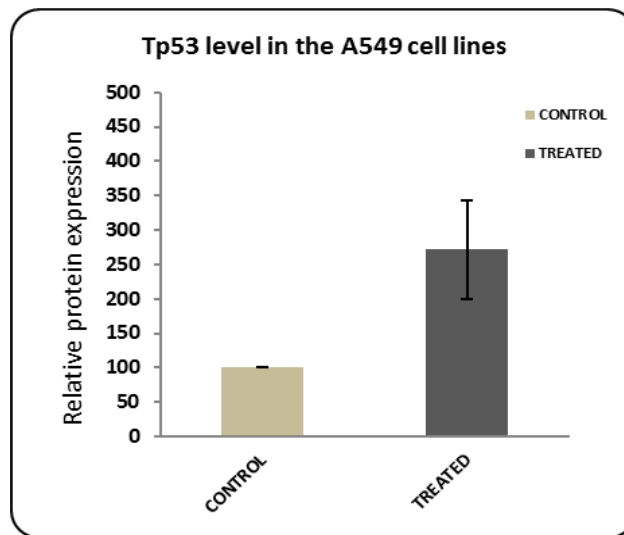


**Figure 3. 2:** Quantification of the total p53 protein levels of the blots shown in figure 3. 1 was carried out using ImageJ software. Band's intensity was normalised to β-Actin in the three independent experiments. Data is representative of the average of three independent experiments +/- SEM. *P*-value ≤0.05 is indicated by \*.

### 3.1.1.2 Analysis of the phosphorylated p53 at Serine 46 protein levels in A549 human Lung cancer cell line

To determine the protein levels of the phosphorylated p53 at Serine 46 in Etoposide treated lung cancer cell line, western blot analysis was applied (figure 3. 3, top panel, lane 1 and 2). DNA damage was induced in A549 cell lines by treating the cells with 20 μM Etoposide for 24 hours, proteins were extracted from control and cells exposed to Etoposide drug, then western blotting was performed using rabbit polyclonal anti- phosphorylated p53 (Ser46)

antibody (Abcam). Three independent cell protein extractions were undertaken and analysed to determine reproducibility of results and  $\beta$ -actin was used as control to ensure equal loading of a protein extract, along with the phosphorylated p53 at Serine 46 protein (figure 3. 3, bottom panel lane 1 and 2). An increase in phosphorylated p53 at Serine 46 protein was observed in Etoposide treated cells (compare lane 1 to lane 2).

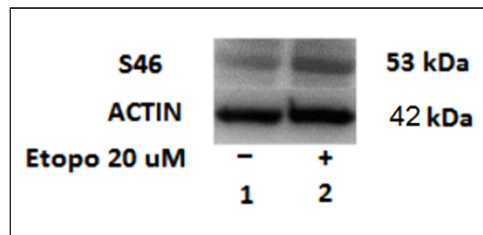


**Figure 3. 3:** Analysis of the phosphorylated p53 at Serine 46 protein levels in A549 cell line with and without DNA damage. Cells were incubated with 20  $\mu$ M Etoposide for 24 hours.  $\beta$ -Actin has used as control of the total proteins loaded on the gel.

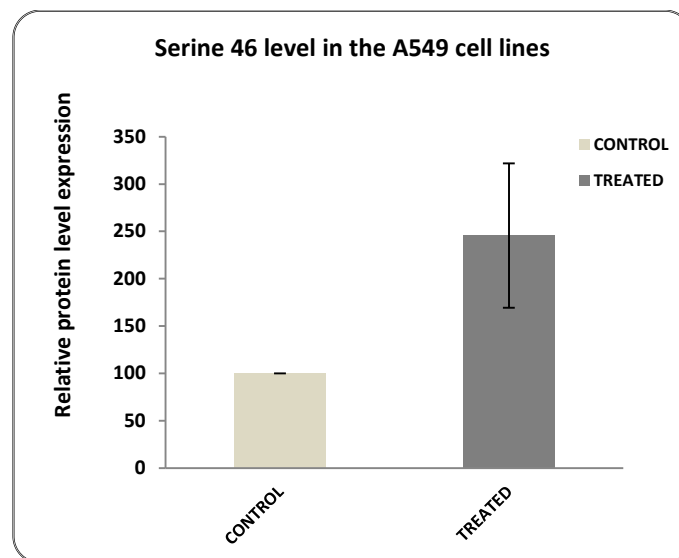


**Figure 3. 4:** Quantification of the phosphorylated p53 at Serine 46 protein level of the blots shown in figure 3. 3. were carried out using ImageJ software. Data is representative of the mean of the phospho-p53 (Ser46) level in three independent experiments with or without induced DNA damage. Samples bands' intensity were normalised to  $\beta$ -actin. Data is representative of the average of three independent experiments  $\pm$  SEM.  $P$ -value  $\leq 0.05$  is indicated by \*.

### 3.1.1.3 Analysis of the acetylated p53 at lysine 382 protein levels in A549 human Lung cancer cell line

For detection of the acetylated p53 at lysine 382 protein levels, A549 cells were treated or not for 24 hours with 20  $\mu$ M of Etoposide. To test the DNA damage effect on the acetylated p53 at lysine 382 levels, the total cellular proteins were extracted. Samples were analysed by SDS page and western blot analysis. Rabbit polyclonal antibody (Cell Signaling Technology) was used and results shown in the Fig. 3. 5. (top panel, lane 1 and 2),  $\beta$ -actin was used as control (bottom panel lane 1 and 2). Three independent cell protein extractions were carried out and analysed to ensure accuracy of results. Elevated expression of this p53 isoform (K382) has been observed (compare lane 1 to lane 2).

Quantification of data for three independent experiments to determine the acetyl-p53 at lysine 382 protein levels has done by using ImageJ software, represented in Figure 3. 6.  $\beta$ -actin was employed as loading control then results normalised and represented in fig. 3. 6. Upregulation of the acetyl-p53 at lysine 382 levels was demonstrated.

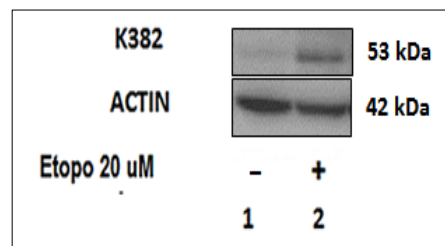


**Figure 3. 5:** Analysis the acetylated p53 at lysine 382 protein levels in lung cancer cell lines (A549) with and without inducing DNA damage. The cell lines were treated with 20 $\mu$ M for 24 hours. Three independent total cell proteins were extracted and acetyl-p53 at lysine 382 was detected by using anti-acetylated p53 (K382) antibody and  $\beta$ -Actin was used as control.

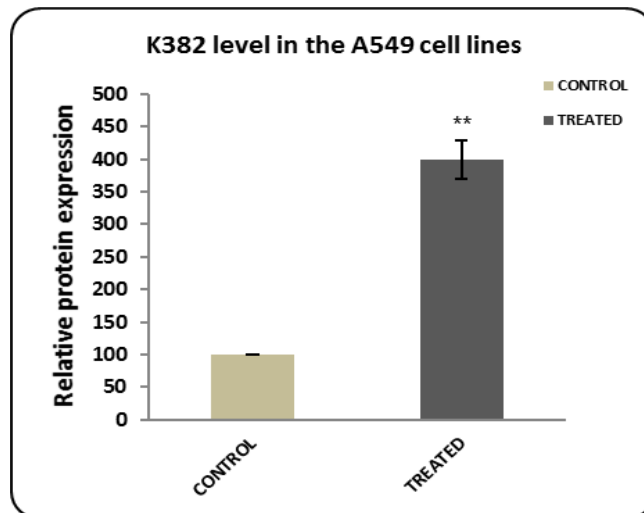


**Figure 3. 6:** Densitometric analysis of acetyl-p53 at lysine 382 in A549 cell lines in presence or absence of induced DNA damage via Etoposide by using ImageJ software. Data is representative of the mean of the acetyl-p53 at lysine 382 level in three independent experiments and bands' intensity was normalised to  $\beta$ -actin. Data is representative of the average of three independent experiments +/- SEM. *P*-value <0.05 is indicated by \*.

#### 3.1.1.4 Analysis of the TTC5 protein levels in A549 human lung cancer cell line

To investigate the expression of the TTC5 protein levels in A549 cell line, the cells were treated as described above. Cell extracts were analysed by the western blotting technique. Three independent experiments were been performed by using Rabbit polyclonal anti-TTC5 antibody (Santa Cruz Biotechnology) to detect the protein expression level (Fig. 3. 7., top panel lane 1 and lane 2). There was no significant change in the TTC5 protein level observed in the three independent experiments and represented in the fig. 3. 7.

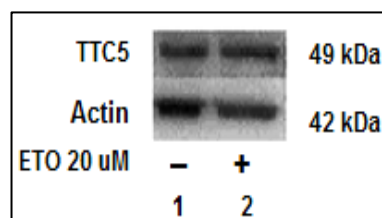


**Figure 3. 7.** Detection of the TTC5 protein in the A549 cell lines in presence or absence of induced DNA damage using SDS PAGE assay. A549 cell lines were incubated for 24 hours after the treatment and anti-TTC5 polyclonal antibody's product has applied in three independent experiments.

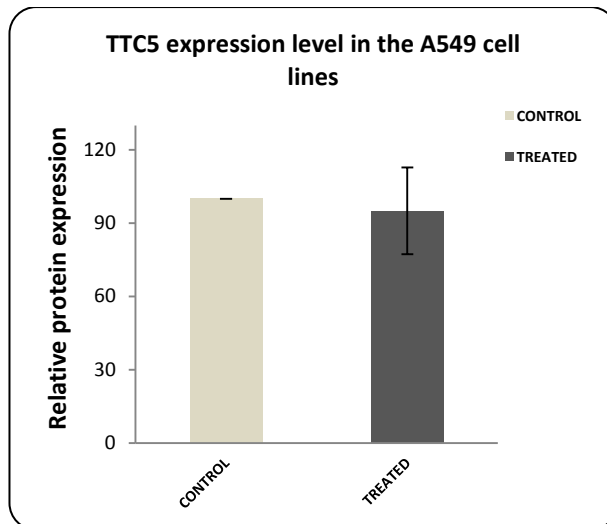


**Figure 3. 8.** Quantification of the TTC5 protein level of the blots in A549 cell lines shown in figure 3. 7 was carried out using ImageJ software as semi-quantitative tool in presence or absence of DNA damage, induced via the mentioned anti-cancer drug. Data is representative of the average of three independent experiments +/- SEM. *P*-value <0.05 is indicated by \*.

As a conclusion of this set of experiments in the A549 lung cancer cell line, upregulation of the total p53 protein expression and its isoforms phospho-p53 at Serine 46 and acetylated p53 at K382 has been observed but no significant change in its co-factor “TTC5” was detected and represented in the figure 3. 9.

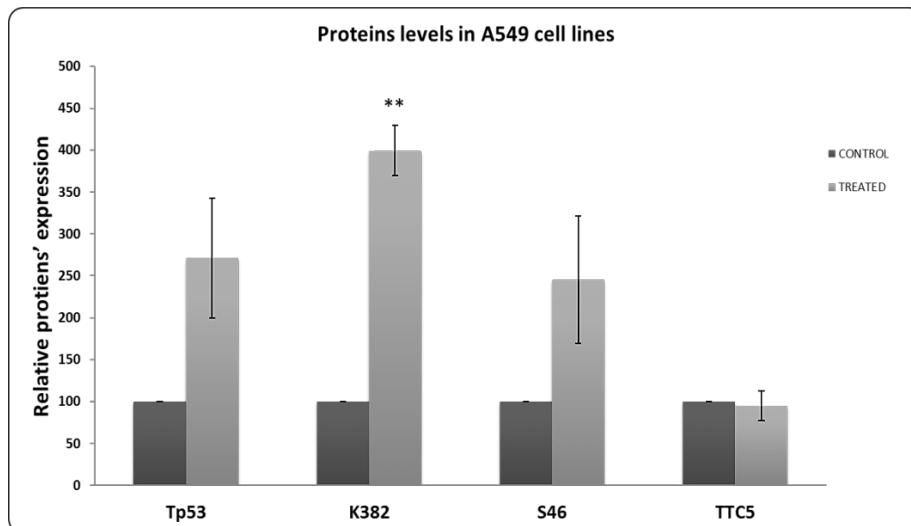


**Figure 3. 9:** Conclusion figure for densitometric analysis of Tp53, P-p53 at S46, acetyl-p53 at lysine 382 and TTC5 proteins in the A549 cell lines with or without of induced DNA damage were carried out by using ImageJ software. Data is representative of the mean of three independent experiments and the samples’ band intensity was normalised to  $\beta$ -actin as mentioned above. Data is

representative of the average of three independent experiments +/- SEM. *P*-value ≤0.05 is indicated by \*.

### 3.1.2.1 Analysis of the total p53 protein levels in Mero-25 human mesothelioma cancer cell line

In order to determine if observed changes are specific for A549 cell line or can be observed in other cell lines and cancer types we detected p53 levels in two mesothelioma cell lines. To detect the protein levels of the wild type p53 in Etoposide treated malignant mesothelioma cell lines, western blot analysis was applied (figure 3. 10, top panel, compare lane 1 and lane 2). For 24 hours incubation, Mero-25 cell lines were treated with the same anti-cancer drug to induce the DNA damage followed by the extraction of the total proteins, to determine the effect on the total p53. Monoclonal antibody DO-1 (Santa Cruz Biotechnology) against the Tp53 protein has applied and under the same conditions, three independent cellular extractions were undertaken and analysed to determine reproducibility of results.

β-actin was also used here as control to ensure equal loading of a protein extract, along with total p53 protein (fig. 3. 10. Bottom panel lane 1 and 2). For densitometric measurements of wtp53 protein's level, ImageJ software has employed and the band's intensity were analysed and normalised to β-actin intensity (Fig. 3. 10), which indicated slight increase that was not significant in the p53 protein level of the treated Mero-25 cells in response to DNA damage when compared to untreated cells.

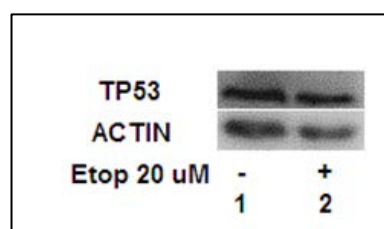


**Figure 3. 10.** Detection of the Total p53 protein level in the Mero-25 cell lines with and without DNA damage by using SDS PAGE and WB. Mesothelioma cell lines were incubated for 24 hours after treated as detailed above.

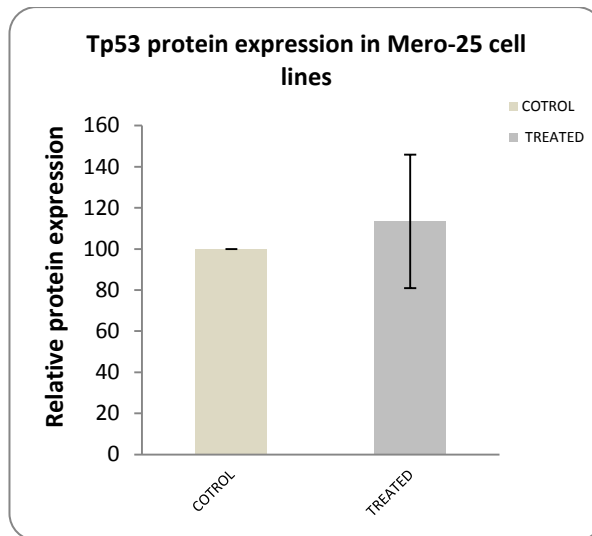


**Figure 3. 11:** Quantification of the wild-type p53 protein level of the blots shown in figure 3. 10. which carried out using ImageJ software. The cells were treated and incubated with 20  $\mu$ M of anti-cancer drug Etoposide for 24 hours as previously described. Data is representative of the average of three independent experiments  $\pm$  SEM. *P*-value  $\leq 0.05$  is indicated by \*.

### 3.1.2.2 Analysis of the phosphorylated p53 at Serine 46 protein levels in Mero-25 human mesothelioma cancer cell line

To determine the protein levels of the phosphorylated p53 at serine 46 in Etoposide treated malignant mesothelioma cell lines, western blot analysis was applied (figure 3. 12, top panel, compare lane 1 and lane 2). Under the same conditions described above, DNA damage were induced by treating them with 20 $\mu$ M Etoposide for 24 hours and total proteins were extracted and used for western blotting technique. Polyclonal anti- phosphorylated p53 at Ser46 antibody from Abcam was used and three independent experiments were analysed to determine reproducibility of results.

$\beta$ -actin was used as control represented in figure 3. 12. bottom panel lane 1 and 2. ImageJ software has employed for densitometric measurements of phospho-p53 at Ser46 protein levels and the intensity of the bands were analysed and normalised to the  $\beta$ -actin (Fig. 3. 13). Analysis of this phosphorylated p53 protein (Ser46) indicated slight increase in the protein level in treated Mero-25 cells comparing to untreated cells (Fig. 3. 13, compare lane 1 to lane 2).

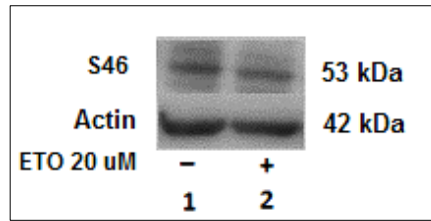


**Figure 3. 12:** Analysis of the phosphorylated p53 at Serine 46 protein levels in Mero-25 cell lines with and without DNA damage. Cells were treated with 20  $\mu$ M Etoposide for 24 hours. Three independent experiments were carried out. Total cell proteins were extracted and the phosphorylation of p53 at Serine 46 protein was detected by using rabbit polyclonal anti- phosphorylated p53 at Ser-46 antibody.  $\beta$ -Actin was used as control of the total proteins loaded on the gel.

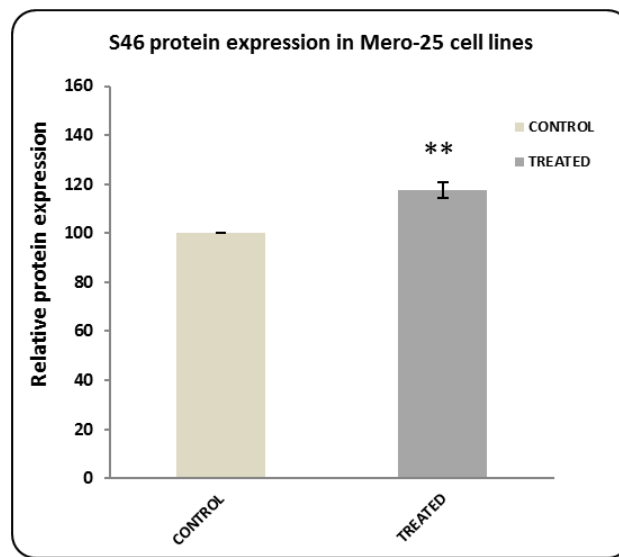


**Figure 3. 13:** Quantification of the phosphorylated p53 at Ser46 protein level has carried out using ImageJ software in the Mero-25 cell lines shown in figure 3. 12. Data is representative of the mean of the phospho-p53 (Ser-46) level in three independent experiments. Samples band intensity were normalised to  $\beta$ -actin. Data is representative of the average of three independent experiments +/- SEM. *P*-value  $\leq 0.05$  is indicated by \*.

### 3.1.2.3 Analysis of the acetylated p53 at lysine 382 protein levels in Mero-25 human Mesothelioma cancer cell line

In this experiment the Mero-25 cell lines were treated or not for 24 hours with Etoposide followed by the extraction of the total cellular proteins and the samples were run through SDS page and western blot analysis. Rabbit polyclonal antibody (Cell Signalling Technology) has used and the results shown in Fig. 3. 14. (top panel, lane 1 and 2).  $\beta$ -actin was used as control (Bottom panel lane 1 and 2). Three independent cell protein extractions were performed and analysed to ensure accuracy of results.

Quantification of three independent data sets to determine the acetyl-p53 at lysine 382 protein level was done by using Image.J software, represented in Figure 3. 15. The results were normalised to  $\beta$ -actin as loading control and represented in fig. 3. 15. Also for this p53 isoform, no significant increase in the acetyl-p53 at lysine 382 levels has observed in this cell line (compare lane 1 to lane 2).

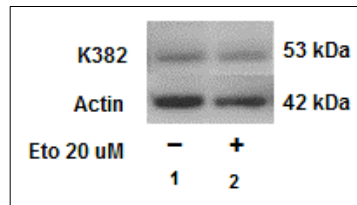


**Figure 3. 14:** Analysis the acetylated p53 at lysine 382 protein levels in mesothelioma cell lines (Mero-25) with and without DNA damage. The cells have grown for 24 hours and treated with the 20  $\mu$ M Etoposide then the whole cell proteins were extracted and acetyl-P53 at lysine 382 protein has detected through using rabbit polyclonal anti-acetylated p53 (K382) antibody.

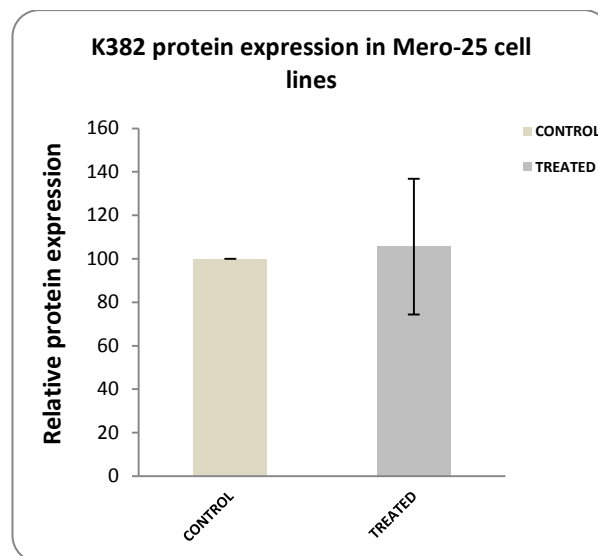


**Figure 3. 15:** Densitometric analysis of acetyl-p53 at lysine 382 in Mero-25 cell lines in presence or absence of DNA damage induced by Etoposide was carried out by using ImageJ software. Data is representative of the mean of the acetyl-p53 at lysine 382 level in three independent experiments and the samples' band intensity were normalised to  $\beta$ -actin. Data is representative of the average of three independent experiments  $\pm$  SEM. *P*-value  $\leq 0.05$  is indicated by \*.

### 3. 1. 2. 4 Analysis of the TTC5 protein levels in Mero-25 human mesothelioma cancer cell line

In order to investigate the expression level of TTC5 p53 cofactor in Mero-25 cell lines, the cells have grown and treated using the same concentration of Etoposide as previously described. The whole cell protein extractions were loaded and analysed by using Western blotting technique and ImageJ software. Three independent experiments have been performed and rabbit polyclonal anti-TTC5 antibody from Santa Cruz Biotechnology was used. There was no significant change in the TTC5 protein level (compare lane 1 to lane 2) was observed in the three independent experiments as represented in the fig. 3. 16.

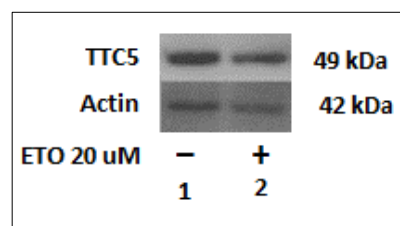


**Figure 3. 16.** Detection of the TTC5 protein in the Mero-25 cell lines in presence or absence of DNA damage via using SDS PAGE and WB. The Mero-25 cells were grown for 24 hours then treated or not with the 20  $\mu$ M Etoposide. Polyclonal rabbit antibody's product was used to detect the TTC5 protein level.  $\beta$ -Actin was used as control of loaded samples and three independent experiments were generated.

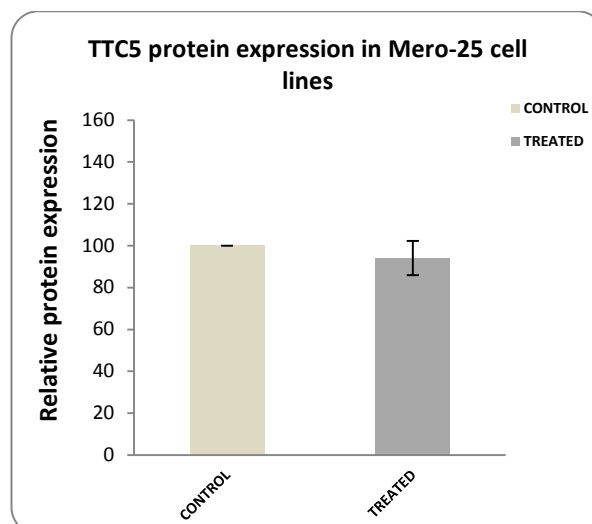


**Figure 3. 17:** Quantification of the TTC5 protein levels shown in figure 3. 16 were carried out using ImageJ software. Data is representative of the TTC5 levels mean in at least three independent experiments with or without Etoposide treatment. Samples' bands intensity were normalised to  $\beta$ -

actin. Data is representative of the average of three independent experiments +/- SEM. *P*-value ≤0.05 is indicated by \*.

Therefore, in Mero-25 cell lines the data showed no significant change in the Tp53 protein levels, K382, and TTC5 protein expression. Whereas; slightly increase observed in S46 levels and the summary of the data is shown in the figure 3. 18.

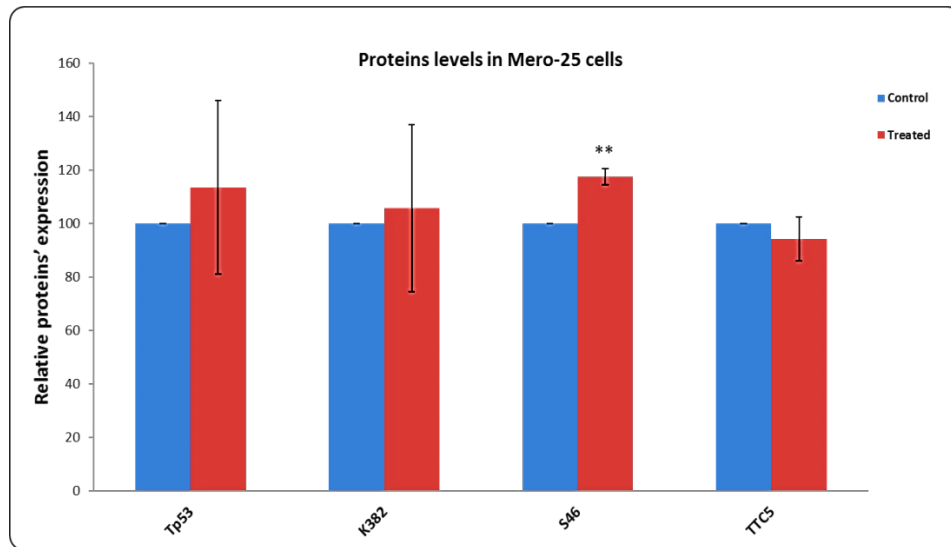


**Figure 3. 18:** Quantification of Tp53, Ser-46 and K382 protein levels in association with TTC5 in the Mero-25 cells summarised in C. Data is representative of all these proteins' levels mean in at least three independent experiments with or without Etoposide treatment. Samples' bands intensity has normalised to  $\beta$ -actin. Data is representative of the average of three independent experiments +/- SEM. *P*-value ≤0.05 is indicated by \*.

### 3.1.3.1 Analysis of the total p53 protein levels in Mero-14 human mesothelioma cancer cell line

In order to test if our results apply to a different mesothelioma cell lines we use analysed Mero-14 cell line as described above. To detect the total p53 protein expression levels, western blotting technique was carried out and membranes were incubated with DO-1 anti-total p53 antibody (Santa Cruz Biotechnology) and generated results showed in figure 3. 19, (top panel, compare lane 1 and lane 2).  $\beta$ -actin was also measured here (fig. 3. 19. bottom panel lane 1 and 2) and three independent experiments and densitometry measurements have been done. ImageJ software was employed and the band's intensity was analysed and

normalised to  $\beta$ -actin intensity (Fig. 3. 20). The results indicated upregulation in the Tp53 protein levels in the treated Mero-14 cells in response to DNA damage compared to untreated cells.

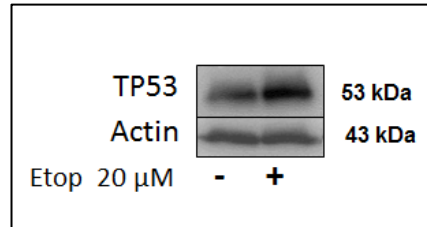


**Figure 3. 19.** Detection of the Total p53 protein level in the Mero-14 cell lines with and without DNA damage by using SDS PAGE and Western Blotting. The cell lines were incubated for 24 hours with 20 $\mu$ M Etoposide.

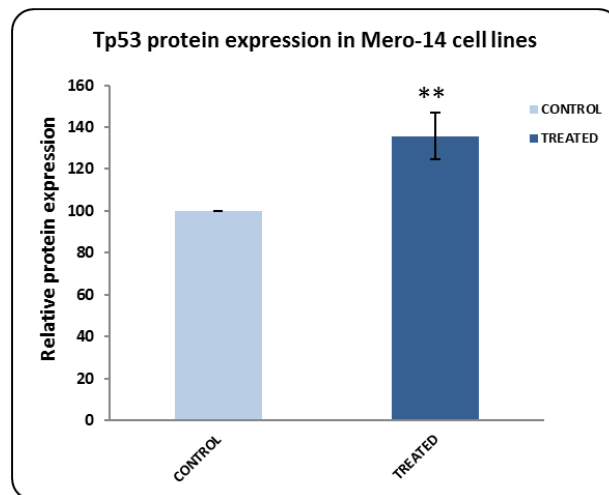


**Figure 3. 20:** Quantification of the wild-type p53 protein levels in the Mero-14 shown in figure 3. 19, which generated by using ImageJ software. Data is representative of the mean of Tp53 protein levels in at least three independent experiments and samples' band intensity have normalised to  $\beta$ -actin. Data is representative of the average of three independent experiments  $\pm$  SEM. *P*-value  $\leq 0.05$  is indicated by \*.

### 3.1.3.2 Analysis of the phosphorylated p53 at Serine 46 protein levels in Mero-14 human mesothelioma cancer cell line

For exploring the protein expression levels of this isoform of p53 (Serine 46) in DNA damage induced in the Mero-14, western blot analysis has applied (figure 3. 21, top panel, compare lane 1 and lane 2). Under the same conditions described above, the Rabbit polyclonal anti-

phosphorylated p53 at Ser46 antibody from Abcam was used in three independent experiments and analysed to determine reproducibility of results.

Again, and as in all previous experiments,  $\beta$ -actin has used as control and represented in figure 3. 21. Bottom panel lane 1 and 2. Employing the ImageJ software for densitometric measurements of phospho-p53 at Ser46 protein levels and the intensity of the bands were analysed then normalised to the  $\beta$ -actin (Figure 3. 22). Data analysis has indicated an increase in this protein levels in treated Mero-14 cells comparing to untreated cells (Fig. 3. 22, compared lane 1 to lane 2).

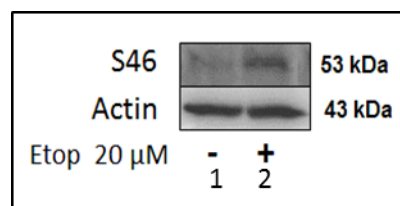


**Figure 3. 21:** detection of the phosphorylated p53 at Serine 46 protein levels in Mero-14 cell lines with and without DNA damage induced with 20  $\mu$ M Etoposide for 24 hours. The total cellular proteins have extracted and the phospho-p53 at Serine 46 proteins were detected by using rabbit polyclonal anti- Ser-46 antibody. Also,  $\beta$ -Actin was used as control of the total proteins loaded on the gel.

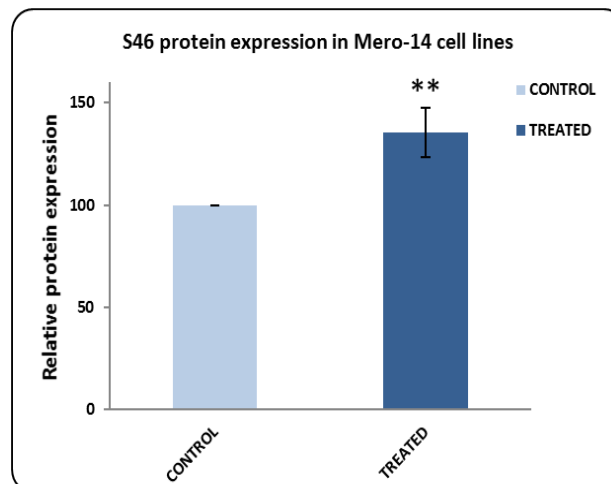


**Figure 3. 22:** Quantification of phospho-p53 at Ser46 protein levels was generated using ImageJ software in the Mero-14 cell lines shown in figure 3. 21. These data is representative of the mean of the protein level in three independent experiments after samples band intensity were normalised to  $\beta$ -actin. Data is representative of the average of three independent experiments  $\pm$  SEM. *P*-value  $\leq 0.05$  is indicated by \*.

### 3.1.3.3 Analysis of the acetylated p53 at lysine 382 protein levels in Mero-14 human mesothelioma cancer cell line

To detect the protein expression, the Mero-14 cell lines were treated or not with Etoposide as described before, followed by protein extraction and SDS page and western blot analysis. Rabbit polyclonal antibody (Cell Signaling Technology) was applied and the results shown in Fig. 3. 23. (Top panel, lane 1 and 2). Loaded samples were normalised to  $\beta$ - actin, which is shown at bottom panel lanes 1 and 2. Three independent cell protein extractions were performed and analysed to ensure accuracy of results.

Quantification data of the three independent experiments was achieved using ImageJ software and represented in Figure 3. 24. The results for this p53 isoform (K382) showed a significant increase in levels of this acetylation form of p53 in the Mero-14 cell lines (compare lane 1 to lane 2).

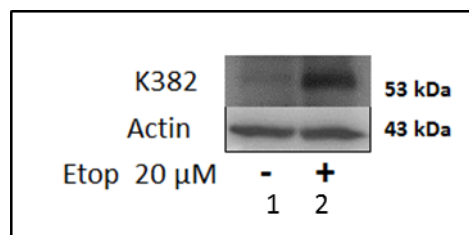


**Figure 3. 23:** Analysis the acetylated p53 at lysine 382 protein levels in Mesothelioma cell lines (Mero-14) with and without an induced DNA damage. The cells were grown for 24 hours and treated with the 20  $\mu$ M Etoposide then the whole cell proteins were extracted and acetyl-p53 at lysine 382 protein was detected through the immunoblotting using a rabbit polyclonal anti-acetylated p53 (K382) antibody.

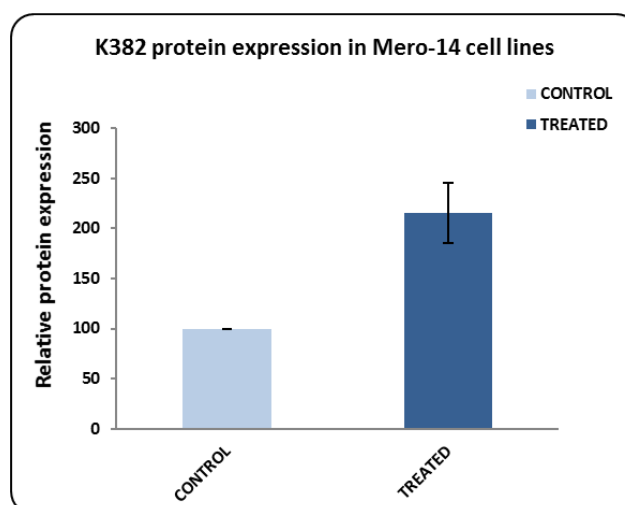


**Figure 3. 24:** Densitometry analysis of the p53 acetylation form (K382) in the Mero-14 cell lines in presence or absence of an induced DNA damage was carried out by using ImageJ software. The data is representative of the mean of the protein levels in three independent experiments and the samples' band intensity were normalised to  $\beta$ -actin. Data is representative of the average of three independent experiments +/- SEM. *P*-value  $\leq 0.05$  is indicated by \*.

### 3.1.3.4 Analysis of the TTC5 protein levels in Mero-14 human mesothelioma cancer cell line

To determine the expression level of TTC5 protein in Mero-14 cell lines, the protocols for growing and treating cells have been followed as previously described. The immunoblotting was done after the whole cell protein extracted and then samples were loaded. TTC5 antibody from Santa Cruz Biotechnology rabbit polyclonal antibody was applied in the three independent experiments. Similar to the TTC5 expression results generated in the previous two different cells, we observed that there was no change in the TTC5 protein levels (compare lane 1 to lane 2) in the three independent experiments represented in the fig. 3. 25.

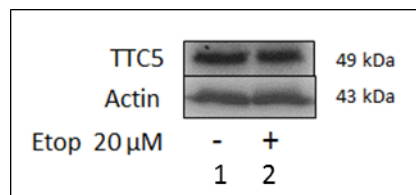


**Figure 3. 25.** Detection of the TTC5 protein expression level in Mero-14 cells with or without of the induced DNA damage using SDS PAGE and immunoblotting assay. The cell lines were grown after 24 hours treatment with or without the 20  $\mu$ M Etoposide. Anti-TTC5 antibody has used to detect the TTC5 protein level.  $\beta$ -Actin used as control of loaded samples in the three independent experiments.

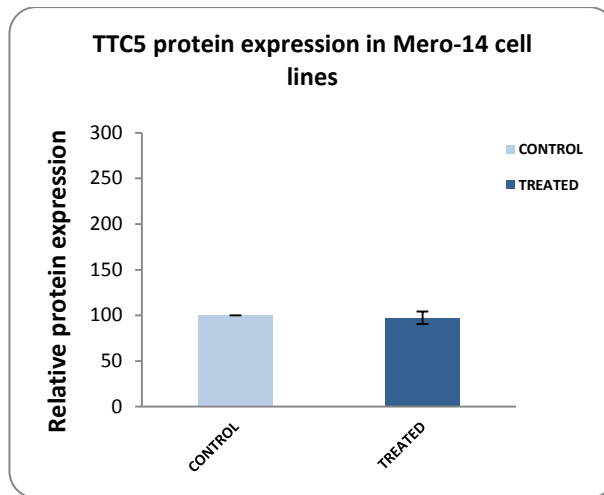


**Figure 3. 26:** Quantification of the TTC5 expression levels in Mero-14 shown in figure 3. 25. by using ImageJ software. This data is representative of the TTC5 levels mean in at least three independent experiments with or without Etoposide treatment. Samples' bands intensity have normalised to  $\beta$ -actin. Data is representative of the average of three independent experiments +/- SEM. *P*-value  $\leq 0.05$  is indicated by \*.

To summarise results generated in the Mero-14 cell lines, the data showed no significant change in TTC5 protein levels. Whereas and in contrast to the other mesothelioma cell lines (Mero-25), significant increases of Tp53, phospho-p53 at S46 and acetylated p53 at lysine 382 have been demonstrated. Data is summarised in the figure 3. 27.

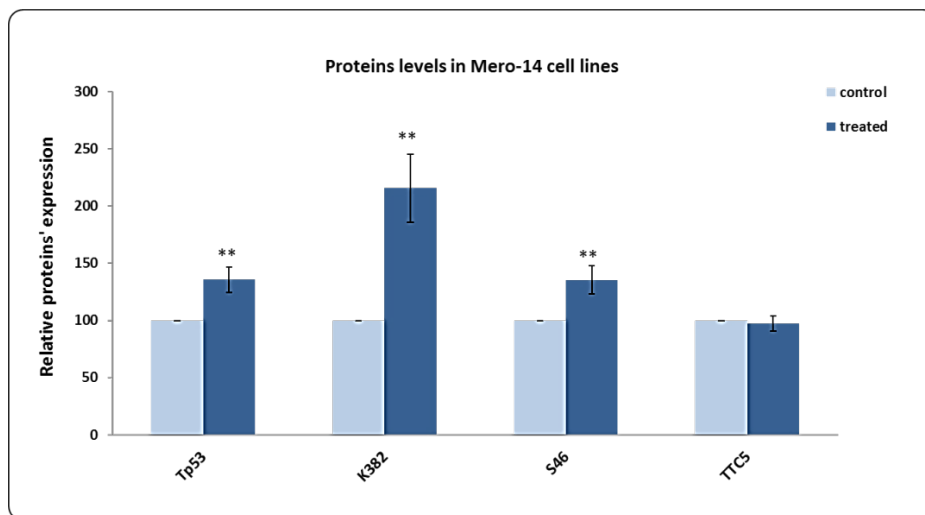


**Figure 3. 27:** Quantification of Total p53, Ser-46 and K382 proteins levels in addition to TTC5 protein in the Mero-14 cell lines. Data is representative of proteins' levels mean in at least three independent experiments in present and absent of the Etoposide treatment. All experiments normalised to the  $\beta$ -actin. Data is representative of the average of three independent experiments +/- SEM. *P*-value  $\leq 0.05$  is indicated by \*.

## **3.2 Immunohistochemistry results**

The immunohistochemistry technique (IHC) became a ubiquitous method, almost in every hospital and pathology diagnostics centres, used for diagnostic, prognostic, and predictive studies. Biomarkers are essential for therapeutic decision- making in terms of prognosis of the cancer progression. Tissue microarray (TMA) technology was described as a potentially influential technology for achieving high- throughput analysis of set of proteins' expressions in large number of normal and cancers tissue specimens' sections. TMA based immunohistochemically staining and proteomics are crucial tools to generate and validate clinically applicable cancer biomarkers. Using formalin-fixed tissue microarray sections with immunohistochemical stains to determine the proteins' expression can be scored manually and semi-quantitatively (Idikio, 2011). One of the main objectives of this project is to detect the total p53 protein expression and its post-translation modification isoforms (Ser46 and K382) and also TTC5 protein in the human lung cancer and mesothelioma tissue microarrays using these techniques. In this series of experiments, we have started the optimization process for obtaining the ideal experimental conditions to use antibodies of interest.

### **3.2.1 The optimization process**

Before analysis of the costly Tissue Microarrays slides (TMA) using the immunohistochemistry technique, extensive optimization was performed. In this process, human COPD patients' lung tissues provided by Dr. Lucy Smyth were used to optimise the antibodies under different conditions. Different antibody dilutions series starting from 1:50 were prepared to determine the best dilution with good quality of staining. Various buffer solutions with different pH included Tri-EDTA pH9 and Tri-sodium citrate pH6 were used and optimal conditions for all four antibodies were determined as summarised in the table3.

**Table 3.** Optimization conditions with the antibodies and buffers

Primary Antibody	Antibody Species	Product's code	Manufacturer	Pre-Treatment Needed (Yes/No)	Pre-Treatment Buffer	The Antibody Dilution
-Ve	N	N	N	N	N	N
WTp53	Mouse Monoclonal	M 7001	DAKO	Y	Tris-EDTA Buffer pH9	1:100
Phosphorylated p53 (Ser46)	Mouse Monoclonal	MAB0659	ABNOVA	Y	Tris-EDTA Buffer pH9	1:100
Acetylated p53 (K382)	Rabbit Polyclonal	bs-0905R	BIOSS	Y	Tri-sodium citrate Buffer pH6	1:50
TTC5	Rabbit Polyclonal	ab36855	ABCAM	Y	Tri-sodium citrate Buffer pH6	1:100

### 3. 2. 2 The tissue microarrays results

Two human lung cancer TMA slides that were obtained from Biomax.us, included 92 cases on slide No.1 and 120 cases placed on slide No.2 which involved 10 cases of normal lung tissue and 110 were cancers lung tissue sections. Most of the lung cancers' tissue sections were squamous cell carcinoma and adenocarcinomas. These samples were placed on the slides as 92 cores for slide No.1 and 120 cores for slide No .2. In total, every core was 4-5µm thick with 1.5 diameter representing 1 case (patient's tissue section), as shown in fig. 3. 28

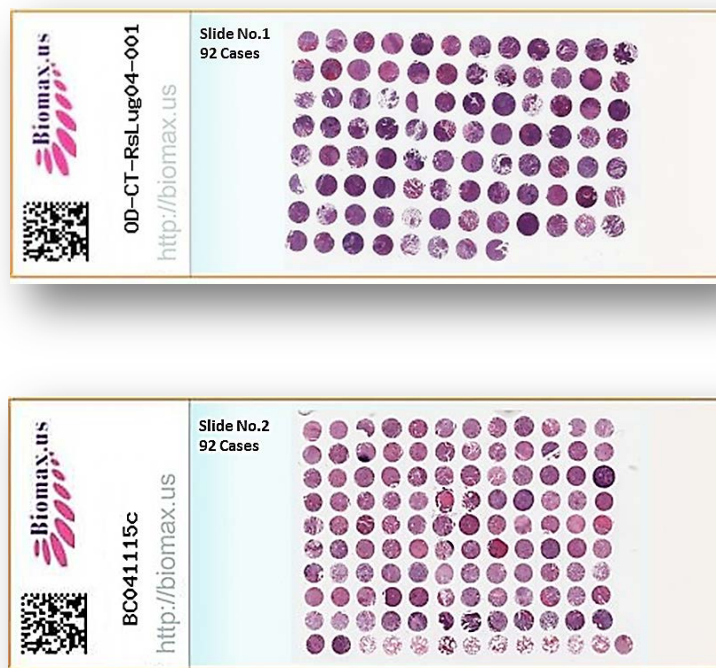


**Figure 3. 28.** Shown the TMA human lung cancer slides 1 and 2 included 92 +120 cases. Adapted from <http://www.biomax.us/tissue-arrays/Lung/OD-CT-RsLug04-001> and <https://www.biomax.us/tissue-arrays/Lung/BC041115c>

Clinicopathological data for every case included the age, the gender, the organ, the type and the grade of the cancer for both slides in addition to the TNM (Tumour, Node, Metastasis) and the stage of the cancer for the slide No. 2 were provided and attached with the product and shown in the following table (Table 4 for the 92 cases) and supplementary table 5 (for the 120 cases).

**Table 4:** Specification Sheet for 92 cases adapted from: <http://www.biomax.us/tissue-arrays/Lung/OD-CT-RsLug04-001>

<b>Pos</b>	<b>No.</b>	<b>Sex</b>	<b>Age</b>	<b>Organ</b>	<b>Pathology diagnosis</b>	<b>Grade</b>	<b>Type</b>
A1	1	M	72	Lung	Squamous cell carcinoma	G1	Tumour
A2	2	M	42	Lung	Squamous cell carcinoma	G1	Tumour
A3	3	M	58	Lung	Squamous cell carcinoma	G1	Tumour
A4	4	M	70	Lung	Squamous cell carcinoma	G1-G2	Tumour
A5	5	M	53	Lung	Squamous cell carcinoma	G1-G2	Tumour
A6	6	M	53	Lung	Squamous cell carcinoma	G2	Tumour
A7	7	M	77	Lung	Squamous cell carcinoma with necrosis		Tumour
A8	8	M	72	Lung	Squamous cell carcinoma	G1-G2	Tumour
A9	9	M	57	Lung	Squamous cell carcinoma	G1-G2	Tumour
A10	10	M	78	Lung	Squamous cell carcinoma	G1-G2	Tumour
A11	11	M	68	Lung	Squamous cell carcinoma	G1-G2	Tumour
A12	12	M	52	Lung	Squamous cell carcinoma	G1-G2	Tumour
B1	13	M	61	Lung	Squamous cell carcinoma	G1-G2	Tumour
B2	14	M	67	Lung	Squamous cell carcinoma	G1-G2	Tumour
B3	15	M	72	Lung	Squamous cell carcinoma	G1-G2	Tumour
B4	16	M	65	Lung	Squamous cell carcinoma	G1-G2	Tumour
B5	17	M	75	Lung	Squamous cell carcinoma	G1-G2	Tumour
B6	18	M	78	Lung	Squamous cell carcinoma	G1-G2	Tumour
B7	19	M	58	Lung	Squamous cell carcinoma	G1-G2	Tumour
B8	20	M	63	Lung	Squamous cell carcinoma	G1-G2	Tumour
B9	21	M	58	Lung	Squamous cell carcinoma	G1-G2	Tumour

<u>Pos</u>	<u>No.</u>	<u>Sex</u>	<u>Age</u>	<u>Organ</u>	<u>Pathology diagnosis</u>	<u>Grade</u>	<u>Type</u>
B10	22	M	64	Lung	Squamous cell carcinoma	G1-G2	Tumour
B11	23	M	53	Lung	Squamous cell carcinoma	G1-G2	Tumour
B12	24	M	68	Lung	Squamous cell carcinoma	G1-G2	Tumour
C1	25	M	71	Lung	Squamous cell carcinoma	G1-G2	Tumour
C2	26	M	75	Lung	Squamous cell carcinoma	G2	Tumour
C3	27	F	57	Lung	Squamous cell carcinoma	G2	Tumour
C4	28	M	57	Lung	Squamous cell carcinoma	G2	Tumour
C5	29	M	69	Lung	Squamous cell carcinoma	G2	Tumour
C6	30	M	61	Lung	Squamous cell carcinoma	G2	Tumour
C7	31	M	62	Lung	Squamous cell carcinoma	G2	Tumour
C8	32	M	70	Lung	Squamous cell carcinoma	G2	Tumour
C9	33	M	61	Lung	Squamous cell carcinoma	G2	Tumour
C10	34	M	71	Lung	Squamous cell carcinoma	G2	Tumour
C11	35	M	68	Lung	Squamous cell carcinoma with necrosis	G2	Tumour
C12	36	M	67	Lung	Squamous cell carcinoma	G2	Tumour
D1	37	M	70	Lung	Squamous cell carcinoma	G2	Tumour
D2	38	M	62	Lung	Squamous cell carcinoma	G2	Tumour
D3	39	M	69	Lung	Squamous cell carcinoma	G2	Tumour
D4	40	M	53	Lung	Squamous cell carcinoma	G2	Tumour
D5	41	M	53	Lung	Squamous cell carcinoma	G2	Tumour
D6	42	M	70	Lung	Squamous cell carcinoma	G2	Tumour
D7	43	M	59	Lung	Squamous cell carcinoma	G2	Tumour

<u>Pos</u>	<u>No.</u>	<u>Sex</u>	<u>Age</u>	<u>Organ</u>	<u>Pathology diagnosis</u>	<u>Grade</u>	<u>Type</u>
D8	44	M	61	Lung	Squamous cell carcinoma	G2	Tumour
D9	45	M	66	Lung	Squamous cell carcinoma	G2	Tumour
D10	46	M	71	Lung	Squamous cell carcinoma	G2	Tumour
D11	47	M	61	Lung	Squamous cell carcinoma	G2	Tumour
D12	48	M	76	Lung	Squamous cell carcinoma	G2	Tumour
E1	49	M	67	Lung	Squamous cell carcinoma	G2	Tumour
E2	50	M	68	Lung	Squamous cell carcinoma	G2	Tumour
E3	51	M	56	Lung	Squamous cell carcinoma	G2	Tumour
E4	52	M	78	Lung	Squamous cell carcinoma	G2	Tumour
E5	53	M	75	Lung	Squamous cell carcinoma	G2	Tumour
E6	54	M	72	Lung	Squamous cell carcinoma	G2	Tumour
E7	55	M	55	Lung	Squamous cell carcinoma	G2	Tumour
E8	56	M	72	Lung	Squamous cell carcinoma	G2	Tumour
E9	57	F	66	Lung	Squamous cell carcinoma	G2	Tumour
E10	58	M	62	Lung	Squamous cell carcinoma	G2	Tumour
E11	59	M	55	Lung	Squamous cell carcinoma	G2	Tumour
E12	60	M	52	Lung	Squamous cell carcinoma	G2	Tumour
F1	61	M	53	Lung	Squamous cell carcinoma	G2	Tumour
F2	62	M	62	Lung	Squamous cell carcinoma	G2	Tumour
F3	63	M	59	Lung	Squamous cell carcinoma	G2	Tumour
F4	64	M	51	Lung	Squamous cell carcinoma	G2	Tumour
F5	65	M	67	Lung	Squamous cell carcinoma	G2	Tumour
F6	66	M	61	Lung	Squamous cell carcinoma with	G2-G3	Tumour

<u>Pos</u>	<u>No.</u>	<u>Sex</u>	<u>Age</u>	<u>Organ</u>	<u>Pathology diagnosis</u>	<u>Grade</u>	<u>Type</u>
					necrosis		
F7	67	M	63	Lung	Squamous cell carcinoma	G2-G3	Tumour
F8	68	M	76	Lung	Squamous cell carcinoma	G2-G3	Tumour
F9	69	M	65	Lung	Squamous cell carcinoma	G2-G3	Tumour
F10	70	M	73	Lung	Squamous cell carcinoma	G2-G3	Tumour
F11	71	M	52	Lung	Squamous cell carcinoma	G2-G3	Tumour
F12	72	M	64	Lung	Squamous cell carcinoma	G2-G3	Tumour
G1	73	M	63	Lung	Squamous cell carcinoma	G2-G3	Tumour
G2	74	M	52	Lung	Squamous cell carcinoma	G2-G3	Tumour
G3	75	M	73	Lung	Squamous cell carcinoma	G2-G3	Tumour
G4	76	M	67	Lung	Squamous cell carcinoma	G2-G3	Tumour
G5	77	M	66	Lung	Squamous cell carcinoma	G3	Tumour
G6	78	M	60	Lung	Squamous cell carcinoma	G3	Tumour
G7	79	M	67	Lung	Squamous cell carcinoma	G3	Tumour
G8	80	M	61	Lung	Squamous cell carcinoma	G3	Tumour
G9	81	M	58	Lung	Squamous cell carcinoma	G3	Tumour
G10	82	M	52	Lung	Squamous cell carcinoma	G3	Tumour
G11	83	M	67	Lung	Squamous cell carcinoma	G3	Tumour
G12	84	M	61	Lung	Squamous cell carcinoma	G3	Tumour
H1	85	M	70	Lung	Squamous cell carcinoma	G3	Tumour
H2	86	F	76	Lung	Squamous cell carcinoma	G3	Tumour
H3	87	M	37	Lung	Squamous cell carcinoma	G3	Tumour
H4	88	M	68	Lung	Squamous cell carcinoma	G3	Tumour

<u>Pos</u>	<u>No.</u>	<u>Sex</u>	<u>Age</u>	<u>Organ</u>	<u>Pathology diagnosis</u>	<u>Grade</u>	<u>Type</u>
H5	89	M	68	Lung	Squamous cell carcinoma	G3	Tumour
H6	90	M	68	Lung	Squamous cell carcinoma	G3	Tumour
H7	91	M	68	Lung	Squamous cell carcinoma	G3	Tumour
H8	92	M	68	Lung	Squamous cell carcinoma	G3	Tumour

The grade 1-3 in pathology diagnosis is equivalent to well- differentiated, moderately-differentiated or poorly differentiated tumour, respectively under the microscope:

Grade 1 or well- differentiated: cells appear normal and are not growing rapidly.

Grade 2 or moderately differentiated: cells appear slightly differentiated than normal.

Grade 3 or poorly differentiated: cells appear abnormal and tend to grow and spread more aggressively.

In addition, TNM staging is used in the clinic for prognosis and for informing the therapeutic schemes. The American Joint Committee on Cancer (AJCC) TNM system involves set of criteria related to the lung cancer outlined below.

### **T-groups**

TX: Primary tumour cannot be assessed

T0: No evidence of primary tumour.

T1: A single tumour (any size) that has not grown into blood vessels

T2: Either a single tumour (any size) that has grown into blood vessels, OR more than one tumour where no tumour is larger than 5 cm (about 2 inches) across.

T3a: Multiple tumours with at least one tumour that is greater than 5 cm (about 2 inches) across.

T3b: At least one tumour (any size) that has grown into a major branch of the large veins of the liver (the portal and hepatic veins).

T4: The tumour has grown into a nearby organ (other than the gallbladder), OR the tumour is growing into the thin layer of tissue covering the liver (called the visceral peritoneum).

### **N-groups**

NX: Regional (nearby) lymph nodes cannot assess.

N0: The cancer has not spread to the regional lymph nodes.

N1: The cancer has spread to the regional lymph nodes.

### **M-groups**

M0: The cancer has not spread to distant lymph nodes or other organs.

M1: The cancer has spread to distant lymph nodes or other organs.

The classification of the samples shown above was all squamous cell carcinoma. The information about both the treatments and surgical procedures or survival time was not available.

#### **3. 2. 2. 1. Total p53 protein expression in the human lung cancer tissue microarrays**

In order to determine the total p53 expression in 202 cases (patients) TMA human lung cancer via IHC technique, deparaffinization and rehydration steps were performed to completely remove the paraffin wax and adding the water to the tissues' cores as described previously in materials and methods. Antigen retrieval has employed through heating the slides in Tris-EDTA Buffer pH 9.0 using the Microwave for 15-20 mins, followed by blocking endogenous peroxidase step as per manufacturer recommendation. 1:100 dilutions of Monoclonal Mouse Anti-Tp53 Protein DO-7 (DAKO, UK) were used and brown nuclear staining was indication of positive immunostaining in the results. The staining was manually assessed and classified according to the intensity of the brown colour to "0, 1, 2 and 3 representing the negative staining, weak, moderate, and strong positive staining respectively. The staining results demonstrating the location (cytoplasmic or nuclear or membrane ...etc.) where the target protein was expressed, whereas the increase of the

colour's intensity reflects the amount of the protein levels in this part of the tissue. Examples of different Tp53 protein staining results are illustrated in fig. 3. 29.

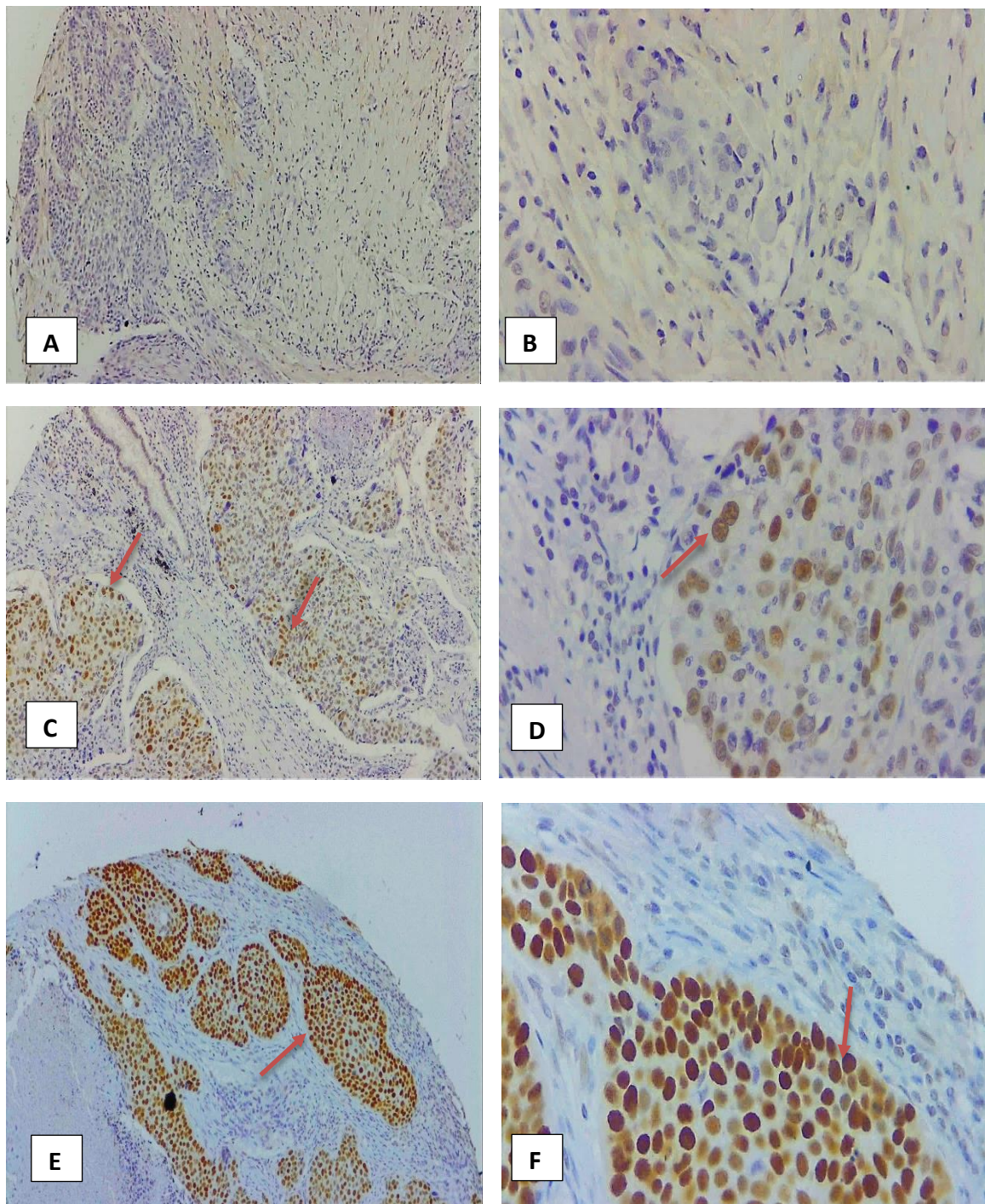


**Figure 3. 29:** Immunoreactivity of the Tp53 protein in paraffin-embedded Human lung cancer tissue microarrays using the Tp53 (DO-7) antibody. A, B shows a negative staining of TMA's case (patient's tissue) at magnification 10x and 40x respectively. C, D Nuclear moderate positive staining (brown staining) of the Tp53 protein in another TMA's case (patient's tissue) at magnification 10x and 40x respectively. E, F Nuclear strong positive staining of Tp53 protein presents the location and the

intensity of the protein in a patient's lung cancer tissue at magnification 10x and 40x respectively. Arrows show the location of positive brown staining.

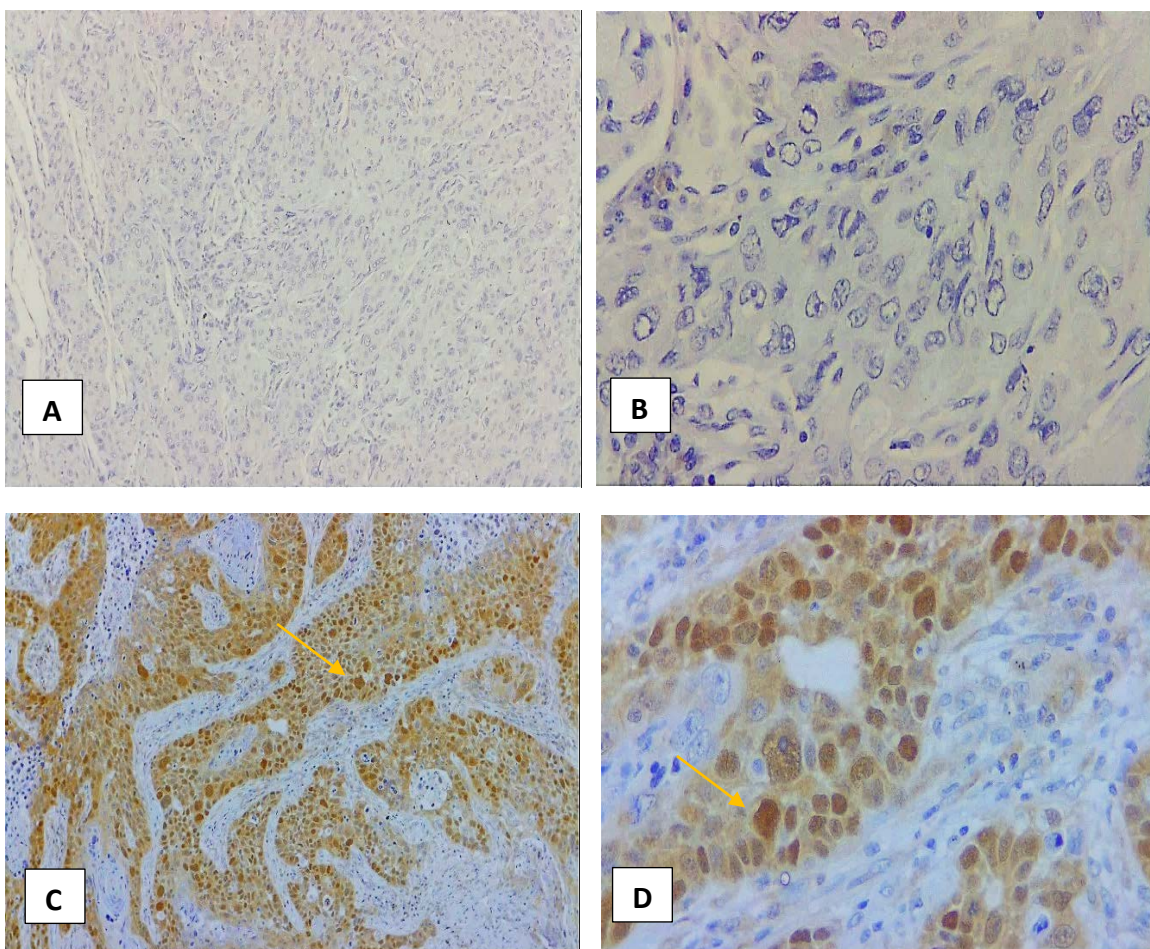
The relationship between Tp53 expression and various clinicopathological features of the non-small cell lung cancer patients' tissues were detected and the analysis was carried out using SPSS Statistics software package. Chi-square tests were conducted for categorical data and  $p$ -value of  $\leq 0.05$  was considered statistically significant. The results were summarized in Table 6. Among the 202 tissue samples, 10 normal lung tissue sections were negative stained and no Tp53 protein expression was demonstrated. For the 192 lung cancer cases, 130 (67.7 %) positively stained for Tp53 in the nuclei of the tumour cells, whereas 62 cases (32.29 %) showed negative staining. Significant correlation ( $p$ -value= 0.001) were found between the Tp53 positive staining and the pathological grade of the cancer for 176 patients. However, no significant correlation was observed between the total p53 expression and age at operation, sex, stage, and the TNM staging ( $p$ -value= 0.527, 0.321, 0.513, 0.558, respectively). Results are represented in table 6.

**Table 6:** The relationship between the total p53 and its acetylated form protein expression and various clinicopathological features of the 202 lung cancer patients using SPSS statistics software and Chi-square test. P- Value = 0.05 was considered as a significant and underlined.

Characteristics	Tp53			K382		
	NO.	Positive	p-Value	NO.	Positive	p-Value
<b>Gender (202 cases)</b>						
Male	171 (84.7 %)	113 (66.1%)	<b>0.231</b>	171 (84.7%)	126 (73.7%)	<b>0.034</b>
Female	31 (15.3 %)	17 (55.9%)		31 (15.3%)	17 (54.8%)	
<b>Age (202 cases)</b>						
>60 y	109 (54 %)	68 (62.4%)	<b>0.527</b>	109 (54.0%)	80 (73.4%)	<b>0.379</b>
<61 y	93 (46 %)	62 (66.7%)		93 (46.0%)	63 (67.7%)	
<b>Grade (176 cases)</b>						
1	6 (3.4 %)	2 (33.3%)	<b>0.001 (***)</b>	6 (3.4%)	4 (66.7%)	<b>0.039</b>
2	88 (50 %)	58 (65.9%)		88 (50.0%)	67 (76.1%)	
3	51 (29 %)	36 (70.6%)		51 (29.0%)	31 (60.8%)	
1-2	20 (11.4 %)	5 (25.0%)		20 (11.4%)	17 (85.0%)	
2-3	11 (6.3 %)	10 (90.9%)		11 (3.6%)	11 (100 %)	
<b>Stage for 110 cases</b>						
I	7 (6.4 %)	4 (57.1%)	<b>0.513</b>	7 (6.4%)	4 (57.1%)	<b>0.884</b>
II	2 (1.8 %)	1 (50.0 %)		2 (1.8%)	1 (50.0%)	
IA	4 (3.6 %)	3 (75.0 %)		4 (3.6%)	3 (75.0%)	
IIA	5 (4.5 %)	3 (60.0 %)		5 (4.5%)	3 (60.0%)	
IIIA	27 (24.5 %)	23 (85.2 %)		27 (24.5%)	16 (59.3%)	
IB	44 (40.0 %)	32 (72.7 %)		44 (40.0%)	25 (56.8%)	
IIB	17 (15.5 %)	9 (52.9 %)		17 (15.5%)	7 (41.2%)	
IIIB	3 (2.7 %)	2 (66.7%)		3 (2.7%)	1 (33.3%)	
IV	1 (0.9 %)	1 (100 %)		1 (0.9%)	1 (100.0%)	
<b>TNM Stage (110 cases)</b>						
T1	9 (8.2%)	6 (66.7 %)	<b>0.558</b>	9 (8.2%)	5 (55.6%)	<b>0.987</b>
T2	78 (70.9%)	53 (67.9%)		78 (70.9%)	44 (56.4%)	
T3	19 (17.3%)	16 (84.2%)		19 (17.3%)	10 (52.6%)	
T4	4 (3.6%)	3 (75.0%)		4 (3.6%)	2 (50.0%)	
M0	109 (99.1%)	77 (70.6%)	<b>0.520</b>	109 (99.1%)	60 (55.0%)	<b>0.368</b>
M1	1 (0.9%)	1 (100%)		1 (0.9%)	1 (100.0%)	
N0	58 (52.7%)	41 (70.7%)	<b>0.957</b>	58 (52.7%)	32 (55.2%)	<b>0.950</b>
N1	52 (47.3 %)	37 (71.2%)		52 (47.3%)	29 (55.8%)	
<b>P53 Intensity</b>						
WEAK		55 (42.3%)		55 (42.3%)	38 (69.1%)	<b>0.195</b>
MODERATE		34 (26.2 %)		34 (26.2%)	24 (70.6%)	
STRONG		41 (31.5%)		41 (31.5%)	35 (85.4%)	
<b>K382 Intensity</b>						
WEAK	67 (46.9%)	45 (67.2%)	<b>0.942</b>		67 (46.9%)	
MODERATE	52 (36.4%)	35 (67.3%)			52 (36.4%)	
STRONG	24 (16.8%)	17 (70.8%)			24 (16.8%)	
<b>S46 Intensity</b>						
WEAK	88 (49.2%)	59 (67.0 %)	<b>0.852</b>	88 (49.2%)	61 (69.3%)	<b>0.89</b>
MODERATE	70 (39.1%)	44 (62.9%)		70 (39.1%)	56 (80.0%)	
STRONG	21 (11.7 %)	14 (66.7%)		21 (11.7%)	12 (57.1%)	
<b>TTC5 Intensity</b>						
WEAK	97 (59.9%)	68 (70.1 %)	<b>0.455</b>	97 (59.9%)	71 (73.2%)	<b>0.130</b>
MODERATE	39 (24.1%)	25 (64.1 %)		39 (24.1%)	29 (74.4%)	
STRONG	26 (16.0%)	15 (57.7%)		26 (16.0%)	14 (53.8%)	

### 3. 2. 2. 2. Detection of the acetylated-p53 at lysine 382 protein expression in the human lung cancer tissue microarrays

In the present study, for detecting the expression of acetylated p53 protein at lysine 382, 1:50 dilutions of rabbit polyclonal antibody (BIOSS) has employed as primary antibody followed by pre-treatment of the sections using heat mediated antigen retrieval with Tris-sodium citrate buffer pH 6 for 15- 20mins. Other IHC procedure's steps were performed as described in the materials and methods and example of the staining results are presented in fig. 3. 30.



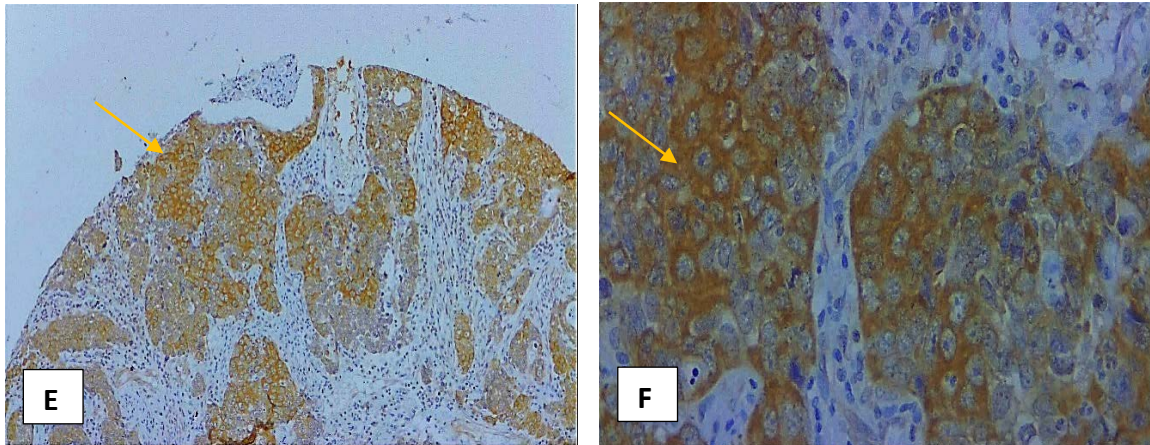


**Figure 3. 30:** Immunostaining of the acetylated-p53 at lysine 382 protein expression in paraffin-embedded human Lung cancer tissue microarrays using the polyclonal anti-acetyl-p53 (K382) antibody. A, B shows a negative staining of TMA's case (patient's tissue) at magnification 10x and 40x respectively. C, D Nuclear and cytoplasmic moderate positive staining (brown staining) in another TMA's cases (patient's tissue) at magnification 10x and 40x respectively. E, F Cytoplasmic strong positive staining showing the location and the intensity of this protein at magnification 10x and 40x respectively. Arrows shown the location of positive brown staining.

The incidence of positive acetylated p53 at lysine 382 expression was 126 (73.7%) and 17 (54.8%) in gender group (Male and Female) of the patients, respectively ( $p$ -value = 0.034), which is considered a significant correlation. In addition, a significant correlation also was indicated between the protein expression and the cancer grade ( $p$ -value = 0.039, whereas; insignificant correlation was determined in each of stage, TNM staging, and Age ( $p$ -Value = 0.884, 0.987, 0.379, respectively). The results are illustrated in Table 6.

### 3. 2. 2. 3. Detection of the phosphorylated-p53 at Ser-46 protein expression in the human lung cancer tissue microarrays

The frequency of phosphorylated-p53 at Ser-46 protein expression was investigated and the prognostic significance of the biological markers, as detected via immunoreactivity using specific mouse monoclonal antibody (Abnova) in 202 TMA cases lung cancers, was analysed. For antigen retrieval step, the TMA's tissues slide was heated in Tris-EDTA buffer pH 9 for 15-20 mins as explained above. The primary anti-phospho-p53 (Ser-46) antibody has diluted at 1:100 and incubated with the sections for one and half hours at RT. The staining results' examples are presented in fig. 3. 31.

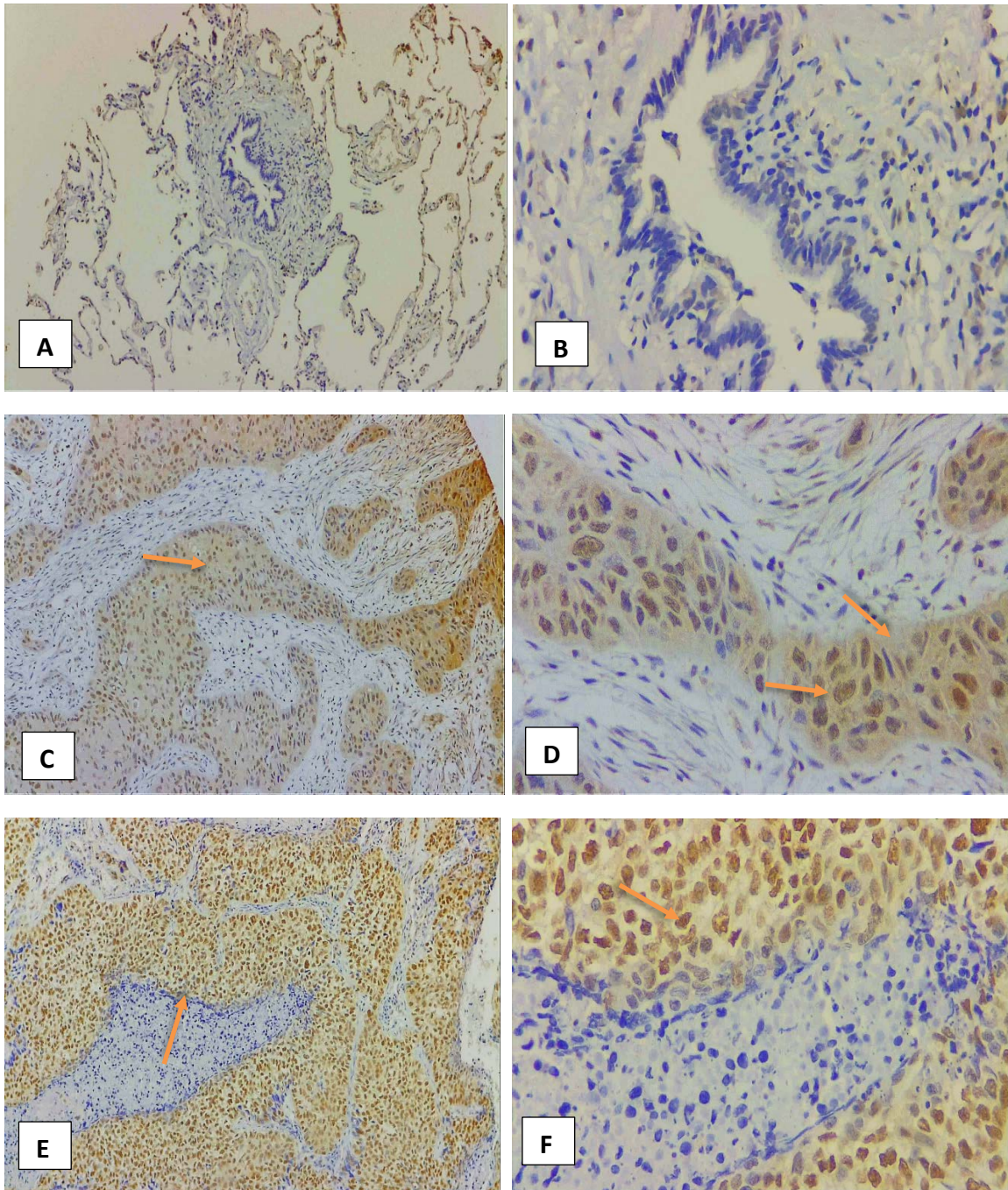


**Figure 3. 31:** Immunostaining of the phospho-p53 at Ser-46 protein expression in paraffin-embedded human Lung cancer tissue microarrays using anti-phospho-p53 (Ser-46) antibody. A, B Shows a negative staining of TMA's case (patient's tissue) at magnification 10x and 40x respectively. C, D Nuclear and cytoplasmic moderate positive staining (brown staining) in another TMA's cases (patient's tissue) at magnification 10x and 40x respectively. E, F Nuclear strong positive staining of the Ser-46 protein, shows the location and the intensity in a patient's lung cancer tissue at magnification 10x and 40x respectively. Arrows show the location of positive brown staining.

The incidence of a positive expression of phosphorylated-p53 at Ser-46 in the 192 TMA cases were 179 (93.2 %) and only 13 (6.77 %) cases showed negative staining. Pathological cancer grade was available in 176 cases (patients) including (n=6) grade 1, (n=88) grade 2, (n=51) grade 3, (n=20) grade 1-2, (n=11) grade 2-3. A highly significant correlation was indicated between the phospho-p53 at Ser-46 and the pathological grade of cancer ( $p$ -value= 0019). Furthermore, a significant correlation between the intensity of this isoform and the expression of the TTC5 protein was detected ( $p$ -Value =0.004). In addition, as the age of patients was classified to two groups, 101 (92.7 %) of the older than 60 years group showed positive staining and 78 (83.9 %) of the younger group of patients (<61 years) expressed the protein. This correlation was determined as a significant with  $p$ - Value = 0.050, whereas no significant correlation was observed between the protein expression and gender, stage of cancer, and TNM staging including the metastasis to distance lymph nodes and other organs ( $p$ -value= 0.336, 0.643, 0.490, 0.308, 0.646, respectively). The results are presented in the table 7.

**Table 7:** The correlation between the phosphorylated form of p53 (Ser-46) and the TTC5 protein expression with various clinicopathological features of the 202 lung cancer patients using SPSS statistics software and Chi-square test. **P- Value = 0.05** considered as a significant.

Characteristics	S46			TTC5				
	NO.	Positive	p-Value	NO	Positive	p-Value		
<b>Gender (202 cases)</b>								
Male	171(84.7%)	153 (89.5%)	<b>0.336</b>	171 (84.7%)	134 (78.4%)	<b>0.124</b>		
Female	31 (15.3%)	26 (83.9%)		31 (15.3%)	28 (90.3%)			
<b>Age (202 cases)</b>								
>60 y	109 (54.0%)	101 (92.7%)	<b>0.050</b>	109 (54.0%)	81 (74.3%)	<b>0.023</b>		
<61 y	93 (46.0%)	78 (83.9%)		93 (46.0%)	81 (87.1%)			
<b>Grade (176 cases)</b>								
1	6 (3.4%)	6 (100.0%)	<b>0.019</b>	6 (3.4%)	5 (83.3%)	<b>0.039</b>		
2	88 (50.0%)	84 (95.5%)		88 (50.0%)	73 (83.0%)			
3	51 (29.0%)	42 (82.4%)		51 (29.0%)	43 (84.3%)			
1-2	20 (11.4%)	20 (100.0%)		20 (11.4%)	12 (60.0%)			
2-3	11(6.3%)	11 (100.0%)		11 (6.3%)	6 (54.5%)			
<b>Stage (110 cases)</b>								
I	7(6.4%)	5 (71.4%)	<b>0.643</b>	7 (6.4%)	6 (85.7%)	<b>0.889</b>		
II	2 (1.8%)	1 (50.0%)		2 (1.8%)	2 (100.0%)			
IA	4 (3.6%)	4 (100.0%)		4 (3.6%)	4 (100.0%)			
IIA	5 (4.5%)	3 (60.0%)		5 (4.5%)	5 (100.0%)			
IIIA	27 (24.5%)	22 (81.5%)		27 (24.5%)	26 (96.3%)			
IB	44 (40.0%)	38 (86.4%)		44 (40.0%)	41 (93.2%)			
IIB	17 (15.5%)	14 (82.4%)		17 (15.5%)	17 (100.0%)			
IIIB	3 (2.7%)	3 (100.0%)		3 (2.7%)	3 (100.0%)			
IV	1 (0.9%)	1 (100.0%)		1 (0.9%)	1 (100.0%)			
<b>TNM staging</b>								
<b>T (110 cases)</b>								
T1	9 (8.2%)	6 (66.7%)		<b>0.490</b>	9 (8.2%)		7 (77.8%)	<b>0.053</b>
T2	78 (70.9%)	65 (83.3%)			78 (70.9%)		75 (96.2%)	
T3	19 (17.3%)	17 (89.5%)			19 (17.3%)		19 (100.0%)	
T4	4 (3.6%)	3 (75.0%)	4 (3.6%)		4 (100.0%)			
<b>M (110 cases)</b>								
M0	109 (99.1%)	90 (82.6%)	<b>0.646</b>	109 (99.1%)	104 (95.4%)	<b>0.826</b>		
M1	1 (0.9%)	1 (100.0%)		1 (0.9%)	1 (100.0%)			
<b>N (110 cases)</b>								
N0	58 (52.7%)	50 (86.2%)	<b>0.308</b>	58 (52.7%)	55 (94.8%)	<b>0.739</b>		
N1	52 (47.3%)	41 (78.8%)		52 (47.3%)	50 (96.2%)			
<b>P53 Intensity (130 cases)</b>								
Weak	55 (42.3%)	50 (90.9%)	<b>0.851</b>	55 (42.3%)	44 (80.0%)	<b>0.334</b>		
Moderate	34 (26.2%)	31 (91.2%)		34 (26.2%)	27 (79.4%)			
Strong	41 (31.5%)	36 (87.8%)		41 (31.5%)	37 (90.2%)			
<b>K382 Intensity (143 cases)</b>								
Weak	67 (46.9%)	58 (86.6%)	<b>0.346</b>	67 (46.9%)	57 (85.1%)	<b>0.327</b>		
Moderate	52 (36.4%)	48 (92.3%)		52 (36.4%)	39 (75.0%)			
Strong	24 (16.8%)	23 (95.8%)		24 (16.8%)	18 (75.0%)			
<b>S46 Intensity (176 cases)</b>								
Weak		88 (49.2%)		88 (49.2%)	64 (72.7%)	<b>0.021</b>		
Moderate		70 (39.1%)		70 (39.1%)	62 (88.6%)			
Strong		21 (11.7%)		21 (11.7%)	19 (90.5%)			
<b>TTC5 Intensity (162 cases)</b>								
Weak	97 (59.9%)	86 (88.7%)	<b>0.381</b>		97 (59.9%)			
Moderate	39 (24.1%)	37 (94.9%)			39 (24.1%)			
Strong	26 (16.0%)	22 (84.6%)			26 (16.0%)			

### 3. 2. 2. 4. Detection of TTC5 protein expression in the human lung cancer tissue microarrays

For investigating the protein expression of the TTC5 (Tetratricopeptide repeat domain 5) in the 202 paraffin embedded human lung cancer TMA, dilution 1:100 of rabbit polyclonal anti-TTC5 antibody from Abcam was used. In addition, Trisodium citrate buffer pH 6 was applied for antigen retrieval procedure and magnification 10x and 40x were used for taking the images and the results' examples presented in the fig. 3. 32.

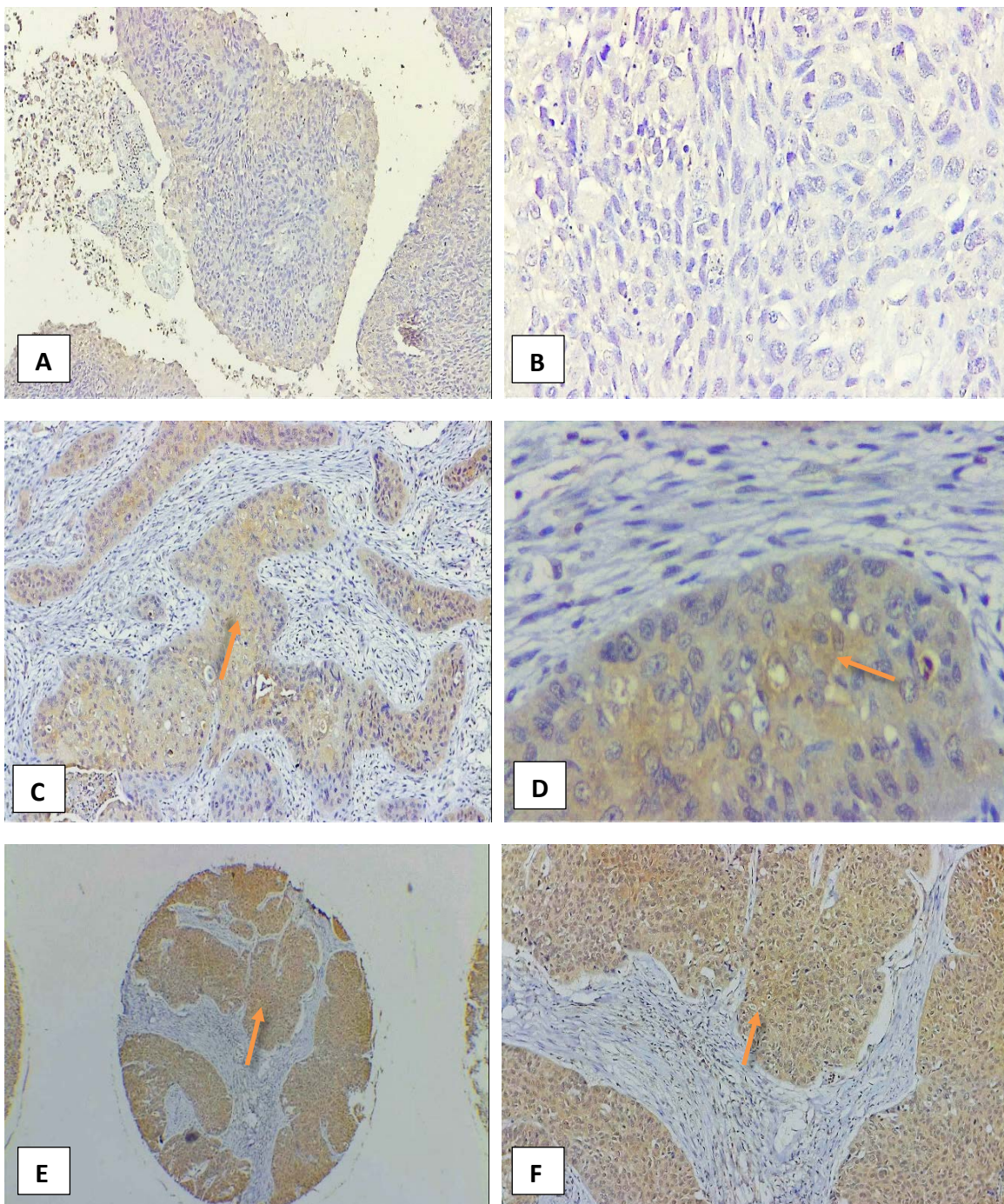


**Figure 3. 32:** The TTC5 protein expression in paraffin-embedded human lung cancer tissue microarrays using the polyclonal anti-TTC5 antibody. A, B Shows a negative TTC5 staining in one of tissue's patients at magnification 10x and 40x respectively. C, D Cytoplasmic weak positive staining (brown staining) in another TMA's cases (patient's tissue) at magnification 10x and 40x respectively. E, F Cytoplasmic and nuclear moderate positive staining of the TTC5 protein shows the intensity of this protein in a patient's lung cancer tissue at magnification 4X and 10X respectively. Arrows show the location of positive brown staining.

The incidence of TTC5 expression was investigated and the prognostic significance of the biological markers, as detected by immunohistochemistry using specific anti-TTC5 antibody in 202 TMA Lung cancers, was analysed. 162 cases (84.4 %) positively stained for TTC5, generally in the cytoplasm of the cancer cells and, only thirty cases (15.6 %) showed negative staining. The staining intensity which reflects the protein expression was between weak to moderate and no strong staining has observed. Significant correlation was observed between the TTC5 protein expression and age, grade, tumour size and the intensity of Ser-46 protein expression ( $P$ -Value = 0.023, 0.039, 0.053, and 0.021 respectively). Furthermore, insignificant correlations were found between the protein expression and other clinicopathological variables including gender, the stage of the lung cancer, metastases to other organs or to the distance of lymph nodes ( $p$ -value= 0.124, 0.889, 0.826, and 0.739 respectively) and with the other proteins' expression including Tp53 and the acetylated form of p53. The results are shown in the table 7.

### 3. 3. CO-Immunoprecipitation results

To investigate the protein– protein interaction between Tp53 and its cofactor TTC5, the CO-IP technique was used. The Mero-14 cancer cells were grown and treated with 20  $\mu$ M Etoposide then the cellular lysate was extracted, and protein concentration measured. About 50  $\mu$ l of the extract was used as input sample and the rest of the samples were divided to two equals amounts. The first divided sample was incubated with the TTC5 antibody and the other sample was incubated with IgG antibody as described in materials and methods. The protein A agarose beads were washed to remove unbound proteins then blotted with the Tp53 antibody (DO-1). The results are presented in figure 3. 33. The same membrane was incubated with Actin Ab (Abcam) after stripping the membrane and the results are presented in the figure 3. 34.

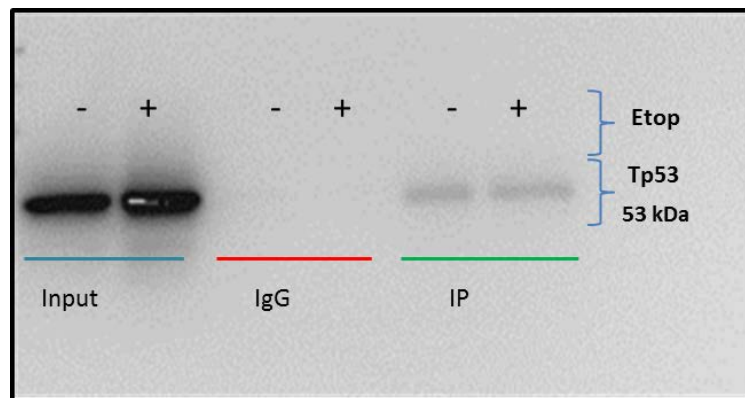


**Figure 3. 33:** CO-Immunoprecipitation results for Mero-14 cells shows the bands with the Tp53 Ab (DO-1). Samples were incubated with mouse anti-Tp53 Ab and bands detected in Input and IP positions but not with IgG.

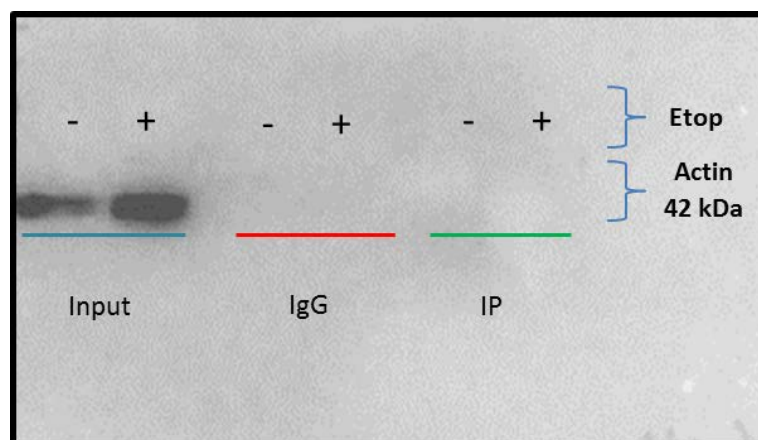


**Figure 3. 34:** CO-Immunoprecipitation results for Mero-14 showed the blotting bands with the Actin. Samples were incubated with rabbit anti-Actin Ab and bands detected in Input positions but not with IP and IgG.

To summarise, this experiment showed an interaction between the p53 protein and its co-factor (TTC5) protein, based on co-immunoprecipitation of the p53 protein after interaction with the TTC5 and confirmed the relation between the p53 and its cofactor.

### 3.4. Immunofluorescence results

Given that IHC results showed a cytoplasmic staining of the acetylated form of p53 at lysine 382 in some tissue samples from lung cancer patients, here we analysed the expression of this isoform in studied cell lines using IF technique.

#### 3.4.1 Determination of the acetylated p53 (K382) expression location in the A549 cell lines:

The lung cancer cells were grown and treated or not using 20  $\mu$ M Etoposide for 24 hours, then the cells were fixed and nucleus stained by DAPI stain (blue). Two primary antibodies, anti-K382 mouse monoclonal Antibody (1G7) and anti-TTC5 Rabbit polyclonal antibody were applied. Secondary antibody anti-Mouse with red fluorescent tag and another secondary antibody anti-Rabbit with green fluorescent tag were used and results presented in figure 3. 35 and 3. 36.

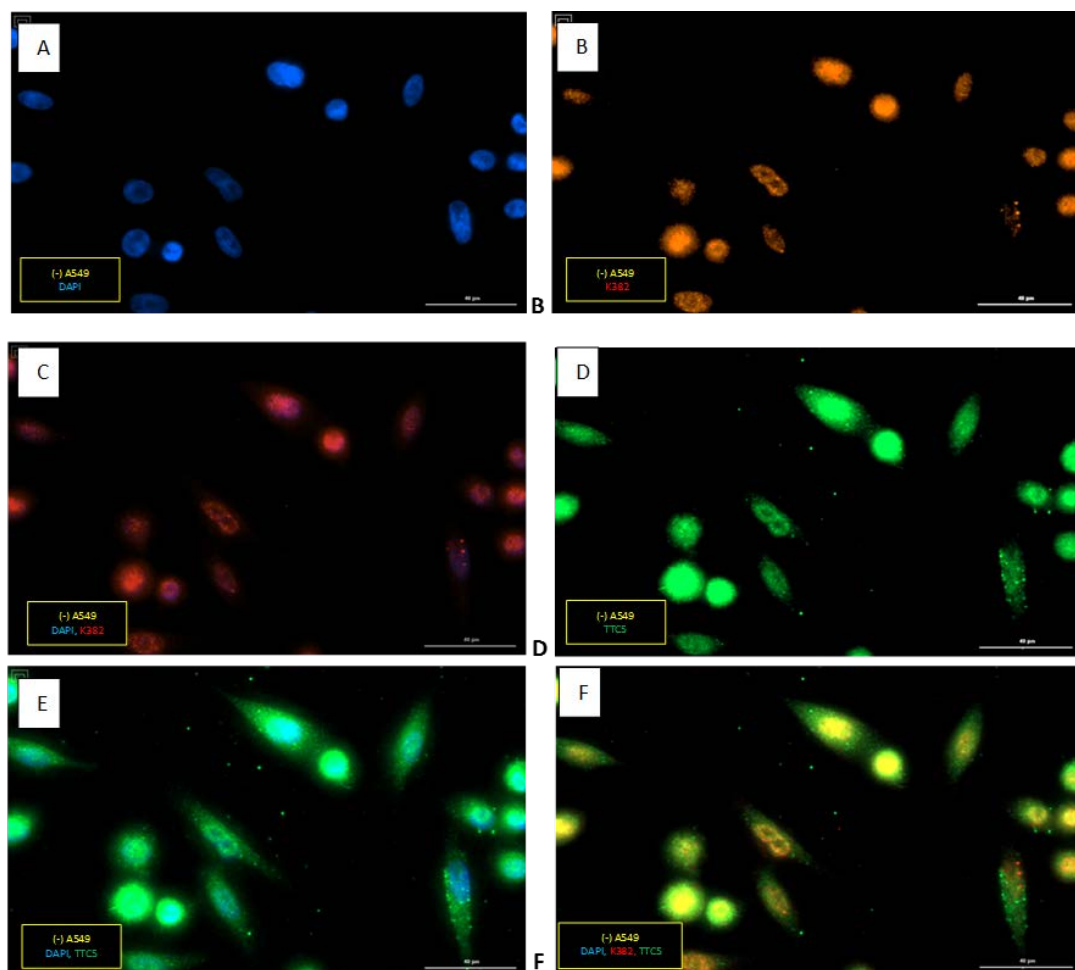


**Figure 3. 35:** The location of p53 acetylated at lysine 382 and TTC5 proteins in untreated A549 cell lines. Blue DAPI staining (A). Nuclear RED fluorescent staining for K382 protein (B, C, F). Nuclear and cytoplasmic GREEN fluorescent staining for TTC5 protein (D, E). Merged images of cells stained with DAPI, K382 and TTC5 staining (F). Magnification 20x was applied to all slides.

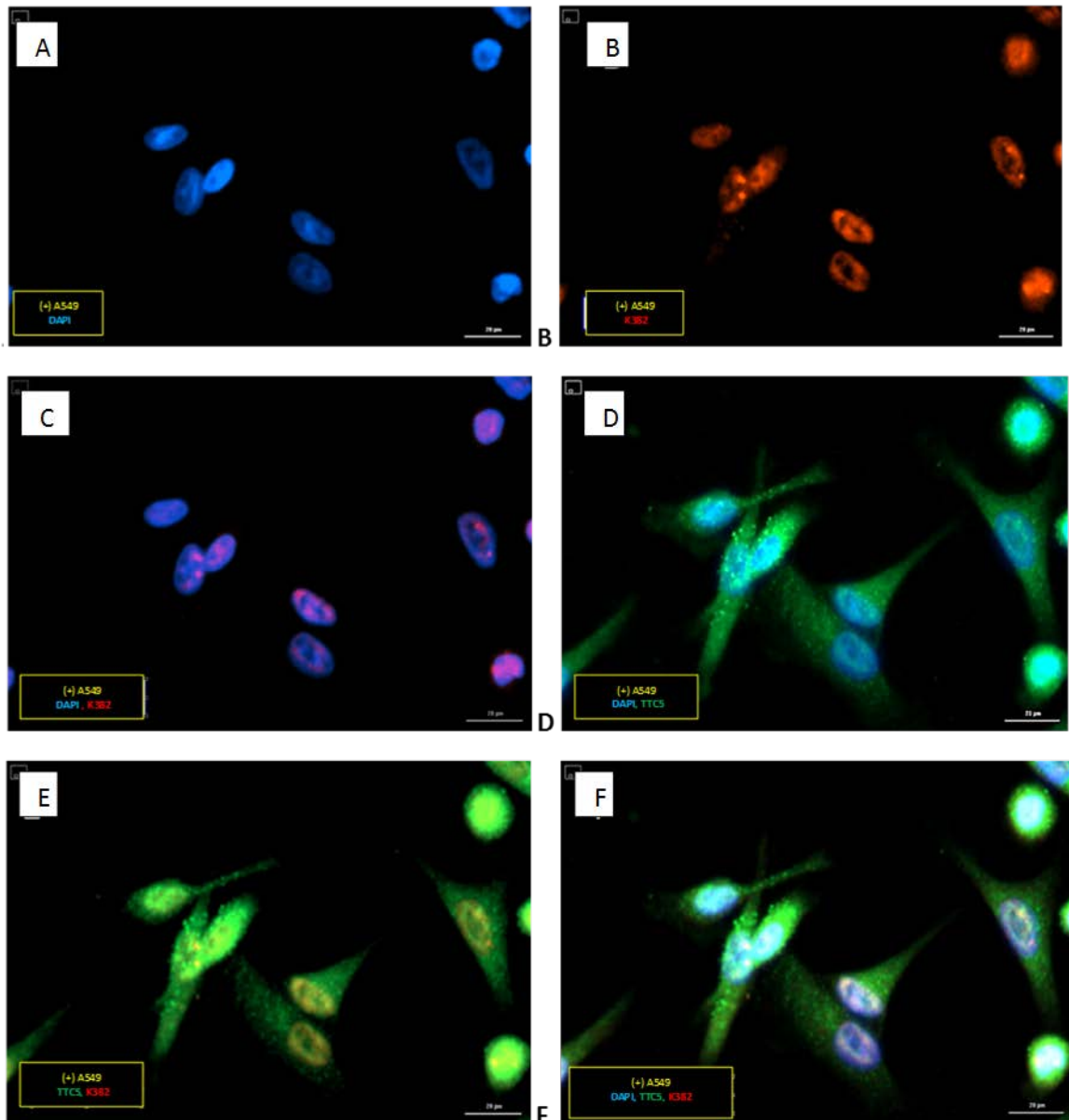


**Figure 3. 36:** The location of p53 acetylated at lysine 382 and TTC5 proteins in treated A549 cell lines. Blue DAPI staining (A). Nuclear RED fluorescent staining for K382 protein (B, C, E, F). Nuclear and cytoplasmic GREEN fluorescent staining for TTC5 protein (D, E). Merged images of cells stained with DAPI, K382 and TTC5 staining (F). Magnification 20x was applied to all slides.

In A549 cells, the immunofluorescence staining of K382 protein were clearly observed to be in the nucleus, while TTC5 protein was observed to be in both nucleus and cytoplasm. Analysis of Mero-14 cells was inconclusive; therefore we carried out this experiment in osteosarcoma cell lines (U2OS) as a control.

### 3.4.2 Determination of the acetylated p53 (K382) expression location in the U2OS cell lines

The U2OS cells were grown as described above in DMEM media. The cells were then fixed and stained by red fluorescent staining for the acetylated p53 protein (K382) and green fluorescent staining for TTC5 protein. The results are presented in the figure 3. 37.

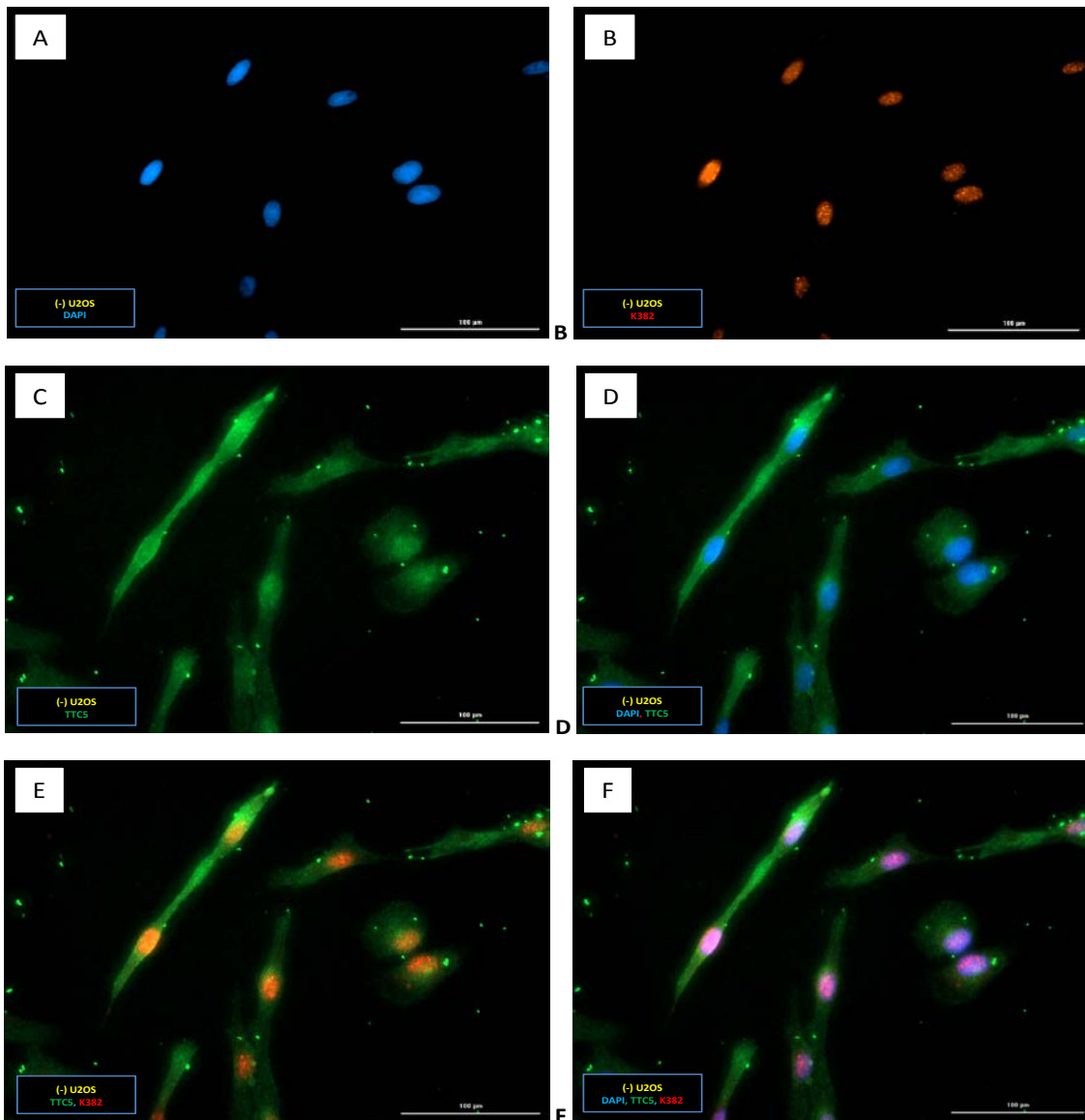


**Figure 3. 37:** The location of p53 acetylated at lysine 382 and TTC5 proteins in U2OS cell line. Blue DAPI staining (A). Nuclear RED fluorescent staining for K382 protein (B, E, F). Nuclear and cytoplasmic GREEN fluorescent staining for TTC5 protein (C, D, E, F). Merged all of staining DAPI, K382 and TTC5 (F). Magnification 10x was applied to all slides.

In the next figure (fig. 3. 38), the same stained U2OS cells images were zoomed in for more clarity of the location of the K382 and TTC5 protein expression.

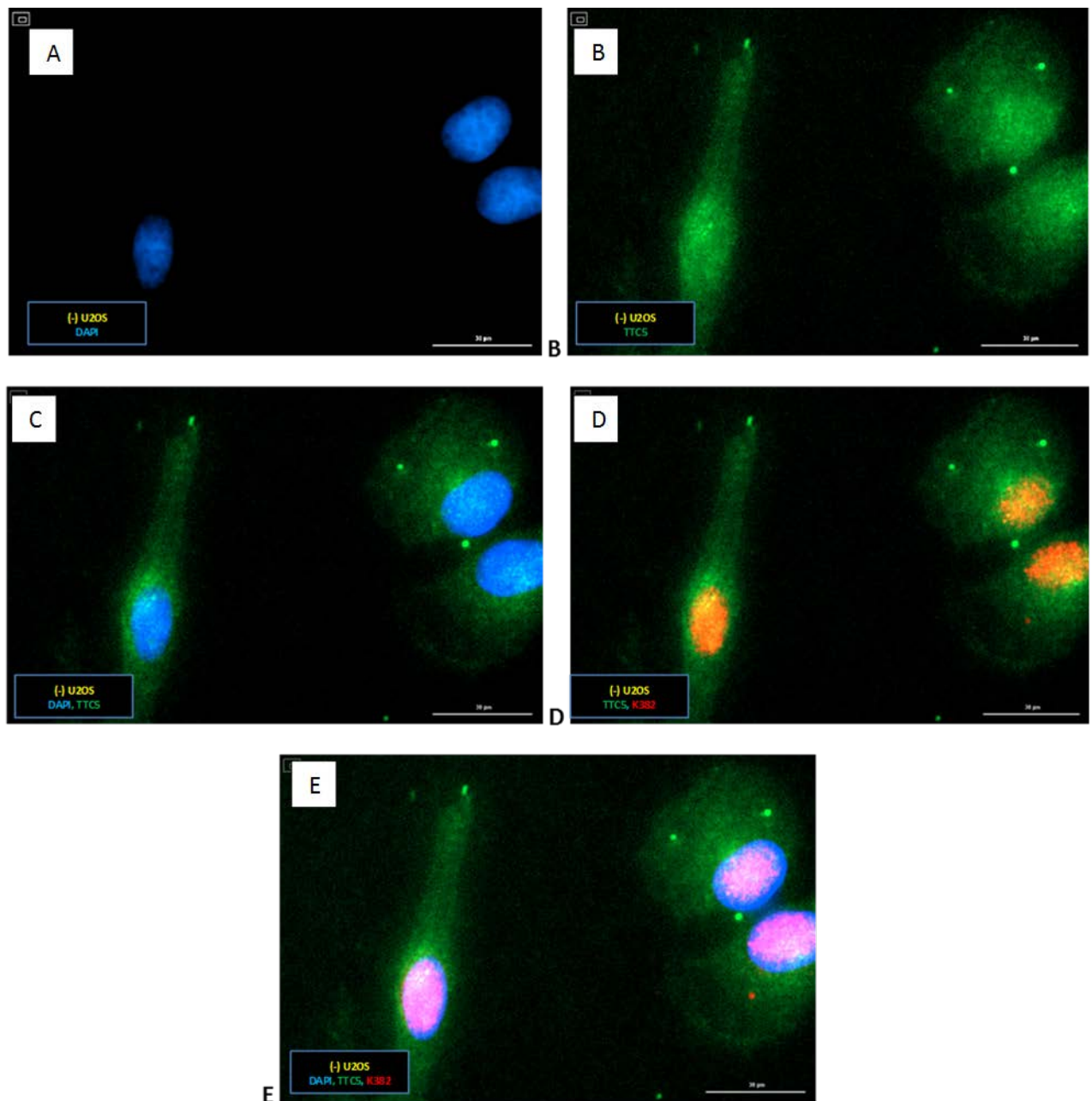


**Figure 3. 38.** Shown the location of K382 protein expression in U2OS cell lines for zoomed images. Nuclear RED fluorescent staining for K382 protein (D, E). Nuclear and cytoplasmic GREEN fluorescent staining for TTC5 protein (B, C, D, E). Blue DAPI staining (A). Merged staining for DAPI, K382 and TTC5 (E). Magnification 40x were applied for all.

In U2OS cell line the results also shown a clear fluorescent staining of K382 protein in the nucleus, whereas, nucleus and cytoplasm staining were observed for the TTC5 protein. As

conclusion of the immunofluorescence staining of cancer cell lines, we demonstrated that the acetylated form of p53 at lysine 382 protein was expressed generally in the nucleus and not in the cytoplasm. On the other hand, the TTC5 protein was expressed and presented in the nucleus and the cytoplasm in all studied cell lines.

### 3. 5 Detection of the expression of microRNA-34 in lung and mesothelioma cell lines using QRT-PCR

Previous publications demonstrated the important impacts of microRNA-34a and b family on the regulation of p53 network; therefore we investigated the expression levels of a specific miRNAs' members (miR-34a, miR-34b) in lung and mesothelioma cell lines using the quantitative real-time RT-PCR technique in the presence and absence of the DNA damage. Applied Biosystems™ TaqMan™ MicroRNA Reverse Transcription Kit was applied to produce the cDNA. The miR-34a, b expression levels were normalized to RNUU44 control.

#### 3. 5. 1 Determination of the expression of miR-34a and miR-34b family members in the lung cancer (A549) cell lines in the presence or absence of DNA damage:

The lung cancer A549 cells were maintained as previously mentioned then treated or not by 20  $\mu$ M Etoposide to induce the DNA damage. The mirVana™ miRNA isolation kit (Ambion) following the manufacturer's protocol was used to convert from total RNA to the template miRNA cDNA as explained in the materials and methods and the experiment was carried out using the qRT-PCR machine (Rotor-Gene Q). The experiments were repeated minimum three times and represented in the figure 3. 39. RNUU44 was used for normalisation, and DDCT calculations were applied. Results with  $p \leq 0.05$  value were considered statistically significant.

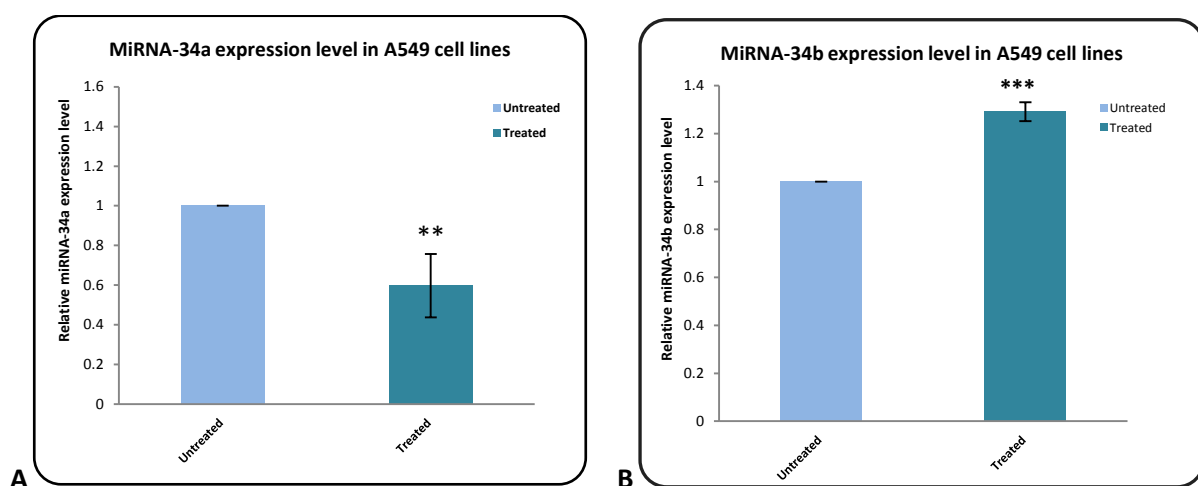


**Figure 3. 39:** Histograms show relative expressions of miR-34a, b in the A549 cancer cells with or without an induced DNA damage by used 20  $\mu$ M of Etoposide for 24 hours. Expression level of miR-

34a (A) and miR-34b (B) was detected in Etoposide treated and untreated cells. Expression levels of miR-34a, b was normalized to RNUU44 and Data is representative of the average of three independent experiments +/- SEM. *P*-value  $\leq 0.05$  is indicated by \*.

Significant downregulation (*p*-Value= 0.0036) of miR-34a expression in this Lung cancer cell lines have observed (0.4 fold), which is in contrast with the upregulation of Tp53 protein level under the same condition. On other hand, a statistically significant and slight (1.3 fold) increase (*p*-Value= 0.0017) of miR-34b expression was determined.

### 3. 5. 2 Determination of the expression of miR-34a and miR-34b family members in the mesothelioma (Mero-25) cell lines in the presence or absence of DNA damage

As previously described in the materials and methods, Mero-25 cells were treated or not with 20  $\mu$ M Etoposide followed by the miRNAs extraction as per manufacturer's guidelines. At least three independent experiments were performed and represented in the figure 3. 40.

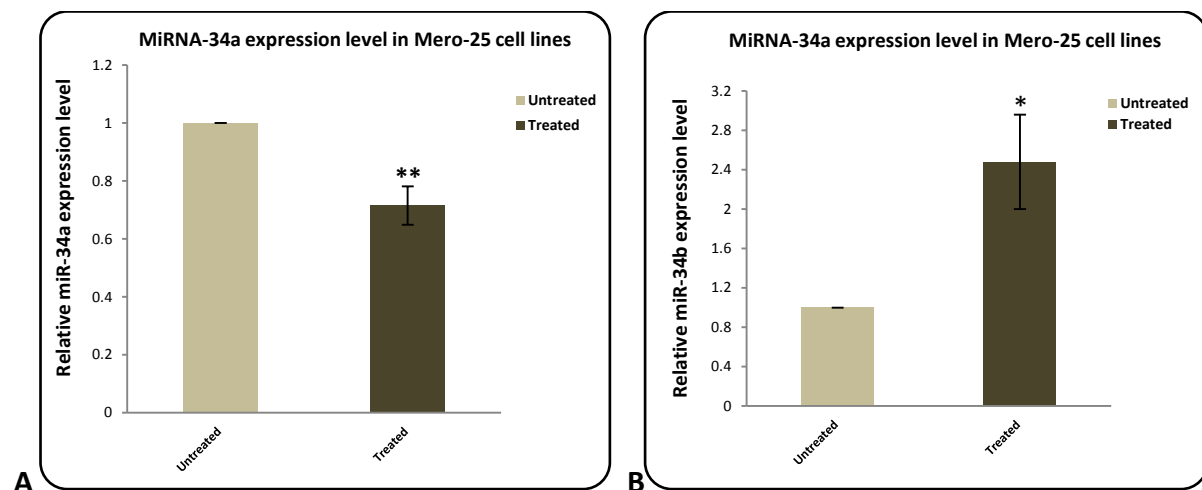


**Figure 3. 40:** Bar charts show the relative miR-34a, b expression in the Mero-25 Mesothelioma cells in presence and absence of DNA damage. Expression level of miR-34a (A) and miR-34b (B) was detected in Etoposide treated and untreated mesothelioma cells. All expression levels of miR-34a, b has normalized to RNUU44 and Data is representative of the average of three independent experiments +/- SEM. *P*-value  $\leq 0.05$  is indicated by \*.

Consistent with the results obtained from analysis of lung cancer cells, a significant decrease (*p*-Value= 0.010) of miR-34a expression level in this type of mesothelioma cell lines were

detected (0.3 fold) compared to untreated cells. Furthermore, high (2.4 fold) and significant increase ( $p$ -Value= 0.023) of miR-34b expressions was observed in at least three independent experiments.

### 3. 5. 3 Determination of the expression of miR-34a and miR-34b family members in the mesothelioma (Mero-14) cell lines in the presence or absence of DNA damage

To determine if the result obtained above was specific for certain cell lines or can be observed in many cell lines, another mesothelioma cell line Mero-14 was used. Mero-14 cell lines were grown and treated as detailed above, followed by extracting and measuring the purity and the concentration of RNAs by using the NanoDrop 2000, before reverse transcription was performed. Samples were prepared for the quantitative real-time RT-PCR according to manufacturer instructions and the results of at least three independent experiments presented at figure 3. 41.

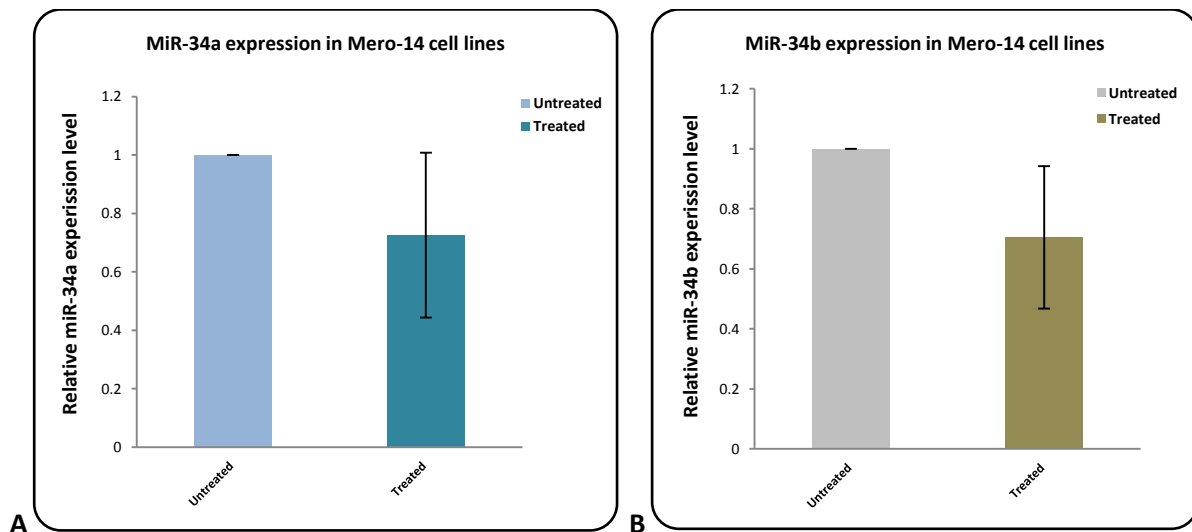


**Figure 3. 41:** Histograms show the relative expression of the two members of miR-34 family (a, b) in the Mero-14 Mesothelioma cells with or without induced DNA damage. Expression level of miR-34a (A) and miR-34b (B) was detected in presence and absence of Etoposide treatment. All expression levels of miR-34a, b has normalized to RNUU44 and Data is representative of the average of three independent experiments +/- SEM.  $P$ -value  $\leq 0.05$  is indicated by \*.

The results revealed that miR-34a expression was lower (0.3 fold) in the treated Mero-14 cells than in untreated cells which was consistent with its expression in each of Mero-25 and

A549 cancer cells, however this was not statistically significant. Furthermore; in contrast with the results of these cell lines, miR-34b expression was decreased (0.3 fold) in treated Mero-14 cells comparing to both Mero-25 and A549 cells, however this change was not statistically significant.

As conclusion, decrease in the miR-34a expression levels was observed in treated A549, Mero-25 with the similar trend observed in Mero-14 cancer cells compared to untreated cells, whereas the expression of miR-34b was elevated in each of treated A549 and Mero-25 but not in treated Mero-14 mesothelioma cell lines.

## Chapter 4. Discussion

The tumour suppressor p53 is a short-lived protein and remains at low expression levels in unstressed cells. P53 is ubiquitinated via binding with MDM2 and other proteins leading to the degradation of p53 protein through the 26S proteasome. The protein levels increase due to posttranslational modifications such as phosphorylation and acetylation in response to the DNA damage, which increases stability and transcriptional activity (Zhao *et al.*, 2006). P300/CREB-binding protein (CBP) and p300/CBP-associated factor (PCAF) are transcriptional co-activators that acetylate p53 at K373/K382 and K320, respectively and are linked to its ability to regulate cell cycle arrest and apoptosis (Guo *et al.*, 2000; Ito *et al.*, 2001; Luo *et al.*, 2000). Furthermore, p53 phosphorylation at Ser15 increases binding to CBP and p300 (Zhao *et al.*, 2006), p53 phosphorylation at the Ser20 or Thr18 plays a vital role in the p300-p53 complex stability (Dornan & Hupp, 2001; MacPherson *et al.*, 2004). P53 phosphorylation at Ser46 was identified as a specific posttranslational modification involved in the programmed cell death (apoptosis) regulation. Inducing DNA damage via ultra violet irradiation or anti-cancer drugs medications like cisplatin and doxorubicin, leads to activation of HIPK2 that specifically phosphorylates p53 at Ser46 and this activation is essential for the apoptosis induction (Rinaldo *et al.*, 2007).

These studies elucidate that the biological consequences of p53 activation promoted via stress signals may be dependent on posttranslational modifications of the p53 at specific sites (Zhao *et al.*, 2006). Previous studies demonstrated that p53 is latent in unstressed cells and it was activated when cells are exposed to DNA damage or genotoxic agents, during which p53 is acetylated or phosphorylated, leading to its accumulation in the nucleus at its target genes (Gu & Roeder, 1997; Hupp & Lane, 1994; Liu *et al.*, 1999).

Tetratricopeptide repeat domain 5 (TTC5), or also called the stress responsive activator of p300 (Strap) is a stress-inducible transcription cofactor, which interacts with EP300 histone acetyltransferase leading to enhanced response of Tp53. TTC5 has essential roles in DNA damage and heat-shock responses and was firstly discovered in complex with (JMY) junction mediating and regulatory protein and the histone acetyltransferase P300 (Demonacos *et al.*, 2001; Demonacos *et al.*, 2004). TTC5 enhances the EP300 and JMY interaction, leading to increase of the HAT activity of EP300, which promotes the Tp53 acetylation, stability and

transcriptional activation leading to appropriate response to DNA damage (Demonacos *et al.*, 2001). In Etoposide-treated cells, phosphorylation of TTC5 via ATM at S203 and CHK2 at S221 promotes its nuclear accumulation and stability and leads to enhanced Tp53 activity and promotion of apoptosis (Demonacos *et al.*, 2004).

In this study, we aim to determine the possible correlation between the p53 posttranslational modifications and the TTC5 (Strap) firstly, in the A549 lung cancer cell lines, Mero-14 and Mero-25 mesothelioma cell lines and secondly, in the human lung cancer tissues to determine if they can be used as biomarkers of these diseases or as a drug targets. To induce DNA damage, the A549 and Mero-25 cell lines were treated with 20  $\mu$ M Etoposide (topoisomerase II inhibitor) which is an anti-neoplastic treatment, generally used to induce double strand DNA damage leading to apoptosis. Topoisomerase II is a nuclear enzyme, which functions throughout both DNA replication and transcription preventing “knots” from forming in DNA by allowing the passage of an intact section of the helical DNA during a transient double strand break. This leads to stabilization of the complex formed via topoisomerase II and induces the 5-cleaved ends of the DNA, therefore DNA double strand breaks (DSBs). This DNA damage leads to activation of the programmed cell death (Karpinich *et al.*, 2002).

#### **4. 1. Analysis of p53 total, its modified isoforms and TTC5 protein levels in cancer cell lines:**

Western blotting technique was performed to detect the total p53 expression level and its isoforms (Ser46 and K382) in addition to TTC5 co-factor. As expected, p53 was significantly upregulated and the protein levels were raised in response to the induced DNA damage in A549 and Mero-14 cell lines (Figure 3. 2 and 3. 20). These significant increases of the total p53 protein levels and its isoforms Ser46 and K382 were observed in all western blotting results. This supports the fact that p53 becomes activated through the DNA damage and the protein levels increase to achieve its functions as transcription factor by targeting and activating transcriptionally specific genes in response to a particular type of the stress signals. One study demonstrated that HIPK2-mediated S46 phosphorylation of p53 is essential for the p53 acetylation at lysine 382, effective p300-p53 co-recruitment onto apoptotic promoters and apoptosis, following DNA damage (Reed & Quelle, 2014). The

results are in agreement with published data describing p53 protein levels in lung cancer cells (Gu *et al.*, 2004; Lakin & Jackson, 1999; Li, Liu, *et al.*, 2014). Recent studies indicated K382 levels were elevated in the human embryonic kidney cells (HEK293) (Koh *et al.*, 2014), colorectal tumour cell line (RKO) (Phang *et al.*, 2015), and osteosarcoma cell lines (U2OS) (Zannini *et al.*, 2012) after Etoposide treatment which is in agreement with our results. Also consistent with the data presented in this thesis is report that the phosphorylated p53 at Ser-46 was increased in U2OS (Smeenk *et al.*, 2011). In addition, high expression levels were observed for Ser46 and K382 modified p53 proteins in the A549 treated cells with Actinomycin D (Krześniak *et al.*, 2014).

We observed that there was no change in the TTC5 protein levels in A549, Mero-14, and Mero-25 cells lines treated with Etoposide when compared to not treated cells. These data are in agreements with the established literature showing no change in the protein level in human colon cancer cells (HCT15) (Adams *et al.*, 2008), whereas; upregulation was demonstrated in U2OS cell lines (Adams *et al.*, 2008; Demonacos *et al.*, 2001). It has been suggested that certain factors could affect the TTC5 protein levels, for instance the phosphorylation of TTC5 was dependent on the activity of Chk2 and the protein level were reduced after treatment of the U2OS cells with Chk2 inhibitor (Adams *et al.*, 2008). So, further research including the protein kinase (Chk2) maybe need to established molecular details of the observed cell type specific change in TTC 5 protein levels in cells exposed to DNA damage.

In Mero-25 cell there were no significant effects on the p53 protein levels or any of its isoforms (phosphorylated p53 at Ser46 and acetylated p53 at lysine 382) when cells were treated with Etoposide. These cells showed potential resistance to the Etoposide treatment, which was also confirmed by the MTT results in Prof. Mutti's team. Their results demonstrated that Mero-25 mesothelioma cell lines showed a high resistance to higher doses of Etoposide (50  $\mu$ M) in comparison to a different mesothelioma cell lines (Mero-14, REN, and Mill) and that might support our findings. Previous research has identified two frequent genetic alterations, commonly being homozygous 9p21 deletions centred on CDKN2A, which have been detected in up to 72% of tumours and more than 80% of malignant pleural mesothelioma cell lines (Bott *et al.*, 2011). Genetic characterization of the tissue sections and cells lines of malignant mesothelioma has illustrated that the majority

are defective in the INK4A/ARF locus, which included p16INK4A and p14ARF genes, but still have the wild-type p53 gene (Lee *et al.*, 2007). Dysfunction of p16 because of deletion leads to upregulation and activities increase of cyclin-dependent kinase 4/6 and consequently phosphorylation of pRb gene, which prompts cell cycle progression. On the other hand, p14 absence enhances Mdm2 activities and subsequently leads to downregulation of p53 levels, and that increases mesothelioma cells resistance to apoptotic pathways (Li *et al.*, 2012). Latest study of A549 and U2OS cell lines treated with actinomycin D showed strong expression of Ser46 in A549 and not in U2OS cells. Moreover, similar expression level of Ser15 was detected in the both cell lines and authors suggested that signalling pathway controlling Ser46 p53 phosphorylation have lower/deregulated activity in U2OS cells when compared to A549 cells (Krześniak *et al.*, 2014). However, mir34b expression levels increased in Etoposide treated Mero25 cell lines (Fig. 3. 40). Given that mir34 is targeted by p53, this result indicates that residual p53 activity may be present in Mero25 cells or that Etoposide induces this miRNA through p53 independent mechanism.

#### **4. 2. Detection of p53 total, its modified isoforms and TTC5 protein levels in cancer tissues**

To detect studied proteins in human tissues, immunohistochemistry technique was used. For optimization process human lung tissue slides from COPD patient from Dr Smith laboratory in University of Salford were used. Different antibodies' dilutions of the wtp53 and its isoforms Ser46 and K382 in addition to TTC5 were applied and ideal dilutions were obtained. These conditions were applied to analysis of the tissue microarrays' slides by immunohistochemistry and their clinicopathological significance evaluated in 202 cases of lung cancer patients. Clinical data, including grade and TNM stage of the cancer, in addition to the patients' age and the gender, were used to identify any significant correlation with the target proteins' expression. Unfortunately, survival rates and treatments were not available from the source. Our data demonstrated that 130 of 202 cases were positively stained with Tp53 (64%), which is consistent with a published study that showed 103 of 156 cases (66%) were positively stained (Lee *et al.*, 1995). This positivity staining which reflected the Tp53 protein expression in the patients' tissues was in a significant correlation with the cancer grade (0.001). Our data is also in agreement with studies were the p53 expression

was determined in 50 samples of lung cancer tissue (Adenocarcinoma and squamous cell carcinoma ) using IHC by Caamano and colleagues (Caamano *et al.*, 1991), and authors concluded that p53 positive staining correlates with advanced disease (Caamano *et al.*, 1991). Our results are in agreement with another study were 52 from 132 cases (39.4%) positively stained and significantly correlated ( $p$ - value = 0.03) with the incidence of p53 positive expression in patients with squamous cell carcinoma and adenocarcinoma (URAMOTO *et al.*, 2006). The results should be interpreted with caution as positive p53 staining sometimes can also indicate presence of mutated p53 depending on mutation effect on p53 protein expression (Melhem *et al.*, 1995). Therefore, IHC staining coupled with sequencing of p53 gene is a better determination of the p53 status. Although mutations of p53 are found in numerous lung cancers, their clinical value is not entirely clear (Bar *et al.*, 2009). These results may support the theory that mutant p53 may play a role as an oncoprotein and lead to lung cancer progressions (Lee *et al.*, 1995). Using immunohistochemical detection of the p53 protein alone cannot determine the function status of the p53 protein. Therefore, assessment of p53 isoforms expression maybe a better indicator of the disease progression and so, we performed additional immunohistochemical staining including the K382 and Ser-46 in addition to TTC5.

These studies have not been frequently performed by other laboratories and limited information is available for IHC with phosphorylated p53 at Ser-15 in mouse tissues and with phosphorylated p53 at Ser-20 in malignant and benign ovarian neoplasms (Bar *et al.*, 2009; Lee & McKinnon, 2009). Also, the phosphorylation of p53 on Ser392 and Ser15 sites in esophageal squamous cell carcinomas was reported (Matsumoto *et al.*, 2004). However, Interesting results were obtained after staining tissues' samples with anti-acetylated p53 (K382) protein Ab. Number of cases showed a cytoplasmic staining of the acetylated p53-K382 rather than the nuclear, were functionally should be (Figure 3. 30). Up-regulation of K382 expression was observed after treatment with histone deacetylase (HDACs) inhibitors, promoting the pro-apoptotic PUMA and induced apoptosis in colon cancer cells (HCT116) or cell cycle arrest through promoting p21 in neuronal cell lines (Brochier *et al.*, 2013). The cytoplasmic expression of the K382 may support the theory that p53 acetylated at this site is targeted by ubiquitination molecules like MDM2 and exported from the nucleus to the cytoplasm for degradation via proteasome (Brooks & Gu, 2011b; Lohrum *et al.*, 2001).

Furthermore, MDM2 has been reported to inhibit the p53 acetylation through protein acetyltransferases (Jin *et al.*, 2002; Kobet *et al.*, 2000) and also to promote deacetylation via HDACs (Ito *et al.*, 2002). Previously it has been illustrated that MDM2 can inhibit p300-mediated p53 acetylation via making a ternary complex with these two proteins (Kobet *et al.*, 2000) and by enhancing p53 deacetylation via the MDM2–HDAC1 complexes (Ito *et al.*, 2002). SIRT1 and SIRT2, members of the HDACs, that are expressed in the nucleus and cytoplasm respectively, were reported to target the acetylated p53-K382, leading to p53 deacetylation and decrease in the stability and activity of p53 (Brooks & Gu, 2011a; Jin *et al.*, 2008). Recently, high expression of SIRT1 protein was demonstrated in brain metastatic tissues of non-small cell lung cancer (NSCLC) (Han *et al.*, 2013), and it correlated with depth of invasion, TNM stage and lymph node metastasis in colorectal cancer (CRC) patients (Zu *et al.*, 2016). The nuclear SIRT1 protein has been reported to be expressed in the cytoplasm in invasive non-small cell lung cancers (NSCLC) tissue microarrays and significantly correlated with large tumour size and lymph node metastasis (Noh *et al.*, 2013). Analysis of SIRT1, 2 proteins expression in TMA lung cancer slides and determination of potential association with the cytoplasmic expression of K382 might be a future direction in our research.

Our data showed a significant correlation between TTC5 expression and p53 phosphorylated at Ser46 but not with each of p53 total protein, and K382 acetylated p53 protein expression in the 202 examined lung cancer tissues. Given that Ser-46 phosphorylation directs p53 to apoptotic genes this may be important for determining cancer cell death. A significant correlation was observed between the TTC5 expression and the clinicopathological features of the patients included the age, grade, tumour size and the intensity of Ser-46 phosphorylated p53 protein expression. Preliminary analysis of TTC5 expression in COPD shows correlation with disease progression (Almusrati, 2015), however, there were no published studies for evaluation the TTC5 protein expression in the lung cancer tissues.

#### **4. 3. Subcellular location of p53, its isoforms and TTC5 in cell lines**

As a result of our findings showed a cytoplasmic expression of the acetylated p53-K382 protein in the patients' tissues, we explored the protein expression *in vitro* by using the

established cancer cell lines and the immunofluorescence approach. Our results have shown a nuclear expression of the acetylated p53-K382 protein in A549 and U2OS cell lines were (Figure 3. 36, 3. 38) functionally should be and in contrast with our IHC results in some cases of lung cancer. This data suggests that the acetylated p53- K382, which is one of activated forms of p53, might be exported to the cytoplasm through a specific nucleocytoplasmic transport system, found only in certain cancer patients, potentially leading later to deacetylation of p53 by HDACs proteins like SIRT2, and to its cytoplasmic degradation.

#### **4. 4. MiR-34 expression detection**

Many published reports elucidated the important roles played by MiR-34 family members through repression of the expression of target genes and base pairing with 3' untranslated region of mRNA leading to inhibition of the translation and the protein production (Bernardo *et al.*, 2012; Lal *et al.*, 2011). This miRNAs' family was involved in the p53 network, and its expression is induced directly by the p53 protein as a response to oncogenic activation or DNA damage (Gallardo *et al.*, 2009). Overexpression of miR-34a in HCT116 cells showed a positive impact on the acetylated p53- K382 protein by decreasing the SIRT1 protein, leading to upregulation of the K382 and pro-apoptotic PUMA protein levels and induction of apoptosis (Yamakuchi *et al.*, 2008). In our data, there was a decrease in the miR-34a level determined in Etoposide treated A549 cells (Figure 3. 39), which in contrast with the p53 protein level in this (NSCLC) cell lines, but in agreement with published report on small cell lung cancer (SCLC) cell lines (Lee *et al.*, 2011). Furthermore, previous data demonstrated that miR-34a was reduced in a frozen NSCLC human tissue samples, also in different types of NSCLC cell lines (Wiggins *et al.*, 2010). MiR-34a levels were also downregulated after the Etoposide treatment in the two types of mesothelioma cells (Mero-14, Mero-25) (fig. 3. 40 and 3. 41). The hypermethylation of miR-34a promoter could decrease the miR-34a expression in lung cancer and different cancer types (Gallardo *et al.*, 2009; Lodygin *et al.*, 2008). High percentage of aberrant methylation in miR-34 (especially in miR-34b, c) was demonstrated in number of mesothelioma cell lines, whereas no methylation was observed in a group of non-malignant mesothelial tissues. The expression of miR-34 family members were silenced in all methylated mesothelioma cell lines included in the research and the

study indicated that methylation can cause gene silencing (Kubo *et al.*, 2010). Therefore, exploring the methylation status at the miR-34 family members should be considered in the future research direction.

#### 4. 5. Conclusions

Upregulation of the total p53 protein expression and its isoforms phospho-p53 at Serine 46 and acetylated p53 at lysine 382 was observed in A549 and Mero-14 cells but not in the Mero-25 cells after DNA damage. Furthermore, significantly no impact on the TTC5 protein was detected in all of cell lines after the treatment. CO-IP approach confirmed the interaction between the p53 protein and its co-factor TTC5.

High percentage (67.7%) of lung cancer tissues expressed the protein and a significant correlation between the Tp53 protein expression and the pathological grade of the lung cancer tissues was demonstrated. These data may argue against the p53 protein's role as tumour suppressor but can support the fact that mutant p53 protein plays a role as an oncoprotein and might lead to cancer progression. DNA sequencing might be the right future step to confirm the status of p53 in these lung cancer samples.

In addition, the expression of phosphorylated p53 at S46 protein also showed a significant correlation between the grade of the cancer, the age of patients and the TTC5 protein expression. Strong staining of TTC5 protein (84.4 %) was detected in the 202 lung cancer cases with a significant correlation found for age, grade, tumour size and the intensity of Ser-46 phosphorylated p53 protein expression ( $P$ -Value = 0.023, 0.039, 0.053, and 0.021 respectively). The correlation between the TTC5 expression and the p53 phosphorylated at S46, which is considered a very important isoform of p53 connected to the apoptosis pathway, suggest the vital role of this co-factor (TTC5) in the cell death programme.

Statistically significant correlation was observed between the expression of acetylated form of p53 (K382), with the pathological grade of the cancer ( $p$ -value = 0.039). Interestingly, the expression of this isoform was observed in the cytoplasm in some cases. This isoform plays a vital role in apoptosis pathway by promoting and activating the expression of the pro-apoptotic PUMA leading to cell death. Moreover, a similar study on the lung cancer also showed a cytoplasmic expression of SIRT1 protein which is a nuclear protein, and a significantly correlated with the tumour size and metastasis. SIRT1 negatively regulates the p53 through K382 deacetylation leading to p53 degradation in the cytoplasm via 26S

proteasome. More investigation is needed to explain this cytoplasmic expression status of the p53 acetylated at lysine 382 protein.

Immunofluorescence approach applied to investigate the expression of K382 in the lung cancer cell line motivated by our findings in the IHC and tissues' staining showed nuclear expression of the K382 protein in the lung cancer cell line A549. These data suggest that cultured cancer cells might behave differently and use various mechanisms for progression comparing with the cancer cells in patients.

Downregulation in the expression of miR-34a levels was observed in treated A549, Mero-25 cell lines with the similar trend observed in Mero-14 cells comparing to the untreated cells, whereas the expression of miR-34b was upregulated in treated A549 and Mero-25 cells but not in treated Mero-14 mesothelioma cell lines. The data suggests that miR-34a might not be involved in the response to this type of DNA damage induced by Etoposide treatment in these cell lines.

#### **4. 6. Future Directions**

Further work is needed to increase understanding of the roles of investigated molecular pathways in the cancer progression. This can involve:

- DNA sequencing to determine the p53 status in these positive stained TMA tissues, which correlated with the grade of the cancer in this study.
- Determination of the SIRT1 protein expression and its localization in comparison to acetylated p53 at lysine 382 protein expression in these examined lung cancer cases.
- Analysis of the methylation status of miRNA-34 promoters in tested cell lines and exploration of the effect on their roles in DNA damage response.

#### 4. 7. Appendix:

**Supplementary table 5:** Specification Sheet for 120 cases adapted from:

<https://www.biomax.us/tissue-arrays/Lung/BC041115c>

Pos.	Age	Sex	Pathology diagnosis	TNM	Grade	Stage	Type
A1	65	M	Squamous cell carcinoma	T3N1M0	1	IIIA	Malignant
A2	43	F	Squamous cell carcinoma	T2N1M0	2	IIA	Malignant
A3	46	M	Squamous cell carcinoma	T2N0M0	2	IB	Malignant
A4	56	M	Squamous cell carcinoma	T2N0M0	2	IB	Malignant
A5	59	M	Squamous cell carcinoma	T2N0M0	2	IB	Malignant
A6	66	M	Squamous cell carcinoma	T2N1M0	2	IIB	Malignant
A7	57	M	Squamous cell carcinoma	T3N2M0	2	IIIA	Malignant
A8	45	M	Squamous cell carcinoma	T2N0M0	2	I	Malignant
A9	68	M	Squamous cell carcinoma	T2N2M0	2	IIIA	Malignant
A10	41	M	Squamous cell carcinoma	T2N2M0	2	IIIA	Malignant
A11	69	M	Squamous cell carcinoma	T2N2M0	2	IIIA	Malignant
A12	65	M	Squamous cell carcinoma	T3N0M0	2	IIB	Malignant
B1	47	M	Squamous cell carcinoma	T1N0M0	2	IA	Malignant
B2	50	F	Squamous cell carcinoma	T2N0M0	2	I	Malignant
B3	44	M	Squamous cell carcinoma	T2N1M0	2	IIB	Malignant
B4	63	M	Squamous cell carcinoma	T2N1M0	2	IB	Malignant
B5	63	M	Squamous cell carcinoma	T3N1M0	2	IIIA	Malignant
B6	61	M	Squamous cell carcinoma	T2N0M0	2	IB	Malignant
B7	50	M	Squamous cell carcinoma	T3N1M0	2	IIIA	Malignant
B8	66	M	Squamous cell carcinoma	T2N0M0	2	IB	Malignant
B9	61	M	Squamous cell carcinoma	T2N0M0	3	IB	Malignant
B10	59	M	Squamous cell carcinoma	T2N1M0	3	II	Malignant
B11	55	M	Squamous cell carcinoma	T2N0M0	3	IB	Malignant
B12	43	M	Squamous cell carcinoma	T2N0M0	3	IB	Malignant
C1	65	M	Squamous cell carcinoma	T2N0M0	3	IB	Malignant
C2	59	M	Adenosquamous carcinoma	T2N0M0	-	IB	Malignant
C3	63	M	Squamous cell carcinoma	T3N2M0	3	IIIA	Malignant
C4	61	M	Squamous cell carcinoma	T2N0M0	3	IB	Malignant
C5	51	M	Squamous cell carcinoma with necrosis	T3N1M0	2	IIIA	Malignant
C6	61	M	Squamous cell carcinoma	T3N1M0	3	IIIA	Malignant
C7	38	M	Squamous cell carcinoma	T2N0M0	3	IB	Malignant
C8	66	M	Squamous cell carcinoma with necrosis	T3N1M0	3	IIIA	Malignant
C9	56	M	Squamous cell carcinoma	T2N1M0	3	IIA	Malignant
C10	56	M	Squamous cell carcinoma	T1N2M0	3	IIIA	Malignant
C11	51	F	Squamous cell carcinoma	T2N2M0	3	IIIA	Malignant
C12	54	M	Squamous cell carcinoma	T2N0M0	3	I	Malignant

D1	60	M	Squamous cell carcinoma	T2N0M0	-	IB	Malignant
D2	44	M	Squamous cell carcinoma	T2N0M0	3	IB	Malignant
D3	55	M	Squamous cell carcinoma	T2N0M0	3	IB	Malignant
D4	71	M	Squamous cell carcinoma	T1N0M0	3	IA	Malignant
D5	61	M	Squamous cell carcinoma	T2N0M0	3	IB	Malignant
D6	68	M	Adenosquamous carcinoma	T2N0M0	-	IIA	Malignant
D7	64	F	Adenosquamous carcinoma	T2N0M0	-	IB	Malignant
D8	42	M	Mucinous adenocarcinoma	T3N1M0	1	IIIA	Malignant
D9	51	M	Mucinous adenocarcinoma	T4N2M0	1	IIIB	Malignant
D10	47	M	Mucinous adenocarcinoma	T2N0M0	2	IB	Malignant
D11	68	M	Adenocarcinoma	T2N1M1	2	IV	Malignant
D12	34	F	Adenocarcinoma	T2N0M0	2	IB	Malignant
E1	58	M	Adenocarcinoma	T2N0M0	2	IB	Malignant
E2	68	M	Adenocarcinoma	T2N1M0	2	IIB	Malignant
E3	51	M	Adenocarcinoma	T3N1M0	2	IIIA	Malignant
E4	63	F	Adenocarcinoma	T2N1M0	2	IIB	Malignant
E5	44	F	Adenocarcinoma	T2N1M0	2	IIB	Malignant
E6	56	F	Adenocarcinoma	T2N1M0	2	II	Malignant
E7	58	F	Adenocarcinoma	T2N0M0	2	IB	Malignant
E8	56	F	Adenocarcinoma	T1N0M0	2	IA	Malignant
E9	67	M	Adenocarcinoma	T2N1M0	2	IIB	Malignant
E10	59	M	Adenocarcinoma	T3N1M0	2	IIIA	Malignant
E11	61	M	Adenocarcinoma with necrosis	T2N0M0	2	IB	Malignant
E12	50	M	Adenocarcinoma with necrosis	T2N0M0	2	IB	Malignant
F1	61	F	Adenocarcinoma	T2N1M0	2	IIB	Malignant
F2	68	F	Adenocarcinoma	T3N1M0	2	IIIA	Malignant
F3	66	M	Adenocarcinoma	T2N1M0	2	IIB	Malignant
F4	72	M	Adenocarcinoma	T1N0M0	2	IA	Malignant
F5	65	F	Adenocarcinoma	T2N0M0	2	IB	Malignant
F6	57	M	Adenocarcinoma	T2N1M0	2	IIB	Malignant
F7	50	M	Adenocarcinoma	T2N1M0	3	IIB	Malignant
F8	70	M	Adenocarcinoma with necrosis	T2N0M0	2	IB	Malignant
F9	68	M	Adenocarcinoma	T2N0M0	2	IB	Malignant
F10	57	M	Adenocarcinoma	T2N0M0	3	IB	Malignant
F11	51	F	Adenocarcinoma	T2N0M0	3	IB	Malignant
F12	71	F	Adenocarcinoma	T2N1M0	3	IIB	Malignant
G1	64	F	Adenocarcinoma	T2N0M0	2	IIA	Malignant
G2	50	M	Adenocarcinoma	T3N1M0	2	IIIA	Malignant
G3	53	M	Adenocarcinoma	T2N0M0	3	IB	Malignant
G4	60	M	Adenocarcinoma	T2N1M0	-	IIA	Malignant
G5	48	F	Adenocarcinoma	T2N0M0	3	IB	Malignant

G6	59	F	Adenocarcinoma	T3N1M0	3	IIIA	Malignant
G7	54	F	Adenocarcinoma	T2N0M0	2	I	Malignant
G8	50	M	Adenocarcinoma	T2N0M0	3	IB	Malignant
G9	60	M	Adenocarcinoma	T2N2M0	3	IIIA	Malignant
G10	60	F	Adenocarcinoma	T2N2M0	3	IIIA	Malignant
G11	35	F	Adenocarcinoma	T2N0M0	3	IB	Malignant
G12	67	M	Adenocarcinoma	T3N0M0	3	IIIA	Malignant
H1	76	M	Adenocarcinoma	T2N1M0	3	IIB	Malignant
H2	57	F	Adenocarcinoma	T2N2M0	3	IB	Malignant
H3	59	M	Adenocarcinoma	T2N1M0	3	IIB	Malignant
H4	65	M	Adenocarcinoma	T3N0M0	3	IIB	Malignant
H5	53	F	Adenocarcinoma	T2N2M0	3	IIIA	Malignant
H6	49	M	Adenocarcinoma	T2N0M0	-	IB	Malignant
H7	65	M	Adenocarcinoma	T2N0M0	2	IB	Malignant
H8	51	F	Bronchioloalveolar carcinoma	T1N0M0	-	I	Malignant
H9	72	M	Bronchioloalveolar carcinoma	T1N0M0	-	I	Malignant
H10	60	M	Bronchioloalveolar carcinoma	T2N1M0	-	IIB	Malignant
H11	52	M	Bronchioloalveolar carcinoma	T2N0M0	-	IB	Malignant
H12	53	M	Large cell carcinoma	T4N0M0	-	IIIB	Malignant
I1	64	F	Large cell carcinoma	T2N0M0	-	IB	Malignant
I2	70	M	Large cell carcinoma	T3N1M0	-	IIIA	Malignant
I3	65	M	Small cell carcinoma	T2N0M0	-	IB	Malignant
I4	48	F	Small cell carcinoma	T2N0M0	-	IB	Malignant
I5	39	M	Small cell carcinoma	T2N1M0	-	IIB	Malignant
I6	42	F	Small cell carcinoma	T4N1M0	-	IIIA	Malignant
I7	73	M	Small cell carcinoma	T3N1M0	-	IIIA	Malignant
I8	73	M	Small cell carcinoma	T2N2M0	-	IB	Malignant
I9	44	M	Small cell carcinoma	T1N1M0	-	IIIA	Malignant
I10	60	M	Small cell carcinoma	T1N0M0	-	I	Malignant
I11	53	M	Atypical carcinoid	T2N0M0	-	IB	Malignant
I12	36	F	Atypical carcinoid	T2N0M0	-	IB	Malignant
J1	49	M	Atypical carcinoid	T4N2M0	-	IIIB	Malignant
J2	43	M	Carcinoid	T2N0M0	-	IB	Malignant
J3	46	M	Lung tissue	-	-	-	Normal
J4	19	M	Lung tissue	-	-	-	Normal
J5	47	M	Lung tissue	-	-	-	Normal
J6	30	M	Lung tissue	-	-	-	Normal
J7	25	M	Lung tissue	-	-	-	Normal
J8	19	F	Lung tissue	-	-	-	Normal
J9	15	F	Lung tissue	-	-	-	Normal
J10	41	F	Lung tissue	-	-	-	Normal
J11	47	M	Lung tissue	-	-	-	Normal
J12	24	M	Lung tissue and fibrous tissue	-	-	-	Normal

## References:

- Adams, C. J., Graham, A. L., Jansson, M., Coutts, A. S., Edelmann, M., Smith, L., . . . La Thangue, N. B. (2008). ATM and Chk2 kinase target the p53 cofactor Strap. *EMBO reports*, *9*(12), 1222-1229.
- Adams, C. J., Pike, A. C., Maniam, S., Sharpe, T. D., Coutts, A. S., Knapp, S., . . . Bullock, A. N. (2012). The p53 cofactor Strap exhibits an unexpected TPR motif and oligonucleotide-binding (OB)-fold structure. *Proceedings of the National Academy of Sciences*, *109*(10), 3778-3783.
- Allis, C. D., Berger, S. L., Cote, J., Dent, S., Jenuwien, T., Kouzarides, T., . . . Shiekhatar, R. (2007). New nomenclature for chromatin-modifying enzymes. *cell*, *131*(4), 633-636.
- Almusrati, W. (2015). *Glucocorticoid resistance in COPD patients and lung cancer*. Environment and life science.
- Alsharafi, W. A., Xiao, B., Abuhamed, M. M., & Luo, Z. (2015). miRNAs: biological and clinical determinants in epilepsy. *Frontiers in molecular neuroscience*, *8*, 59.
- Amodio, N., Leotta, M., Bellizzi, D., Di Martino, M. T., D'Aquila, P., Lionetti, M., . . . Passarino, G. (2012). DNA-demethylating and anti-tumour activity of synthetic miR-29b mimics in multiple myeloma. *Oncotarget*, *3*(10), 1246.
- Antonini, D., Russo, M. T., De Rosa, L., Gorrese, M., Del Vecchio, L., & Missero, C. (2010). Transcriptional repression of miR-34 family contributes to p63-mediated cell cycle progression in epidermal cells. *Journal of Investigative Dermatology*, *130*(5), 1249-1257.
- Asghar, U., Witkiewicz, A. K., Turner, N. C., & Knudsen, E. S. (2015). The history and future of targeting cyclin-dependent kinases in cancer therapy. *Nature Reviews Drug Discovery*, *14*(2), 130-146.
- Bar, J. K., Slomska, I., Rabczynski, J., Noga, L., & Grybos, M. (2009). Expression of p53 protein phosphorylated at serine 20 and serine 392 in malignant and benign ovarian neoplasms: correlation with clinicopathological parameters of tumours. *International Journal of Gynecological Cancer*, *19*(8), 1322-1328.
- Barnes, P. J., Drazen, J. M., Rennard, S. I., & Thomson, N. C. (2009). *Asthma and COPD: basic mechanisms and clinical management*: Elsevier.
- Bartel, D. P. (2009). MicroRNAs: target recognition and regulatory functions. *cell*, *136*(2), 215-233.
- Baylin, S. B., & Ohm, J. E. (2006). Epigenetic gene silencing in cancer—a mechanism for early oncogenic pathway addiction? *Nature Reviews Cancer*, *6*(2), 107.
- Berger, S. L. (2010). Keeping p53 in check: a high-stakes balancing act. *cell*, *142*(1), 17-19.
- Bernardo, B. C., Charchar, F. J., Lin, R. C., & McMullen, J. R. (2012). A microRNA guide for clinicians and basic scientists: background and experimental techniques. *Heart, Lung and Circulation*, *21*(3), 131-142.

- Bott, M., Brevet, M., Taylor, B. S., Shimizu, S., Ito, T., Wang, L., . . . Reva, B. (2011). The nuclear deubiquitinase BAP1 is commonly inactivated by somatic mutations and 3p21.1 losses in malignant pleural mesothelioma. *Nature genetics*, *43*(7), 668.
- Brochier, C., Dennis, G., Riviuccio, M. A., McLaughlin, K., Coppola, G., Ratan, R. R., & Langley, B. (2013). Specific acetylation of p53 by HDAC inhibition prevents DNA damage-induced apoptosis in neurons. *Journal of Neuroscience*, *33*(20), 8621-8632.
- Brooks, C. L., & Gu, W. (2006). p53 ubiquitination: Mdm2 and beyond. *Molecular cell*, *21*(3), 307-315.
- Brooks, C. L., & Gu, W. (2011a). The impact of acetylation and deacetylation on the p53 pathway. *Protein & cell*, *2*(6), 456-462.
- Brooks, C. L., & Gu, W. (2011b). p53 regulation by ubiquitin. *FEBS letters*, *585*(18), 2803-2809.
- Caamano, J., Ruggeri, B., Momiki, S., Sickler, A., Zhang, S., & Klein-Szanto, A. (1991). Detection of p53 in primary lung tumours and nonsmall cell lung carcinoma cell lines. *The American journal of pathology*, *139*(4), 839.
- Carbone, M., Pass, H., Miele, L., & Bocchetta, M. (2003). New developments about the association of SV40 with human mesothelioma. *Oncogene*, *22*(33), 5173-5180.
- Chan, H. M., & La Thangue, N. B. (2001). p300/CBP proteins: HATs for transcriptional bridges and scaffolds. *Journal of cell science*, *114*(13), 2363-2373.
- Chehab, N. H., Malikzay, A., Stavridi, E. S., & Halazonetis, T. D. (1999). Phosphorylation of Ser-20 mediates stabilization of human p53 in response to DNA damage. *Proceedings of the National Academy of Sciences*, *96*(24), 13777-13782.
- Chen, W. Y., Wang, D. H., Yen, R. C., Luo, J., Gu, W., & Baylin, S. B. (2005). Tumour suppressor HIC1 directly regulates SIRT1 to modulate p53-dependent DNA-damage responses. *cell*, *123*(3), 437-448.
- Chipuk, J. E., & Green, D. R. (2008). How do BCL-2 proteins induce mitochondrial outer membrane permeabilization? *Trends in cell biology*, *18*(4), 157-164.
- Clayton, A. L., Hazzalin, C. A., & Mahadevan, L. C. (2006). Enhanced histone acetylation and transcription: a dynamic perspective. *Molecular cell*, *23*(3), 289-296.
- Collins, L. G., Haines, C., Perkel, R., & Enck, R. E. (2007). Lung cancer: diagnosis and management. *Am Fam Physician*, *75*(1), 56-63.
- Coutts, A. S., & La Thangue, N. B. (2005). The p53 response: emerging levels of co-factor complexity. *Biochemical and biophysical research communications*, *331*(3), 778-785.
- Degterev, A., Boyce, M., & Yuan, J. (2003). A decade of caspases. *Oncogene*, *22*(53), 8543-8567.
- Demonacos, C., Krstic-Demonacos, M., & La Thangue, N. B. (2001). A TPR motif cofactor contributes to p300 activity in the p53 response. *Molecular cell*, *8*(1), 71-84.
- Demonacos, C., Krstic-Demonacos, M., Smith, L., Xu, D., O'Connor, D. P., Jansson, M., & La Thangue, N. B. (2004). A new effector pathway links ATM kinase with the DNA damage response. *Nature cell biology*, *6*(10), 968-976.

- Di Martino, M. T., Campani, V., Misso, G., Cantafio, M. E. G., Gullà, A., Foresta, U., . . . Gigantino, V. (2014). *In vivo* activity of miR-34a mimics delivered by stable nucleic acid lipid particles (SNALPs) against multiple myeloma. *PLoS ONE*, *9*(2), e90005.
- Di Martino, M. T., Gullà, A., Cantafio, M. E. G., Lionetti, M., Leone, E., Amodio, N., . . . Cannataro, M. (2013). *In vitro* and *in vivo* anti-tumour activity of miR-221/222 inhibitors in multiple myeloma. *Oncotarget*, *4*(2), 242.
- Dijkstra, M., van Lom, K., Tielemans, D., Elstrodt, F., Langerak, A., Van't Veer, M., & Jongen-Lavrencic, M. (2009). 17p13/TP53 deletion in B-CLL patients is associated with microRNA-34a downregulation. *Leukemia*, *23*(3), 625.
- Dimopoulos, K., Gimsing, P., & Grønbæk, K. (2013). Aberrant microRNA expression in multiple myeloma. *European journal of haematology*, *91*(2), 95-105.
- Dornan, D., & Hupp, T. R. (2001). Inhibition of p53-dependent transcription by BOX-I phospho-peptide mimetics that bind to p300. *EMBO reports*, *2*(2), 139-144.
- Dulić, V., Kaufmann, W. K., Wilson, S. J., Tlsty, T. D., Lees, E., Harper, J. W., . . . Reed, S. I. (1994). p53-dependent inhibition of cyclin-dependent kinase activities in human fibroblasts during radiation-induced G1 arrest. *cell*, *76*(6), 1013-1023.
- El-Deiry, W. S., Kern, S. E., Pietenpol, J. A., Kinzler, K. W., and Vogelstein, B. (1992). Definition of a consensus binding site for p53. *Nat. Genet.*, *1*, 45-49.
- Emery, N. J., & Clayton, N. S. (2009). Tool use and physical cognition in birds and mammals. *Current Opinion in Neurobiology*, *19*(1), 27-33. doi:10.1016/j.conb.2009.02.003
- Esquela-Kerscher, A., & Slack, F. J. (2006). Oncomirs—microRNAs with a role in cancer. *Nature Reviews Cancer*, *6*(4), 259.
- Fakharzadeh, S., Trusko, S., & George, D. (1991). Tumourigenic potential associated with enhanced expression of a gene that is amplified in a mouse tumour cell line. *The EMBO journal*, *10*(6), 1565.
- Filipowicz, W., Bhattacharyya, S. N., & Sonenberg, N. (2008). Mechanisms of post-transcriptional regulation by microRNAs: are the answers in sight? *Nature reviews genetics*, *9*(2), 102.
- Fujita, Y., Kojima, K., Hamada, N., Ohhashi, R., Akao, Y., Nozawa, Y., . . . Ito, M. (2008). Effects of miR-34a on cell growth and chemoresistance in prostate cancer PC3 cells. *Biochemical and biophysical research communications*, *377*(1), 114-119.
- Fulda, S., & Debatin, K. (2006). Extrinsic versus intrinsic apoptosis pathways in anticancer chemotherapy. *Oncogene*, *25*(34), 4798-4811.
- Fulda, S., Meyer, E., & Debatin, K.-M. (2002). Inhibition of TRAIL-induced apoptosis by Bcl-2 overexpression. *Oncogene*, *21*(15), 2283.
- Gallardo, E., Navarro, A., Viñolas, N., Marrades, R. M., Diaz, T., Gel, B., . . . Ramirez, J. (2009). miR-34a as a prognostic marker of relapse in surgically resected non-small-cell lung cancer. *Carcinogenesis*, *30*(11), 1903-1909.
- Glozak, M. A., Sengupta, N., Zhang, X., & Seto, E. (2005). Acetylation and deacetylation of non-histone proteins. *gene*, *363*, 15-23.

- Gu, J., Zhang, L., Swisher, S. G., Liu, J., Roth, J. A., & Fang, B. (2004). Induction of p53-regulated genes in lung cancer cells: implications of the mechanism for adenoviral p53-mediated apoptosis. *Oncogene*, *23*(6), 1300-1307.
- Gu, W., & Roeder, R. G. (1997). Activation of p53 sequence-specific DNA binding by acetylation of the p53 C-terminal domain. *cell*, *90*(4), 595-606.
- Guessous, F., Zhang, Y., Kofman, A., Catania, A., Li, Y., Schiff, D., . . . Abounader, R. (2010). microRNA-34a is tumour suppressive in brain tumours and glioma stem cells. *Cell Cycle*, *9*(6), 1031-1036.
- Guo, A., Salomoni, P., Luo, J., Shih, A., Zhong, S., Gu, W., & Pandolfi, P. P. (2000). The function of PML in p53-dependent apoptosis. *Nature cell biology*, *2*(10), 730-736.
- Han, L., Liang, X.-H., Chen, L.-X., Bao, S.-M., & Yan, Z.-Q. (2013). SIRT1 is highly expressed in brain metastasis tissues of non-small cell lung cancer (NSCLC) and in positive regulation of NSCLC cell migration. *International journal of clinical and experimental pathology*, *6*(11), 2357.
- Hanahan, D., & Weinberg, R. A. (2011). Hallmarks of cancer: the next generation. *cell*, *144*(5), 646-674.
- Haupt, S., Berger, M., Goldberg, Z., & Haupt, Y. (2003). Apoptosis-the p53 network. *Journal of cell science*, *116*(20), 4077-4085.
- He, L., He, X., Lim, L. P., De Stanchina, E., Xuan, Z., Liang, Y., . . . Ridzon, D. (2007). A microRNA component of the p53 tumour suppressor network. *Nature*, *447*(7148), 1130.
- Hengartner, M. O. (2000). The biochemistry of apoptosis. *Nature*, *407*(6805), 770-776.
- Hermeking, H. (2010). The miR-34 family in cancer and apoptosis. *Cell death and differentiation*, *17*(2), 193.
- Hirao, A., Kong, Y.-Y., Matsuoka, S., Wakeham, A., Ruland, J., Yoshida, H., . . . Mak, T. W. (2000). DNA damage-induced activation of p53 by the checkpoint kinase Chk2. *Science*, *287*(5459), 1824-1827.
- Hofmann, T. G., Möller, A., Sirma, H., Zentgraf, H., Taya, Y., Dröge, W., . . . Schmitz, M. L. (2002). Regulation of p53 activity by its interaction with homeodomain-interacting protein kinase-2. *Nature cell biology*, *4*(1), 1.
- Hupp, T. R., & Lane, D. P. (1994). Allosteric activation of latent p53 tetramers. *Current Biology*, *4*(10), 865-875.
- Idikio, H. A. (2011). Quantitative analysis of p53 expression in human normal and cancer tissue microarray with global normalization method. *International journal of clinical and experimental pathology*, *4*(5), 505.
- Ismail-Khan, R., Robinson, L. A., Williams, C. C., Garrett, C. R., Bepler, G., & Simon, G. R. (2006). Malignant pleural mesothelioma: a comprehensive review. *Cancer control*, *13*(4), 255.
- Ito, A., Kawaguchi, Y., Lai, C. H., Kovacs, J. J., Higashimoto, Y., Appella, E., & Yao, T. P. (2002). MDM2-HDAC1-mediated deacetylation of p53 is required for its degradation. *The EMBO journal*, *21*(22), 6236-6245.

- Ito, A., Lai, C. H., Zhao, X., Saito, S. i., Hamilton, M. H., Appella, E., & Yao, T. P. (2001). p300/CBP-mediated p53 acetylation is commonly induced by p53-activating agents and inhibited by MDM2. *The EMBO journal*, 20(6), 1331-1340.
- Jang, K. Y., Hwang, S. H., Kwon, K. S., Kim, K. R., Choi, H. N., Lee, N.-R., . . . Chung, M. J. (2008). SIRT1 expression is associated with poor prognosis of diffuse large B-cell lymphoma. *The American journal of surgical pathology*, 32(10), 1523-1531.
- Jang, K. Y., Noh, S. J., Lehwald, N., Tao, G.-Z., Bellovin, D. I., Park, H. S., . . . Sylvester, K. G. (2012). SIRT1 and c-Myc promote liver tumour cell survival and predict poor survival of human hepatocellular carcinomas. *PLoS ONE*, 7(9), e45119.
- Jen, P. H. S., & Wu, C. H. (2008). Echo duration selectivity of the bat varies with pulse-echo amplitude difference. *Neuroreport*, 19(3), 373-377. doi:10.1097/WNR.0b013e3282f52c61
- Jenkins, L. M. M., Durell, S. R., Mazur, S. J., & Appella, E. (2012). p53 N-terminal phosphorylation: a defining layer of complex regulation. *Carcinogenesis*, 33(8), 1441-1449.
- Jenuwein, T., & Allis, C. D. (2001). Translating the histone code. *Science*, 293(5532), 1074-1080.
- Ji, Q., Hao, X., Meng, Y., Zhang, M., DeSano, J., Fan, D., & Xu, L. (2008). Restoration of tumour suppressor miR-34 inhibits human p53-mutant gastric cancer tumourspheres. *BMC cancer*, 8(1), 266.
- Jin, Y.-H., Kim, Y.-J., Kim, D.-W., Baek, K.-H., Kang, B. Y., Yeo, C.-Y., & Lee, K.-Y. (2008). Sirt2 interacts with 14-3-3  $\beta/\gamma$  and down-regulates the activity of p53. *Biochemical and biophysical research communications*, 368(3), 690-695.
- Jin, Y., Zeng, S. X., Dai, M.-S., Yang, X.-J., & Lu, H. (2002). MDM2 inhibits PCAF (p300/CREB-binding protein-associated factor)-mediated p53 acetylation. *Journal of Biological Chemistry*, 277(34), 30838-30843.
- Kandoth, C., McLellan, M. D., Vandin, F., Ye, K., Niu, B., Lu, C., . . . Wyczalkowski, M. A. (2013). Mutational landscape and significance across 12 major cancer types. *Nature*, 502(7471), 333-339.
- Karpinich, N. O., Tafani, M., Rothman, R. J., Russo, M. A., & Farber, J. L. (2002). The Course of Etoposide-induced apoptosis from damage to DNA and p53 activation to mitochondrial release of cytochrome c. *Journal of Biological Chemistry*, 277(19), 16547-16552.
- Kerr, J. F., Wyllie, A. H., & Currie, A. R. (1972). Apoptosis: a basic biological phenomenon with wide-ranging implications in tissue kinetics. *British journal of cancer*, 26(4), 239.
- Kim, D. H., Sætrom, P., Snøve, O., & Rossi, J. J. (2008). MicroRNA-directed transcriptional gene silencing in mammalian cells. *Proceedings of the National Academy of Sciences*, 105(42), 16230-16235.
- Knippschild, U., Milne, D., Campbell, L., DeMaggio, A., Christenson, E., Hoekstra, M., & Meek, D. (1997). p53 is phosphorylated *in vitro* and *in vivo* by the delta and epsilon

- isoforms of casein kinase 1 and enhances the level of casein kinase 1 delta in response to topoisomerase-directed drugs. *Oncogene*, *15*(14), 1727-1736.
- Kobet, E., Zeng, X., Zhu, Y., Keller, D., & Lu, H. (2000). MDM2 inhibits p300-mediated p53 acetylation and activation by forming a ternary complex with the two proteins. *Proceedings of the National Academy of Sciences*, *97*(23), 12547-12552.
- Kodama, M., Otsubo, C., Hirota, T., Yokota, J., Enari, M., & Taya, Y. (2010). Requirement of ATM for rapid p53 phosphorylation at Ser46 without Ser/Thr-Gln sequences. *Molecular and cellular biology*, *30*(7), 1620-1633.
- Koh, D.-I., Han, D., Ryu, H., Choi, W.-I., Jeon, B.-N., Kim, M.-K., . . . Clarke, A. R. (2014). KAISO, a critical regulator of p53-mediated transcription of CDKN1A and apoptotic genes. *Proceedings of the National Academy of Sciences*, *111*(42), 15078-15083.
- Komander, D., & Rape, M. (2012). The ubiquitin code. *Annual review of biochemistry*, *81*, 203-229.
- Krześniak, M., Zajkovicz, A., Matuszczyk, I., & Rusin, M. (2014). Rapamycin prevents strong phosphorylation of p53 on serine 46 and attenuates activation of the p53 pathway in A549 lung cancer cells exposed to actinomycin D. *Mechanisms of ageing and development*, *139*, 11-21.
- Kubo, T., Toyooka, S., Tsukuda, K., Asano, H., Sakaguchi, M., Soh, J., . . . Oto, T. (2010). Frequent silencing of tumour suppressive MicroRNA-34b/c by aberrant methylation in malignant mesothelioma: AACR.
- Lacroix, M., Toillon, R.-A., & Leclercq, G. (2006). p53 and breast cancer, an update. *Endocrine-related cancer*, *13*(2), 293-325.
- Lakin, N. D., & Jackson, S. P. (1999). Regulation of p53 in response to DNA damage. *Oncogene*, *18*(53), 7644-7655.
- Lal, A., Thomas, M. P., Altschuler, G., Navarro, F., O'Day, E., Li, X. L., . . . Rajani, D. K. (2011). Capture of microRNA-bound mRNAs identifies the tumour suppressor miR-34a as a regulator of growth factor signaling. *PLoS genetics*, *7*(11), e1002363.
- Lane, D. P., Cheok, C. F., & Lain, S. (2010). p53-based cancer therapy. *Cold Spring Harbor perspectives in biology*, *2*(9), a001222.
- Lavrik, I., Golks, A., & Krammer, P. H. (2005). Death receptor signaling. *Journal of cell science*, *118*(2), 265-267.
- Lee, A. Y., Raz, D. J., He, B., & Jablons, D. M. (2007). Update on the molecular biology of malignant mesothelioma. *Cancer*, *109*(8), 1454-1461.
- Lee, J.-H., Song, M.-Y., Song, E.-K., Kim, E.-K., Moon, W. S., Han, M.-K., . . . Park, B.-H. (2008). Overexpression of SIRT1 protects pancreatic  $\beta$ -cells against cytokine toxicity through suppressing NF- $\kappa$ B signaling pathway. *Diabetes*.
- Lee, J.-H., Voortman, J., Dingemans, A.-M. C., Voeller, D. M., Pham, T., Wang, Y., & Giaccone, G. (2011). MicroRNA expression and clinical outcome of small cell lung cancer. *PLoS ONE*, *6*(6), e21300.
- Lee, J., & Gu, W. (2010). The multiple levels of regulation by p53 ubiquitination. *Cell Death & Differentiation*, *17*(1), 86-92.

- Lee, J. S., Yoon, A., Kalapurakal, S. K., Ro, J. Y., Lee, J. J., Tu, N., . . . Hong, W. K. (1995). Expression of p53 oncoprotein in non-small-cell lung cancer: a favorable prognostic factor. *Journal of clinical oncology*, *13*(8), 1893-1903.
- Lee, Y., & McKinnon, P. J. (2009). Detection of apoptosis in the central nervous system *Apoptosis* (pp. 273-282): Springer.
- Leotta, M., Biamonte, L., Raimondi, L., Ronchetti, D., Di Martino, M. T., Botta, C., . . . Giordano, A. (2014). A p53-Dependent Tumour Suppressor Network Is Induced by Selective miR-125a-5p Inhibition in Multiple Myeloma Cells. *Journal of cellular physiology*, *229*(12), 2106-2116.
- Levine, A., Hu, W., & Feng, Z. (2006). The P53 pathway: what questions remain to be explored? *Cell Death & Differentiation*, *13*(6), 1027-1036.
- Levine, A. J. (1997). p53, the cellular gatekeeper for growth and division. *cell*, *88*(3), 323-331.
- Li, J., Liu, A., & Wang, Y. (2014).  $\beta$ -Elemene against human lung cancer via up-regulation of P53 protein expression to promote the release of exosome. *Lung Cancer*, *86*(2), 144-150.
- Li, N., Fu, H., Tie, Y., Hu, Z., Kong, W., Wu, Y., & Zheng, X. (2009). miR-34a inhibits migration and invasion by down-regulation of c-Met expression in human hepatocellular carcinoma cells. *Cancer letters*, *275*(1), 44-53.
- Li, Q., Kawamura, K., Yamanaka, M., Okamoto, S., Yang, S., Yamauchi, S., . . . Takiguchi, Y. (2012). Upregulated p53 expression activates apoptotic pathways in wild-type p53-bearing mesothelioma and enhances cytotoxicity of cisplatin and pemetrexed. *Cancer gene therapy*, *19*(3), 218-228.
- Li, X., Ren, Z., & Tang, J. (2014). MicroRNA-34a: a potential therapeutic target in human cancer. *Cell death & disease*, *5*(7), e1327.
- Li, X., Xu, H., Xu, C., Lin, M., Song, X., Yi, F., . . . Kim, S. S. (2013). The yin-yang of DNA damage response: roles in tumorigenesis and cellular senescence. *International journal of molecular sciences*, *14*(2), 2431-2448.
- Liu, C., Kelnar, K., Liu, B., Chen, X., Calhoun-Davis, T., Li, H., . . . Honorio, S. (2011). The microRNA miR-34a inhibits prostate cancer stem cells and metastasis by directly repressing CD44. *Nature medicine*, *17*(2), 211.
- Liu, L., Scolnick, D. M., Trievel, R. C., Zhang, H. B., Marmorstein, R., Halazonetis, T. D., & Berger, S. L. (1999). p53 sites acetylated *in vitro* by PCAF and p300 are acetylated *in vivo* in response to DNA damage. *Molecular and cellular biology*, *19*(2), 1202-1209.
- Lodygin, D., Tarasov, V., Epanchintsev, A., Berking, C., Knyazeva, T., Körner, H., . . . Hermeking, H. (2008). Inactivation of miR-34a by aberrant CpG methylation in multiple types of cancer. *Cell Cycle*, *7*(16), 2591-2600.
- Lohrum, M. A., Woods, D. B., Ludwig, R. L., Bálint, É., & Vousden, K. H. (2001). C-terminal ubiquitination of p53 contributes to nuclear export. *Molecular and cellular biology*, *21*(24), 8521-8532.
- Long, J., & Ryan, K. (2012). New frontiers in promoting tumour cell death: targeting apoptosis, necroptosis and autophagy. *Oncogene*, *31*(49), 5045-5060.

- Longo, D., Fauci, A., Kasper, D., Hauser, S., Jameson, J., & Loscalzo, J. (2012). *Harrison's Principles of Internal Medicine 18E Vol 2 EB*: McGraw Hill Professional.
- Lovaas, J. D., Zhu, L., Chiao, C. Y., Byles, V., Faller, D. V., & Dai, Y. (2013). SIRT1 enhances matrix metalloproteinase-2 expression and tumour cell invasion in prostate cancer cells. *The Prostate*, *73*(5), 522-530.
- Luan, S., Sun, L., & Huang, F. (2010). MicroRNA-34a: a novel tumour suppressor in p53-mutant glioma cell line U251. *Archives of medical research*, *41*(2), 67-74.
- Luo, J., Nikolaev, A. Y., Imai, S.-i., Chen, D., Su, F., Shiloh, A., . . . Gu, W. (2001). Negative control of p53 by Sir2 $\alpha$  promotes cell survival under stress. *cell*, *107*(2), 137-148.
- Luo, J., Solimini, N. L., & Elledge, S. J. (2009). Principles of cancer therapy: oncogene and non-oncogene addiction. *cell*, *136*(5), 823-837.
- Luo, J., Su, F., Chen, D., Shiloh, A., & Gu, W. (2000). Deacetylation of p53 modulates its effect on cell growth and apoptosis. *Nature*, *408*(6810), 377-381.
- MacPherson, D., Kim, J., Kim, T., Rhee, B. K., van Oostrom, C. T., DiTullio, R. A., . . . de Vries, A. (2004). Defective apoptosis and B-cell lymphomas in mice with p53 point mutation at Ser 23. *The EMBO journal*, *23*(18), 3689-3699.
- Manfredi, J. J. (2010). The Mdm2-p53 relationship evolves: Mdm2 swings both ways as an oncogene and a tumour suppressor. *Genes & development*, *24*(15), 1580-1589.
- Marine, J.-C. W., Dyer, M. A., & Jochemsen, A. G. (2007). MDMX: from bench to bedside. *Journal of cell science*, *120*(3), 371-378.
- Matsumoto, M., Furihata, M., Kurabayashi, A., Sasaguri, S., Araki, K., Hayashi, H., & Ohtsuki, Y. (2004). Prognostic significance of serine 392 phosphorylation in overexpressed p53 protein in human esophageal squamous cell carcinoma. *Oncology*, *67*(2), 143-150.
- Mayer, B., & Oberbauer, R. (2003). Mitochondrial regulation of apoptosis. *Physiology*, *18*(3), 89-94.
- Meek, D. (1994). *Post-translational modification of p53*. Paper presented at the Seminars in cancer biology.
- Melhem, M. F., Law, J. C., El-Ashmawy, L., Johnson, J. T., Landreneau, R. J., Srivastava, S., & Whiteside, T. L. (1995). Assessment of sensitivity and specificity of immunohistochemical staining of p53 in lung and head and neck cancers. *The American journal of pathology*, *146*(5), 1170.
- Milczarek, G. J., Martinez, J., & Bowden, G. T. (1996). p53 Phosphorylation: biochemical and functional consequences. *Life sciences*, *60*(1), 1-11.
- Misso, G., Di Martino, M. T., De Rosa, G., Farooqi, A. A., Lombardi, A., Campani, V., . . . Tassone, P. (2014). Mir-34: a new weapon against cancer? *Molecular Therapy-Nucleic Acids*, *3*.
- Momand, J., Zambetti, G. P., Olson, D. C., George, D., & Levine, A. J. (1992). The mdm-2 oncogene product forms a complex with the p53 protein and inhibits p53-mediated transactivation. *cell*, *69*(7), 1237-1245.
- Nagata, T., Shirakawa, K., Kobayashi, N., Shiheido, H., Tabata, N., Sakuma-Yonemura, Y., . . . Yanagawa, H. (2014). Structural basis for inhibition of the MDM2: p53 interaction by

- an optimized MDM2-binding peptide selected with mRNA display. *PLoS ONE*, 9(10), e109163.
- Nalls, D., Tang, S.-N., Rodova, M., Srivastava, R. K., & Shankar, S. (2011). Targeting epigenetic regulation of miR-34a for treatment of pancreatic cancer by inhibition of pancreatic cancer stem cells. *PLoS ONE*, 6(8), e24099.
- Noh, S. J., Baek, H. A., Park, H. S., Jang, K. Y., Moon, W. S., Kang, M. J., . . . Chung, M. J. (2013). Expression of SIRT1 and cortactin is associated with progression of non-small cell lung cancer. *Pathology-Research and Practice*, 209(6), 365-370.
- Oda, K., Arakawa, H., Tanaka, T., Matsuda, K., Tanikawa, C., Mori, T., . . . Nakamura, Y. (2000). p53AIP1, a potential mediator of p53-dependent apoptosis, and its regulation by Ser-46-phosphorylated p53. *cell*, 102(6), 849-862.
- Ohki, R., Kawase, T., Ohta, T., Ichikawa, H., & Taya, Y. (2007). Dissecting functional roles of p53 N-terminal transactivation domains by microarray expression analysis. *Cancer science*, 98(2), 189-200.
- Oliner, J. D., Pietenpol, J. A., Thiagalingam, S., Gyuris, J., Kinzler, K. W., & Vogelstein, B. (1993). Oncoprotein MDM2 conceals the activation domain of tumour suppressor p53.
- Oliveto, S., Mancino, M., Manfrini, N., & Biffo, S. (2017). Role of microRNAs in translation regulation and cancer. *World journal of biological chemistry*, 8(1), 45.
- Oren, M. (2003). Decision making by p53: life, death and cancer. *Cell death and differentiation*, 10(4), 431.
- Pepperberg, I. M. (2004). Cognitive and communicative capacities of grey parrots — implications for the enrichment of many species. *Animal Welfare*, 13, S203-S208.
- Perfettini, J.-L., Castedo, M., Nardacci, R., Ciccocanti, F., Boya, P., Roumier, T., . . . Kroemer, G. (2005). Essential role of p53 phosphorylation by p38 MAPK in apoptosis induction by the HIV-1 envelope. *Journal of Experimental Medicine*, 201(2), 279-289.
- Peto, J., Decarli, A., La Vecchia, C., Levi, F., & Negri, E. (1999). The European mesothelioma epidemic. *British journal of cancer*, 79(3-4), 666.
- Phang, B. H., Othman, R., Bougeard, G., Chia, R. H., Frebourg, T., Tang, C. L., . . . Sabapathy, K. (2015). Amino-terminal p53 mutations lead to expression of apoptosis proficient p47 and prognosticate better survival, but predispose to tumourigenesis. *Proceedings of the National Academy of Sciences*, 112(46), E6349-E6358.
- Puca, R., Nardinocchi, L., Sacchi, A., Rechavi, G., Givol, D., & D'Orazi, G. (2009). HIPK2 modulates p53 activity towards pro-apoptotic transcription. *Molecular cancer*, 8(1), 85.
- Raimondi, L., Amodio, N., Di Martino, M. T., Altomare, E., Leotta, M., Caracciolo, D., . . . D'Aquila, P. (2014). Targeting of multiple myeloma-related angiogenesis by miR-199a-5p mimics: *in vitro* and *in vivo* anti-tumour activity. *Oncotarget*, 5(10), 3039.
- Rajendran, R., Garva, R., Krstic-Demonacos, M., & Demonacos, C. (2011). Sirtuins: molecular traffic lights in the crossroad of oxidative stress, chromatin remodeling, and transcription. *BioMed Research International*, 2011.

- Raver-Shapira, N., Marciano, E., Meiri, E., Spector, Y., Rosenfeld, N., Moskovits, N., . . . Oren, M. (2007). Transcriptional activation of miR-34a contributes to p53-mediated apoptosis. *Molecular cell*, *26*(5), 731-743.
- Reed, S. M., & Quelle, D. E. (2014). p53 acetylation: regulation and consequences. *Cancers*, *7*(1), 30-69.
- Rinaldo, C., Prodosmo, A., Mancini, F., Iacovelli, S., Sacchi, A., Moretti, F., & Soddu, S. (2007). MDM2-Regulated Degradation of HIPK2 Prevents p53Ser46 Phosphorylation and DNA Damage-Induced Apoptosis. *Molecular cell*, *25*(5), 739-750. doi:10.1016/j.molcel.2007.02.008
- Robinson, B. W., & Lake, R. A. (2005). Advances in malignant mesothelioma. *New England Journal of Medicine*, *353*(15), 1591-1603.
- Saelens, X., Festjens, N., Walle, L. V., Van Gorp, M., van Loo, G., & Vandenabeele, P. (2004). Toxic proteins released from mitochondria in cell death. *Oncogene*, *23*(16), 2861-2874.
- Salwiczek, L. H., Emery, N. J., Schlinger, B., & Clayton, N. S. (2009). The development of caching and object permanence in western scrub-jays (*Aphelocoma californica*): Which emerges first? *Journal of Comparative Psychology*, *123*(3), 295-303. doi:10.1037/a0016303
- Saunders, L., & Verdin, E. (2007). Sirtuins: critical regulators at the crossroads between cancer and aging. *Oncogene*, *26*(37), 5489.
- Scaffidi, C., Fulda, S., Srinivasan, A., Friesen, C., Li, F., Tomaselli, K. J., . . . Peter, M. E. (1998). Two CD95 (APO-1/Fas) signaling pathways. *The EMBO journal*, *17*(6), 1675-1687.
- Scherpereel, A. (2006). The experts' conference of the Societe de Pneumologie de Langue Francaise (SPLF) on malignant pleural mesothelioma (MPM): useful and necessary recommendations. *Revue des maladies respiratoires*, *23*(4 Pt 3), 11S15.
- Scherpereel, A., Astoul, P., Baas, P., Berghmans, T., Clayson, H., De Vuyst, P., . . . Hillerdal, G. (2010). Guidelines of the European Respiratory Society and the European Society of Thoracic Surgeons for the management of malignant pleural mesothelioma. *European Respiratory Journal*, *35*(3), 479-495.
- Scherpereel, A., & Group, F. S. S. f. C. M. E. (2007). Guidelines of the French Speaking Society for Chest Medicine for management of malignant pleural mesothelioma. *Respiratory medicine*, *101*(6), 1265-1276.
- Scoumanne, A., & Chen, X. (2008). Protein methylation: a new regulator of the p53 tumour suppressor. *Histology and histopathology*, *23*(9), 1143.
- Shahbazian, M. D., & Grunstein, M. (2007). Functions of site-specific histone acetylation and deacetylation. *Annu. Rev. Biochem.*, *76*, 75-100.
- Smeenk, L., Van Heeringen, S. J., Koeppel, M., Gilbert, B., Janssen-Megens, E., Stunnenberg, H. G., & Lohrum, M. (2011). Role of p53 serine 46 in p53 target gene regulation. *PLoS ONE*, *6*(3), e17574.
- Stankevics, L., da Silva, A. P. A., dos Passos, F. V., dos Santos Ferreira, E., Ribeiro, M. C. M., David, M. G., . . . de Almeida, C. E. (2013). MiR-34a is up-regulated in response to low

- dose, low energy X-ray induced DNA damage in breast cells. *Radiation oncology*, 8(1), 231.
- Sun, F., Fu, H., Liu, Q., Tie, Y., Zhu, J., Xing, R., . . . Zheng, X. (2008). Downregulation of CCND1 and CDK6 by miR-34a induces cell cycle arrest. *FEBS letters*, 582(10), 1564-1568.
- Suzuki, K., & Matsubara, H. (2011). Recent advances in p53 research and cancer treatment. *BioMed Research International*, 2011.
- Tait, S. W., & Green, D. R. (2010). Mitochondria and cell death: outer membrane permeabilization and beyond. *Nature reviews Molecular cell biology*, 11(9), 621-632.
- Tibbetts, R. S., Brumbaugh, K. M., Williams, J. M., Sarkaria, J. N., Cliby, W. A., Shieh, S.-Y., . . . Abraham, R. T. (1999). A role for ATR in the DNA damage-induced phosphorylation of p53. *Genes & development*, 13(2), 152-157.
- Tokino, T., & Nakamura, Y. (2000). The role of p53-target genes in human cancer. *Critical reviews in oncology/hematology*, 33(1), 1-6.
- Tsvetkov, P., Reuven, N., & Shaul, Y. (2010). Ubiquitin-independent p53 proteasomal degradation. *Cell Death & Differentiation*, 17(1), 103-108.
- URAMOTO, H., SUGIO, K., OYAMA, T., NAKATA, S., ONO, K., NOZOE, T., & YASUMOTO, K. (2006). Expression of the p53 family in lung cancer. *Anticancer research*, 26(3A), 1785-1790.
- Vaziri, H., Dessain, S. K., Eaton, E. N., Imai, S.-I., Frye, R. A., Pandita, T. K., . . . Weinberg, R. A. (2001). hSIR2SIRT1 functions as an NAD-dependent p53 deacetylase. *cell*, 107(2), 149-159.
- Vogelstein, B., Lane, D., & Levine, A. J. (2000). Surfing the p53 network. *Nature*, 408(6810), 307-310.
- Vogt, M., Munding, J., Grüner, M., Liffers, S.-T., Verdoodt, B., Hauk, J., . . . Hermeking, H. (2011). Frequent concomitant inactivation of miR-34a and miR-34b/c by CpG methylation in colorectal, pancreatic, mammary, ovarian, urothelial, and renal cell carcinomas and soft tissue sarcomas. *Virchows Archiv*, 458(3), 313-322.
- Vousden, K. H., & Prives, C. (2009). Blinded by the light: the growing complexity of p53. *cell*, 137(3), 413-431.
- Wade, M., Wang, Y. V., & Wahl, G. M. (2010). The p53 orchestra: Mdm2 and Mdmx set the tone. *Trends in cell biology*, 20(5), 299-309.
- Wagner, J., Sleggs, C., & Marchand, P. (1960). Diffuse pleural mesothelioma and asbestos exposure in the North Western Cape Province. *British journal of industrial medicine*, 17(4), 260-271.
- Walczak, H., & Krammer, P. H. (2000). The CD95 (APO-1/Fas) and the TRAIL (APO-2L) apoptosis systems. *Experimental cell research*, 256(1), 58-66.
- Wei, J. S., Song, Y. K., Durinck, S., Chen, Q.-R., Cheuk, A. T. C., Tsang, P., . . . Shohet, J. (2008). The MYCN oncogene is a direct target of miR-34a. *Oncogene*, 27(39), 5204.
- Wiggins, J. F., Ruffino, L., Kelnar, K., Omotola, M., Patrawala, L., Brown, D., & Bader, A. G. (2010). Development of a lung cancer therapeutic based on the tumour suppressor microRNA-34. *Cancer research*, 70(14), 5923-5930.

- Wu, X., Bayle, J. H., Olson, D., & Levine, A. J. (1993). The p53-mdm-2 autoregulatory feedback loop. *Genes & development*, 7(7a), 1126-1132.
- Xu-Monette, Z. Y., Medeiros, L. J., Li, Y., Orlowski, R. Z., Andreeff, M., Bueso-Ramos, C. E., . . . Young, K. H. (2012). Dysfunction of the TP53 tumour suppressor gene in lymphoid malignancies. *Blood*, blood-2011-2011-366062.
- Xu, D., & La Thangue, N. B. (2008). Strap: A versatile transcription co-factor. *Cell Cycle*, 7(16), 2456-2457.
- Yamakuchi, M., Ferlito, M., & Lowenstein, C. J. (2008). miR-34a repression of SIRT1 regulates apoptosis. *Proceedings of the National Academy of Sciences*, 105(36), 13421-13426.
- Yamakuchi, M., & Lowenstein, C. J. (2009). MiR-34, SIRT1, and p53: The feedback loop. *Cell Cycle*, 8(5), 712-715.
- Yan, D., Zhou, X., Chen, X., Hu, D.-N., Da Dong, X., Wang, J., . . . Qu, J. (2009). MicroRNA-34a inhibits uveal melanoma cell proliferation and migration through downregulation of c-Met. *Investigative ophthalmology & visual science*, 50(4), 1559-1565.
- Zannini, L., Buscemi, G., Kim, J.-E., Fontanella, E., & Delia, D. (2012). DBC1 phosphorylation by ATM/ATR inhibits SIRT1 deacetylase in response to DNA damage. *Journal of molecular cell biology*, 4(5), 294-303.
- Zhao, Y., Lu, S., Wu, L., Chai, G., Wang, H., Chen, Y., . . . Zheng, Q. (2006). Acetylation of p53 at lysine 373/382 by the histone deacetylase inhibitor depsipeptide induces expression of p21Waf1/Cip1. *Molecular and cellular biology*, 26(7), 2782-2790.
- Zhu, J., Zhang, S., Jiang, J., & Chen, X. (2000). Definition of the p53 functional domains necessary for inducing apoptosis. *Journal of Biological Chemistry*, 275(51), 39927-39934.
- Zorina, Z. A. (2005). Animal intelligence: Laboratory experiments and observations in nature. *Zoologicheskyy Zhurnal*, 84(1), 134-148.
- Zu, G., Ji, A., Zhou, T., & Che, N. (2016). Clinicopathological significance of SIRT1 expression in colorectal cancer: A systematic review and meta analysis. *International Journal of Surgery*, 26, 32-37.

## Web References

- WHO, 2015. Cancer. [online] available at: <http://www.who.int/mediacentre/factsheets/fs297/en/> [Accessed 09 March 2015].
- WHO, 2014. World cancer report 2014. [online] available at: [http://www.iarc.fr/en/mediacentre/pr/2014/pdfs/pr224\\_E.pdf](http://www.iarc.fr/en/mediacentre/pr/2014/pdfs/pr224_E.pdf) [Accessed 09 March 2015]
- UK, C. R. (2013). CANCER INCIDENCE Statistics IN THE UK IN 2011. Retrieved 10 MAR, 2015, from <http://jsna.reading.gov.uk/living-working/health-protection/cancer/>
- NICE, 2011. Lung cancer: The diagnosis and treatment of lung cancer. [online] available at: <https://www.nice.org.uk/guidance/cg121/chapter/introduction> [Accessed 31 MAY 2015]